



THE HONG KONG  
POLYTECHNIC UNIVERSITY

香港理工大學

Pao Yue-kong Library

包玉剛圖書館

---

## Copyright Undertaking

This thesis is protected by copyright, with all rights reserved.

**By reading and using the thesis, the reader understands and agrees to the following terms:**

1. The reader will abide by the rules and legal ordinances governing copyright regarding the use of the thesis.
2. The reader will use the thesis for the purpose of research or private study only and not for distribution or further reproduction or any other purpose.
3. The reader agrees to indemnify and hold the University harmless from and against any loss, damage, cost, liability or expenses arising from copyright infringement or unauthorized usage.

### IMPORTANT

If you have reasons to believe that any materials in this thesis are deemed not suitable to be distributed in this form, or a copyright owner having difficulty with the material being included in our database, please contact [lbsys@polyu.edu.hk](mailto:lbsys@polyu.edu.hk) providing details. The Library will look into your claim and consider taking remedial action upon receipt of the written requests.

**STUDIES OF *IN VIVO* EFFICACY OF  
FLAVONOID DIMERS IN MODULATING  
P-GLYCOPROTEIN (P-GP)  
MEDIATED DRUG RESISTANCE**

YAN CLARE SAU WOON

Ph.D

The Hong Kong Polytechnic University

2017

The Hong Kong Polytechnic University  
Department of Applied Biology and Chemical Technology

**STUDIES OF *IN VIVO* EFFICACY OF  
FLAVONOID DIMERS IN MODULATING  
P-GLYCOPROTEIN (P-GP)  
MEDIATED DRUG RESISTANCE**

YAN CLARE SAU WOON

A thesis submitted in partial fulfillment of the requirements for the  
degree of Doctor of Philosophy

September 2016

## **CERTIFICATE OF ORIGINALITY**

I hereby declare that this thesis is my own work and that, to the best of my knowledge and belief, it reproduces no material previously published or written, nor material that has been accepted for the award of any other degree or diploma, except where due acknowledgement has been made in the text.

YAN Clare Sau Woon

## Abstract

A series of apigenin based novel flavonoid dimers were synthesized to tackle cancer MDR mediated by P-gp. Lead optimization through the introduction of an amine group within the PEG linker of parent compound 61 has led to the discovery of FD18. FD18 is more potent than 61, with an  $EC_{50}$  towards PTX decreased from 360 nM to 148nM and enhanced aqueous solubility. FD18, together with its derivatives, were characterized *in vivo* with the use of a newly established LCC6/MDR P-gp overexpressed human cancer nude mice model. This model is highly resistant to PTX treatment at 12 mg/kg (q.o.d. x 4 for 2-cycle), making it favorable to become an ideal testing platform. Subsequent treatment of these flavonoid compounds at 45 mg/kg together with PTX at 12 mg/kg (q.o.d. x 12) had demonstrated tumor inhibition effects, in which, FD18 was the most potent compound resulted in a promising %T-C of 54%. The safety profile of FD18 was also demonstrated through injections to healthy Balb/c mice and histopathological studies. No treated mice exerted toxicity deaths or weight loss >15% as well as cellular toxicities. DMPK study of FD18 has proposed one of its metabolite is an active P-gp inhibitor. This metabolite, namely FM04, has significantly increased in its aqueous solubility with a  $clogP$  value of 4.06 ( $clogP$  for FD18 is 7.07) and 50% more potent compared to FD18 in reversing PTX resistance from LCC6/MDR cells ( $EC_{50} = 70nM$ ). It was compared with FD18 with essentially the same in inhibiting DOX transport and the role as a P-gp substrate. Finally, FM04 was better in *in vivo* P-gp modulating activity towards PTX treatment over FD18 with a %T-C of 57%. Together with its druggability as defined by the Lipinski Rule of 5, makes FM04 more favorable than FD18 as a drug candidate.

## List of publications and conference presentation

### Publications

Chan, K. F.; Zhao, Y.; Chow, T. W.; **Yan, C. S.**; Ma, D. L.; Burkett, B. A.; Wong, I. L.; Chow, L. M.; Chan, T. H. (2009). "Flavonoid dimers as bivalent modulators for p-glycoprotein-based multidrug resistance: structure-activity relationships." ChemMedChem 4(4): 594-614.

Kan, J. W.; Chan, K.F.; **Yan, C.S.**; Wong, I.L.K.; Chan, T.H.; Chow, L. M. Pharmacokinetics and interaction study of flavonoid dimer, a P-glycoprotein reversing agent, with Paclitaxel in rodent. Drug Metab Rev (2009), 41(Suppl.)

Chan, K.F.; Wong, I.L.K.; Burkett, B.A.; Zhao, Y.; **Yan, C.S.**; Kan, J. W.; Tsang, K.H.; Lam, C.Y.; Chow, T.W.S.; Chan, T.H.; Chow, L. M. (2010) Flavonoid dimer as modulator of drug resistance in cancer. Progress in Nutrition 12: 1-7.

Chan, K. F.; Wong, I. L.; Kan, J. W.; **Yan, C. S.**; Chow, L. M.; Chan, T. H. (2012). "Amine linked flavonoid dimers as modulators for P-glycoprotein-based multidrug resistance: structure-activity relationship and mechanism of modulation." Journal of medicinal chemistry 55(5): 1999-2014.

**Yan, C. S.**, I. L. Wong, et al. (2015). "A New Class of Safe, Potent, and Specific P-gp Modulator: Flavonoid Dimer FD18 Reverses P-gp-Mediated Multidrug Resistance in Human Breast Xenograft in Vivo." Molecular pharmaceutics 12(10): 3507-17. (Appendix 1)

### Conference presentation

**Yan C.S.**; Chan K.F.; Kan J.W.; Wong I.L.; Zhao Y.; Chow L.M.; Chan T.H. (2010). "Studies of *in vivo* Efficacy of Flavonoid Dimer (FD2010) in Modulating P-glycoprotein (P-gp) Mediated Drug Resistance." Gordon Research Conference on Membrane Transport Proteins, University of New England, Biddeford, Maine, U.S.A. August 15-20

## Acknowledgements

Foremost, I would like to express my sincere gratitude to my supervisor, Professor Chow Larry Ming-cheung, for his guidance and inspirations since undergraduate and throughout my PhD study. His enthusiasm in education and research has very much encouraged me to strive for my best. It is my honor and pleasure to be able to participate in this project.

Besides, thanks must be given to Professor Chan Tak-hang for all of his constructive comments and Dr. Chan Kin-fai for his endless efforts in chemical synthesis and optimizations. Another two persons who must be mentioned are Dr. Chan Shun-wan and Ms. Lam Wai-man, who have given me essential trainings in animal experimental techniques. Kind assistance was also received from Dr. Leung Gina from the Department of Health Technology and Informatics at HKPU and Dr. Tse Gary Man-kit at the Department of Anatomical and Cellular Pathology in CUHK for their professional guidance in my histopathological studies. Without all these important people, the project would not be able to conduct.

Appreciation is also sent to all teammates from Professor Chow's research team, especially Dr. Wong Iris for her well managed *in vitro* assay platform; Dr. Kan Jason for his excellent work in DMPK and Mr. Chong Tsz-cheung for his support in many aspects. Thanks were also given to Dr. Choy Kit-ying and Dr. Chung Tabris, for their cheerful time and sharing of my life moments.

Thank you to those who have ever facilitated this project. Including staff and technicians in particular Mr. Cheng Chor-hing, Ms. Yeung Sarah, Ms. Wan Echo and

Mr. Cheng Yung from the Department of ABCT and all staff from the Centralized Animal Facilities.

My sincere thanks also go a number of friends: Dr. Cheung Chartia, Mr. Chia Kia, Dr. Kong Hang-kin, Mr. Kim Stephen, Dr. Tang Angie, Dr. Lee Fred and Dr. Chong Steve for their continuous support since the day we have met.

Last but not least, thank you to my family, for giving me birth at the first place. Thanks to Mr. Arshid Adnan for brightening up my days. Their unconditional love, understandings and patience have supported me throughout my PhD study.

## **Table of Contents**

<b>Certificate of Originality .....</b>	<b>I</b>
<b>Abstract .....</b>	<b>II</b>
<b>List of publications and conference presentation .....</b>	<b>III</b>
<b>Acknowledgements .....</b>	<b>IV</b>
<b>List of figures .....</b>	<b>XII</b>
<b>List of tables .....</b>	<b>XIV</b>
<b>List of abbreviations .....</b>	<b>XV</b>
<b>Chapter 1 Introduction .....</b>	<b>1</b>
1.1 What is cancer? .....	2
1.2 Cancer Resistance and Multidrug resistance (MDR).....	2
1.2.1 P-glycoprotein and the adenosine triphosphate-binding cassette (ABC) transporter .....	3
1.2.2 The structure and working mechanism of P-gp .....	4
1.3 The MDR1/P-gp Reversing Agents (P-gp Modulators) .....	9
1.3.1 First generation MDR modulators .....	9
1.3.2 Second generation MDR modulators .....	13
1.3.3 Third generation MDR modulators .....	16
1.4 Flavonoids and Their Reversal Activities in MDR Cancer Cells .....	18

1.4.1 The synthetic flavonoid dimers as P-gp modulators .....	19
1.4.2 Lead optimization of flavonoid dimers and previous work .....	20
1.5 Objectives of this project .....	23
 <b>Chapter 2 Establishment of MDA435/LCC6, MDA435/LCC6MDR</b>	
<b>Human Breast Cancer Xenograft Models .....24</b>	
2.1 Introduction .....	25
2.1.1 The development of animal models for drug screening purposes .....	25
2.1.2 Human tumor xenograft models and their importance in anticancer drug research .....	26
2.2 Materials and reagents .....	29
2.2.1 Cell lines and reagents .....	29
2.2.2 Cell culturing methods and conditions .....	30
2.2.3 Cell counting and trypan blue exclusion assay for viable cells .....	30
2.2.4 Preparation of Drug and flavonoid dimers for cell proliferation assay .....	31
2.2.5 Cell proliferation assay (MTS assay) .....	31
2.2.6 Animal husbandry .....	32
2.2.7 Establishment of LCC6 and LCC6/MDR Ascitic Model .....	32
2.2.8 Confirmation of PTX resistance in ascitic cells by cell proliferation assay .....	33
2.2.9 Construction of LCC6 and LCC6/MDR xenografts from ascitic fluid .....	34
2.2.10 Maintenance of LCC6 and LCC6/MDR subcutaneous xenograft model .....	34

2.2.11 Sample preparation for P-gp level analysis on LCC6 and LCC6/MDR ascitic cells and its solid tumor .....	35
2.2.12 P-gp expression analysis by Western Blotting .....	36
2.2.13 Preparation of Drugs for PTX efficacy studies .....	36
2.2.14 <i>In vivo</i> reversal activities on LCC6 and LCC6/MDR xenografts towards PTX ..	37
2.3 Results.....	39
2.3.1 Establishment of LCC6 and LCC6/MDR Ascitic Model .....	39
2.3.2 Confirmation of PTX resistance in ascitic LCC6/MDR cancer cells .....	41
2.3.3 Permeability glycoprotein (P-gp) expression analysis on LCC6 and LCC6/MDR ascitic cells and their solid tumors .....	42
2.3.4 Efficacy of LCC6 and LCC6/MDR tumor model towards PTX treatment .....	43
2.4 Discussion .....	47
<b>Chapter 3 <i>In vitro</i> screening of flavonoid dimers; their <i>in vivo</i> toxicities and efficacies .....</b>	<b>49</b>
3.1 Introduction.....	50
3.2 Materials and methods .....	51
3.2.1 <i>In vitro</i> P-gp reversing activities towards PTX .....	51
3.2.2 Cytotoxicities of flavonoid modulators .....	55
3.2.3 Drug preparation for animal experiments .....	55
3.2.4 Pharmacokinetic study of FD18 .....	56

3.2.5 <i>In vivo</i> short term toxicity study .....	57
3.2.6 Tissue processing and embedding for histopathological studies .....	58
3.2.7 Histopathological evaluation of selected flavonoid modulators .....	58
3.2.8 <i>In vivo</i> modulating activity towards PTX in LCC6/MDR xenografts .....	59
3.2.9 Evaluation of treatment efficacy .....	61
3.2.10 <i>In vivo</i> Paclitaxel accumulation study .....	61
3.2.11 Extraction of PTX from LCC6/MDR tumors for HPLC analysis .....	61
3.2.12 Dose optimization of FD18 in reversing P-gp mediated PTX resistance in LCC6/MDR xenografts .....	62
3.3 Results.....	62
3.3.1 <i>In vitro</i> screening of flavonoid dimers for their P-gp modulating activities towards PTX .....	62
3.3.2 Pharmacokinetic study of FD18 .....	66
3.3.3 Evaluation of <i>in vivo</i> short-term toxicity study for selected dimers .....	67
3.3.4 Histopathological study of FD18, 4MeO, 4Cl and N-Pip .....	70
3.3.5 <i>In vivo</i> modulating activity of FD18 towards P-gp mediated PTX resistance .....	81
3.3.6 <i>In vivo</i> accumulation of PTX in LCC6/MDR tumors .....	91
3.3.7 Dose optimization of FD18 in reversing P-gp mediated PTX resistance in LCC6/MDR xenografts .....	92
3.4 Discussion .....	97

<b>Chapter 4 <i>In vivo</i> comparison study of FD18 metabolite, FM04 .....</b>	<b>101</b>
4.1 Introduction .....	102
4.1.1 <i>In vitro</i> working mechanism of FD18 and its metabolic study .....	103
4.1.2 Pharmacokinetic properties of FM04 .....	107
4.2 Materials and methods .....	108
4.2.1 <i>In vitro</i> P-gp ATPase activity study .....	108
4.2.2 Effect of FD18 and FM04 on intracellular DOX accumulation in LCC6/MDR cells .....	109
4.2.3 Intracellular accumulation of FM04 .....	110
4.2.4 Drug preparation for animal studies .....	110
4.2.5 Comparison study of FD18 and FM04 <i>in vivo</i> modulation activity .....	111
4.3 Results .....	112
4.3.1 <i>In vitro</i> P-gp ATPase activity study .....	112
4.3.2 Effect of FD18 and FM04 on intracellular DOX accumulation in LCC6/MDR cells .....	114
4.3.3 Intracellular accumulation of FM04 .....	115
4.3.4 <i>In vivo</i> comparison study of FD18 and FM04 in treating PTX resistance tumor bearing mice .....	116
4.4 Discussion .....	121
<b>Chapter 5 Conclusion and future perspectives .....</b>	<b>124</b>

5.1 Summary of work .....	125
5.2 Importance of current study .....	128
5.3 Future work .....	128
5.4 Conclusion .....	128
<b>Appendix 1 Publication .....</b>	<b>130</b>
<b>References .....</b>	<b>141</b>

## List of figures

Figure 1.1 Topology structure of P-gp .....	5
Figure 1.2 The crystal structure of Sav1866.....	6
Figure 1.3 The crystal structure of mouse P-gp .....	7
Figure 1.4 Structure of Verapamil .....	9
Figure 1.5 Structure of CsA .....	10
Figure 1.6 Structure of PSC833 .....	13
Figure 1.7 Structure of GF120918 .....	15
Figure 1.8 Structure of LY335979.....	16
Figure 1.9 Structure of XR9576.....	16
Figure 1.10 Structure of apigenin .....	20
Figure 1.11 Structure of 9d .....	20
Figure 1.12 Structure of 1d-(5,7H) (Compound 61).....	21
Figure 1.13 Structure of 1d-(5,7H)-7F(Compound 62) .....	22
Figure 1.14 Structure of 1d-(5,7H)-6Me(Compound 69) .....	22
Figure 2.1 Confirmation of PTX resistance in ascitic LCC6/MDR cancer cells .....	41
Figure 2.2 P-glycoprotein (P-gp) expression analyses by western blotting .....	43
Figure 2.3 Tumor response curve for LCC6 and LCC6/MDR human cancer xenograft	46
Figure 3.1 Plasma concentration of FD18 against time .....	67
Figure 3.2 Images showing mice with auricular chondritis .....	70

Figure 3.3 Histopathological evaluations of vital organs .....	80
Figure 3.4 <i>In vivo</i> modulating activity of FD18 towards P-gp mediated PTX resistance .....	85
Figure 3.5 <i>In vivo</i> modulating activities of FD18 derivatives towards P-gp mediated PTX resistance .....	90
Figure 3.6 <i>In vivo</i> PTX accumulation in tumor after FD18 treatment .....	92
Figure 3.7 Dose optimization of FD18 in treating LCC6/MDR xenografts towards PTX .....	96
Figure 4.1 A proposed metabolic pathway for FD18 .....	104
Figure 4.2 Pharmacokinetic profile of FM04.....	108
Figure 4.3 <i>In vitro</i> P-gp ATPase activity study of FM04 and FD18 .....	113
Figure 4.4 Effect of FD18 and FM04 on intracellular DOX accumulation in LCC6/MDR cells .....	114
Figure 4.5 Intracellular accumulation of FM04 in LCC6 and LCC6/MDR cells .....	115
Figure 4.6 <i>In vivo</i> modulating activity of FM04 towards P-gp mediated PTX resistance .....	120

## List of tables

Table 2.1 Summary of ascitic model with LCC6 and LCC6/MDR cell lines .....	40
Table 3.1 Structures of modulators .....	52
Table 3.2 Histopathological grading criteria .....	59
Table 3.3 Treatment groups and schedule .....	60
Table 3.4 Summary of P-gp modulating activities of flavonoid dimers towards PTX ...	64
Table 3.5 Therapeutic indexes for selected modulators .....	66
Table 3.6 Summary of toxicity data .....	69
Table 3.7 Summary of histopathological grading .....	72
Table 3.8 Summary of <i>In vivo</i> modulating activity of FD18 .....	86
Table 3.9 Summary of <i>in vivo</i> modulating activity of FD18 derivatives.....	91
Table 3.10 Summary of dose optimization of FD18 in treating LCC6/MDR towards PTX .....	96
Table 4.1 Summary table for <i>in vitro</i> P-gp modulation activity studies of FD18 and its metabolites .....	106
Table 4.2 Summary of <i>in vivo</i> modulating activity of FM04 .....	121

## List of abbreviations

%T-C	% of tumor inhibition
<	Smaller than
>	Greater than
$\mu\text{M}$	Micromolar
AD	Actinomycin D
ADME	Absorption, distribution, metabolism and excretion
AUC	Area under the plasma concentration-time curve
$C_{\text{max}}$	Maximum plasma concentration
CHO	Chinese Hamster Cells
DMPK	Drug metabolism and pharmacokinetics
DMSO	Dimethyl sulfoxide
DOX	Doxorubicin
EC50	Concentration of a drug that gives half-maximal response
F	Bioavailability
H&E	Hematoxylin and eosin
HPLC	High performance liquid chromatography
i.p. injection	Intraperitoneal injection
i.v. injection	Intravenous injection
LCC6	MDA-MB-435/LCC6
LCC6/MDR	MDA-MB-435/LCC6MDR
mL	Milliliter

MTD	Maximum tolerated dosage
MTX	Mitoxantrone
MUD	Maximum usable dosage
NBF	Neutral buffered formalin
NCI	National Cancer Institute
ng	Nanogram
nM	Nanomolar
PBS	Phosphate buffered saline
PEG	Polyethylene glycol
P-gp	Permeability-glycoprotein
PK	Pharmacokinetics
PMSF	Phenylmethylsulfonyl fluoride
PTX	Paclitaxel
PVDF	Polyvinylidene fluoride
q	Every
q.o.d	Every other day
Ro5	Lipinski's Rules of 5
s.c. injection	subcutaneous injection
SAR	Structural activity relationship
SCID mice	Severe combined immunodeficiency mice
SDS-PAGE	Sodium dodecyl sulfate-polyacrylamide gel electrophoresis
SEM	Standard error of means
T.I.	Therapeutic Index

$T_d$	Tumor doubling time
$T_{max}$	Time to maximum plasma concentration
TTBS	Tween 20 tris-buffered saline
UPLC-MS/MS	Ultra performance liquid chromatography tandem mass spectrometry
VBL	Vinblastine
VCR	Vincristine
VER	Verapamil
$\lambda_{emit}$	Emission wavelength
$\lambda_{excite}$	Excitation wavelength

# **Chapter 1**

## **Introduction**

## 1.1 What is Cancer?

Cancer is a disease where cells exhibit uncontrollable growth due to oncogenes or tumor suppressors; abnormal cells failed to go through apoptosis, having the ability of invading nearby tissues and expanding limitlessly through blood and lymphatic circulation. Malignant cancer is further divided into four major types: a) Carcinomas, arise from cells that were located on body surfaces, on both internal and external surfaces, it is the most common type of cancer; b) Sarcomas, cancers arise from supportive tissues such as bone, muscle and so on; c) Lymphomas, cancers that involve the lymphatic system and the immune system; and, d) Leukemia, cancer with abnormal growth in blood or bone marrow. (American Cancer Society, 2016)

## 1.2 Cancer Resistance and Multidrug resistance (MDR)

The cause of cancer resistance can be classified in two aspects: host factors and specific genetic alternations. (Gottesman, 2002) Host factors such as poor absorption to drugs with large molecular sizes, high metabolic rates or rapid excretion, led to low serum drug concentration and resulting the inability of anticancer agent being diffused into tumor.

Overexpression of drug resistance genes, or suppressions in cell surface drug transporter genes can ultimately led to the overexpression of drug efflux pump (e.g. P-glycoprotein and the MDR-associating protein), causing drug resistance to structural related and unrelated drug or decreased in the transportation of certain drug into the cytoplasm of a cancer cell for the latter case.

The phenomenon of multidrug resistance was first described in 1970 during the selection of Actinomycin D (AD) resistance in Chinese Hamster Ovary Cells (CHO), where AD resistance CHO cells exert cross-resistance to more than five other agents that were structurally unrelated including Vincristine and Daunomycin in correlation with increased molecular weights with increased cross-resistances. (Biedler et. al, 1970) Elegant studies on the characterization of drug binding domains and mechanisms for P-gp were conducted by Loo and Clarke since 1995 through cysteine-less mutation and crosslinking studies, the drug binding mechanism “Substrate-induced fit” mechanism has been introduced. (Loo and Clarke, 2005) Under this model, drug substrates share a common drug binding domain by creating their own binding sites using different combination of transmembrane domain (TMD) amino acid residues. This can explain -why such transporter is resistant to multiple drugs with different structures.

### **1.2.1 P-glycoprotein and the adenosine triphosphate-binding cassette (ABC) transporter**

Since Biedler’s published work in 1970, extensive work has been done to identify possible cellular mechanisms and transporters associating with this phenomenon in human cancers. Pioneer researches have overexpressed and amplified genes that play important roles in multidrug resistance within CHO cell. These genes, including a 170kDa overexpressed membrane protein came from multiple drug resistance CHO cell, namely Permeability glycoprotein (P-gp) (Juliano and Ling, 1976; Van der Bliek et al., 1986), MDR1 or the ABCB1 (Gottesman, 2002), referring to the affection in permeability on plasma membrane when exposed to cytotoxic drugs. (Juliano and Ling, 1976; Loo and Clarke, 2005) Ueda and co-worker have successfully shown P-gp from multiple drug resistant

human KB carcinoma cell line is encoded by a gene called the *mdr1* gene. (Ueda et. al, 1986) The expression of this gene can be found on various cell types such as liver, kidney, intestinal cells as well as on the blood-brain-barrier, functioning as transporter for nutrients, biological important molecules and some harmful xenobiotics in and out from the cell, which apparently give protection and monitoring the survival for cells. (Gottesman 1988, Ling 1997, Gottesman 2002) *In vivo* gene knockout studies demonstrated that the loss of this gene product is not lethal nor influencing fertility; but causing hypersensitivities to drugs. (Loo and Clarke, 2005) In human, forty-nine ABC transporters have been identified and were being classified into 7 sub-families. Three of them have been confirmed for their involvement of MDR in cancer namely ABCB1 (MDR1), ABCC3 (MRP1) and ABCG2 (BCRP).

### **1.2.2 The structure and working mechanism of P-gp**

The primary structure of *mdr1* was as an energy-efflux pump-liked transporter with about 1280 residues found on chromosome 7; having two pseudo homologous parts found on the N- and C-terminus of the protein with six transmembrane domains (TMDs) on each half, containing two highly conserved cytosolic nucleotide-binding domains (NBDs). (Chen et al., 1986) (Figure 1.1)

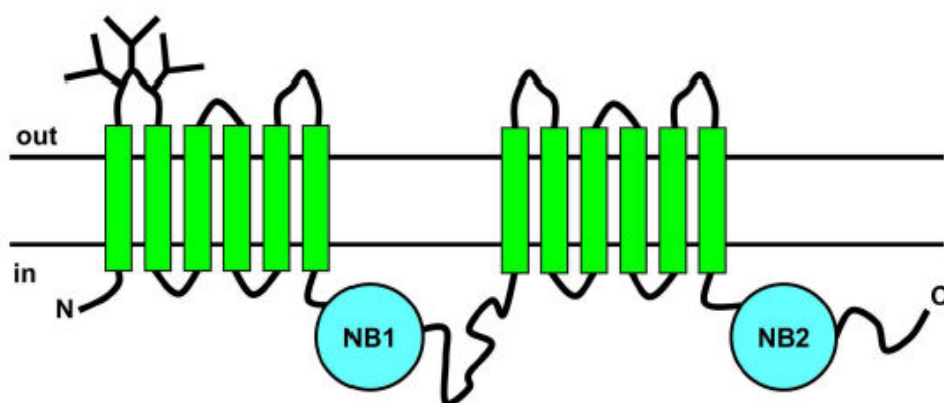


Figure 1.1 Topology structure of P-gp. Topology of P-gp showed that it is formed by a single protein strand with two homologous halves. Each half contains six transmembrane (TM) segments (green) and a nucleotide binding (NB) domain (blue) on the cytoplasmic side which can bind and hydrolyze ATP. (Sharom, 2014)

To understand the mechanisms of P-gp, its structure is essential, however, crystal structure P-gp from human is not available so far and was only observed under low resolution microscopy. The revelation of crystal structures from bacteria (Dawson and Locher, 2006), mouse (Aller et al., 2009), *Caenorhabditis elegans* (Jin et al., 2012) and *Candida albicans* (Kodan et al., 2014) have provided further information to the functional mechanistic understandings for P-gp. The crystal structure of a bacterial P-gp, Sav1866, was described by Dawson and Locher in 2006. With an overall shape that is consistent with human MDR1, Sav1866 was crystallized from *Staphylococcus aureus* at a resolution of 3Å in the presence of ADP. (Figure 1.2)

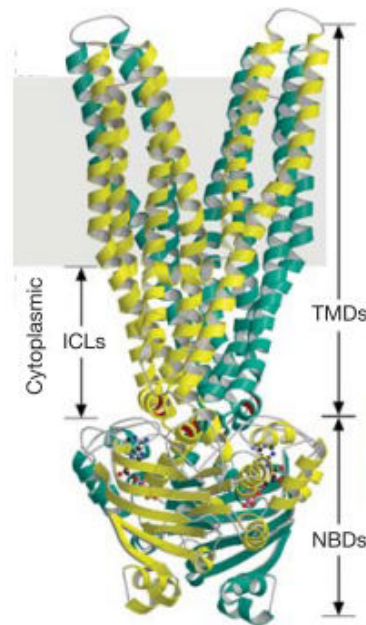


Figure 1.2 The crystal structure of Sav1866. Sav1866 was crystallized from *Staphylococcus aureus* and its structure was resolved at 3 Å. It was recognized as a homodimer with two subunits twisted and embraced with each other. TMDs: transmembrane domains; NBDs: nucleotide-binding domains; ICL: intracellular loops. (Dawson and Locher, 2006)

Sav1866 is an outward facing homodimeric protein with dimensions of 120 Å long, 65 Å wide and 55 Å deep. Each halves of the transporter appeared to be twisted with each other and on each subunit, the two major domains, a transmembrane domain (TMD) at the amino-terminus and a nucleotide binding domain (NBD) at the carboxy-terminus were found to interact with each other. This led to the proposal of a transporting mechanism involving the binding and hydrolysis of ATP which induced conformational changes of the protein, with subsequent signal transduction occurred at the intracellular loops 1 and 2 on the TMD interface, eventually allowing substrate binding and transport. (Dawson and Locher, 2006)

Mouse P-gp structure was obtained subsequently, with an even higher resolution of 3.8Å. The mouse P-gp, unlike Sav1866, exists as an inward facing P-gp at pre-transport state. (Figure 1.3)

The TMs helices from the two subunits (TMs 1 to 3, 6, 10, 11 and TMs 4, 5, 7 to 9, 12) spanned through the lipid bilayer, resulted in a large internal cavity of 6000Å open to both

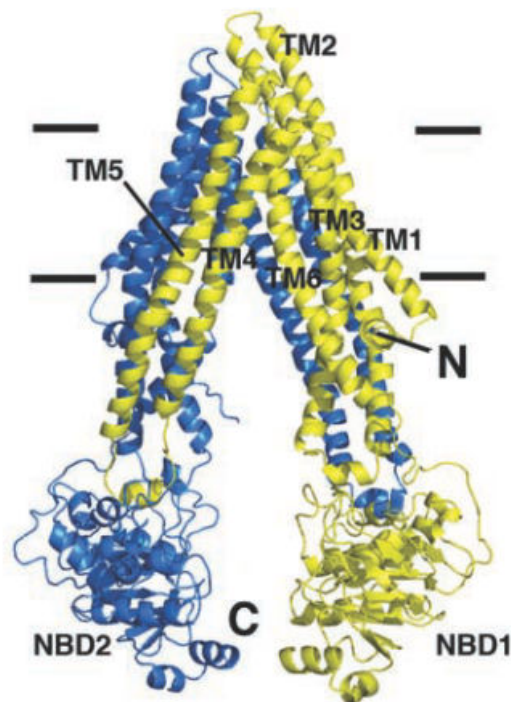


Figure 1.3 The crystal structure of mouse P-gp. Crystal structure of mouse P-gp shows an inward facing conformation at a resolution of 3.8Å. It has a pseudodimer arrangement where the two halves were distinguished in blue and yellow. Bundles of TM helices spanning through the lipid bilayer formed a cavity for substrate binding. Two NBDs separated by 30Å allows ATP binding and hydrolysis. (Aller et al., 2009)

the cytoplasm and inner leaflet. (Aller et al., 2009) The presence of such cavity allow hydrophobic substrate to diffuse through and bind at different orientations, together with

the binding of ATP, causing conformational changes of the protein thus dimerization of the NBD followed by ATP hydrolysis. Substrates could either be released back to the cytoplasm by decreasing binding affinity caused by changes in amino residues that interact with the protein or facilitated by ATP hydrolysis. (Aller et al., 2009) Present structural analysis supported the notion that P-gp works as a “hydrophobic vacuum cleaner”, which refers to hydrophobic drugs being removed directly across the cell membrane. (Raviv et al., 1990; Gottesman and Ambudkar, 2009)

The ABC transporter is an energy driven transporter and the efflux of their substrates requires the hydrolysis of ATP. Binding of drug substrate to P-gp led to conformational change on the transporter which will stimulate the first ATP binding and hydrolysis, through ATPase activities. This will expel the drug molecule back to the extracellular space, subsequently followed by the hydrolysis of the second ATP at the other ATP binding domain to restore its original shape and orientation. (Horio et al., 1988; Gottesman 2002; Loo and Clarke, 2005)

To become an appropriate drug substrate of P-gp, several criteria have to be fulfilled; first, the drug itself has to be relatively hydrophobic in order to be able to diffuse through the lipid bilayer from the plasma membrane and binds to the transporter. Second, cationic drug ligands such as the vinca alkaloids (e.g. Vinblastine), or weak bases having positive charges when exposed to the environment under a neutral pH. (Gottesman, 1993) Numerous structurally unrelated natural anticancer drugs such as Paclitaxel and vinca alkaloids were reported as the substrate of P-gp.

### 1.3 The MDR1/P-gp Reversing Agents (P-gp Modulators)

Three generations of MDR modulators have been identified with the ultimate goal of reversing clinical MDR.

#### 1.3.1 First generation MDR modulators

The first generation of MDR modulators were generally non-specific and being used clinically for other purposes, examples including Verapamil (VER) (Figure 1.4); a calcium channel blocker being used as vasodilator; and an immunosuppressor Cyclosporin A (CsA).

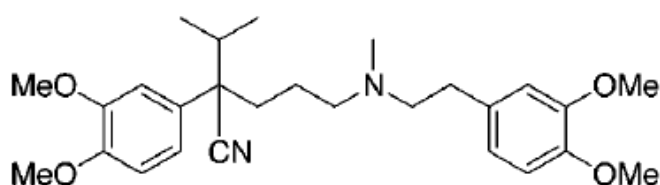


Figure 1.4 Structure of Verapamil. (Tsuruo et al., 1981)

Tsuruo et al in 1981 successfully demonstrated the complete reversal of Vinblastine (VBL) and Vincristine (VCR) resistance in resistant murine leukemia cell line P388/VCR using Verapamil (VER) at a nontoxic level *in vitro*. (Tsuruo et al., 1981) In the same study, they have also investigated the therapeutic effects on P388 and P388/VCR tumor bearing mice. The *in vivo* data suggested that Verapamil, when administered together with a 3-fold higher VCR concentration, it can almost completely overcome the VCR resistance in P388/VCR tumor bearing mice with an increased life span up to 50%. However, when the same animal model was treated with VBL and VER, it could only overcome the

resistance by increasing their life spans slightly. (Tsuruo et al., 1981; Krishna and Mayer, 2000)

Verapamil was evaluated later in clinical trials in both adults and children. In one study conducted by Cairo's group (Cairo et al., 1989), VER was used together with VBL and Etoposide (VP-16) in pediatric patient with advance stage cancer. Due to past experiences of serious cardiac toxicity when higher concentration of VER was being used (Ozols et al., 1987), lowered doses of VER had been employed in this study. Results had shown that 45% of the patients suffered from first degree heart block while close to half of them had hematological toxicity. These adverse effects, although acceptable, had only accompanied with partial treatment responses, which is far from satisfactory in drug safety and the requirement of sustainable treatment results.

Another modulator, CsA (Figure 1.5), is a naturally occurring cyclic peptide produced by fungus *Tolypocladium inflatum* Gams. (Twentyman et al., 1992; Loor et al., 2002) It is an anti-fungal agent as well as an immunosuppressant being used in organ transplantation patients for over forty years (Kahan, 2009).

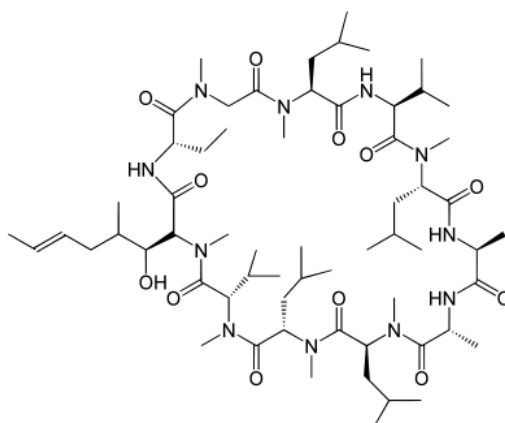


Figure 1.5 Structure of CsA. (Slater et al., 1986)

CsA was first shown to have reversal activities on Daunorubicin in Daunorubicin resistant Ehrlich ascites carcinoma in mice (Slater et al., 1986a) and Vincristine in human T cell acute lymphatic leukemia cells. (Slater et al., 1986b) Since then, different studies had been conducted to compare the potencies between Verapamil and CsA (Twentyman et al., 1990, Leite et al., 2006) and to CsA analogues (Twentyman et al., 1987; Twentyman et al., 1992; Loor et al., 2002) on modifying P-gp activities. One of these studies done by Twentyman (Twentyman et al., 1987) also shown that, apart from Vincristine and Daunorubicin, three other cytotoxic agents: Adriamycin (ADM), etoposide (VP-16) and Colchicines (COL) were also being sensitized by CsA, being used at 3-fold lesser concentration (2.1 $\mu$ M) than in Verapamil, in MDR variants mouse mammary carcinosarcoma cells and in MDR1 overexpressed Chinese Hamster Ovary cells CHO-CH<sup>R</sup>C5 (de Bruijn et al., 1986). CsA was subsequently taken into clinical trials because of the extensive use in organ transplantation and its comparable potency to Verapamil. In clinical trials, investigations were mainly done on cancer types with rapid growth kinetics such as hematological malignancies especially acute myeloid leukemia (AML), because CsA did not show satisfactory responses when it was used in patients having cancer with a slower growth kinetics (Toffoli et al., 1997). Phase I trial focused on the combinatory use of CsA with existing chemotherapy drugs on patients who have no responses on previous conventional treatments and/or the development of refractory drug resistant tumors, the main objective from this stage was to determine the maximum tolerated dose for CsA. Problem aroused when CsA was found to affect anticancer drug metabolism, especially on hindering the elimination of the anticancer drug. (Erlichman et al., 1993) Beside drug metabolism, toxicities due to CsA treatment can further be classified into

hematological and non-hematological toxicities. Hematological toxicity, although is not severe in some reported CsA combination treatments, is often associated with neutropenia which is the major dose limiting factor in CsA treatments. Myelosuppression has also been observed in one the studies done by Stiff et al. (Stiff et al., 1995), causing high rate bacteremia and caused death in their test subjects. Non hematological toxicity including vomiting, nausea, constipation, diarrhea, pain at tumor site, weight gain due to edema, hypertension and hyperbilirubin are occurring in approximately hundred percent on the patients. Fortunately, these toxic effects can be restored once CsA treatment has ceased. (Erllichman et al., 1993; Chambers et al., 1996; Toffoli et al., 1997; Warner et al., 1995; Stiff et al., 1995) In phase II and phase III trials, CsA was being used in shortened duration at a higher dose, via alternative administration route or being used with multidrug treatment such as EVE/CsA treatment. (Warner et al., 1995; Bisogno et al., 1998; Davidson et al., 2002; Sonneveld et al., 2001) Results from these trials were mostly unsatisfactory with limitations on hematological toxicities major in myelosuppression and produced stable responses for a short period of time only.

Other first generation MDR modulators including calmodulin inhibitors (Tsuruo et al., 1983), quercetin and quinidine (Tsuruo et al., 1984) also showed modulating activities on P-gp, but of a lesser clinical interest and was not taken into clinical trials.

The main problems of the first generation modulators are the low selectivity, therefore requiring a high dosage to be used (e.g. Verapamil was administrated at 50-100mg/kg in murine model (Tsuruo et al., 1981)). Furthermore, cytotoxicities towards normal cells *in vitro* (Leite et al., 2006; Lopes et al., 2003) and dose limiting toxicity in combination therapy in clinical trials were observed.

### 1.3.2 Second generation MDR modulators

Second generation non-toxic MDR modulators such as structural analog of VER: DexVerapamil and Emopamil, CsA analog SDZ PSC833 (PSC833 or Valspodar) (Figure 1.6). PSC833 was a marked discovery as it demonstrated superior MDR modulation activities in different cell lines *in vitro* and *in vivo*, it remains as one of the most powerful MDR modulators with its phase I clinical trials started in 2001. (Boesch et al., 1991; Watanabe et al., 1995; Krishna et al., 2000a; Krishna et al., 2000b; Advani et al., 2001; Atadja et al., 1998; Lee et al., 2004; Tan et al., 2000)

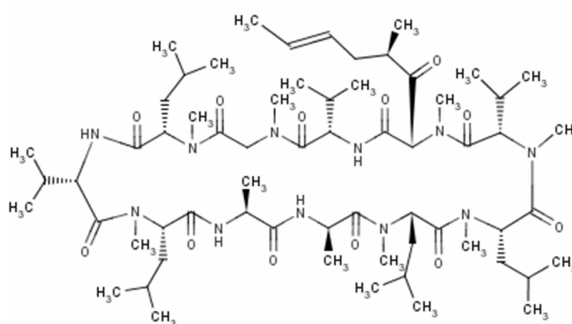


Figure 1.6 Structure of PSC833. (Boesch et al., 1991)

P833 is a highly lipophilic oral administrable Cyclosporin D analogue having much higher potency than CsA on P-gp modulation with no immunosuppression effects. PSC833 is highly specific to P-gp but not to other resistance mechanisms such as platinum resistance. (Lopes de Menezes et al., 2003) Earlier studies already shown the reversing P-gp activity at least ten fold higher than CsA without apoptotic effects. (Watanabe et al., 1995, Grey et al., 1997, Lopes et al., 2001) It was later shown to increase intracellular DOX and vinca alkaloids intracellular accumulation when used with PSC833. (Colombo

et al., 1996; Song et al., 1998) This results in the reversal of *in vitro* MDR of P388 murine leukemia cell and its MDR subtype towards various anticancer drugs. (Boesch et al., 1991) *In vivo* studies in different cancer models showed remarkable effects in prolonging animal life span, retarding tumor growth (Boesh et al., 1991; Watanabe et al., 1995; Lopes de Menezes et al., 2003) and reducing incident rate of chemically induced cancer (Kankesan et al., 2004). Phase I trials suggested that dosage of anticancer agents used with PSC833 should be reduced. PSC833 significantly altered the pharmacokinetics (PK) profiles of common cytotoxic drugs including Doxorubicin, Paclitaxel, mitoxantrone and etoposide. (Advani et al., 2001; Chico et al., 2001; Patnaik et al., 2000; Chauncey et al., 2000) As expected, most patients suffered from mild to moderate neutropenia and non-hematological toxicities; however, these are reversible and can be tolerated. The dose finding stage had suggested PSC833 may be used at 5 – 10 mg/kg with reduced level of cancer drugs. (Pataik et al., 2000; Covelli et al., 1997; Baekelandt et al., 2001) In more recent clinical trials, attempts had been done on more complicated treatment protocols by using several different cancer drugs on randomized studies. Although increased myelosuppression has been observed and some patient died of septic shocks, the overall treatment responses rate was improved. (Tan et al., 2000; Baekelandt et al., 2001) Phase III study on untreated AML patients of age over 60 was conducted by Cancer and Leukemia Group B (Baer et al. 2002), the results were unsatisfactory and led to early closure of the trial due to unacceptable toxicities causing death. No significant improvements on treatment response rates was found. It was concluded that a less toxic regimen should be tested on these elderly patients when available. Other phase III studies attempted to combine PSC833 with Vincristine-Doxorubicin-Dexamethasone (VAD)

(Friedenberg et al.,2006) and Paclitaxel-Carboplatin (Lhomme et al., 2008). In the VAD/VAD-PSC833 study, administration of PSC833 not significantly prolonged median survival time and treatment responses did in multiple myeloma patients when compared to patients who received VAD treatment. Increased grade 3 toxicities were also observed and predominantly due to Doxorubicin since PSC833 increased Doxorubicin and its metabolite Doxorubicinol level from PK study.

PSC833 was the most potent MDR modulator compared to the other second generation modulators like R-Verapamil and GF120918 (Elacridar). (Figure 1.7) It is not immunospressing like CsA, and was highly specific to P-gp. No significant improvement however; was found in clinical trials and for Elacridar. (Planting et al., 2004; Kuppens et al., 2007)

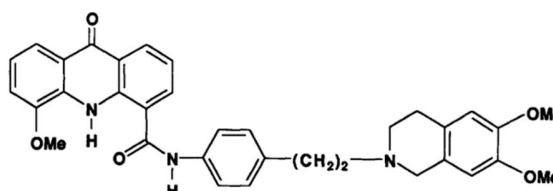


Figure 1.7 Structure of GF120918. (Hyafil et al., 1993)

### 1.3.3 Third generation MDR modulators

Third generation modulators, including LY 335979 (Zosuquidar) (Figure 1.8) and XR 9576 (Tariquidar) (Figure 1.9), have reversal effect at nanomolar levels.

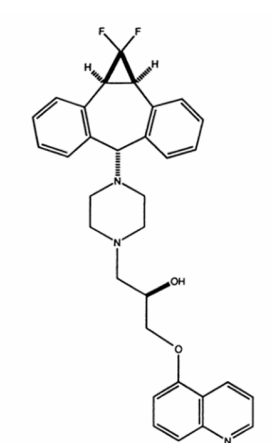


Figure 1.8 Structure of LY335979. (Slate et al., 1995)

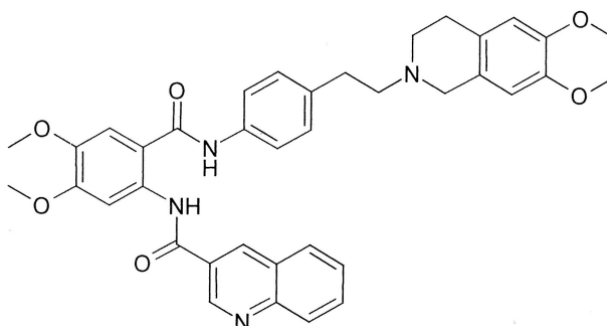


Figure 1.9 Structure of XR9576. (Mistry et al., 1999)

Dantzig and co-workers from Lilly research laboratory in 1996 shows that LY 335979 (former RS-33295-128 by Slate et al., 1995), which is a cyclopropylidene-dibenzosuberone compound, was able to modulate Doxorubicin and; Paclitaxel resistance, LY335979 did

not affect Doxorubicin AUC while CsA increased Doxorubicin AUC by 200%. (Dantzig et al., 1996, Slapak et al., 2001) Similar observation was made in [<sup>99m</sup>Tc]Sestamibi efflux studies (Slapak et al., 2001) by LY335979 can also modulate other transporters like MRP1, BCRP, MXR (Dantzig et al., 1996; Shepard et al., 2003). Unlike CsA, which interacts with cytochrome P450 3A4 (CYP3A4) (Pal et al., 2006), LY335979 only inhibits to 4 major CYP enzymes slightly. These suggests that LY335979 is highly selective and causes less pharmacokinetic interaction. (Dantzig et al., 1999; Dantzig et al., 2001) In phase I trials, zosuquidar was administrated with anthracyclines to advance, recurrent or resistant malignancies (Sandler et al., 2004, Lancet et al., 2009), docetaxel (Fracasso et al., 2004) and CHOP regimen for lymphoma patients. (Morschhauser et al., 2007) All studies showed that LY335979 have minimal effects on AUC and clearance of these anticancer agents. Only low grades toxicities including neutropenia and others tolerable non-hematological toxicities were observed. The suggested doses for these anticancer drugs could be used as high as 100 mg/m<sup>2</sup>, in the case of Doxorubicin, which was a great improvement compared to previous studies when PSC833 or CsA were being used. Randomized phase II study by Ruff et al. in 2009 on breast cancer patients, suggested that, while was non-toxic, it did not improve its overall response rates. (Ruff et al., 2009) Similar results were generated in a recent study conducted by ECOG using standard induction therapy with or without zosuquidar on elderly AML patients with poor prognosis. (Cripe et al., 2010)

Another modulator, XR9576, was improved from XR9051. XR9576 is approximately 15 fold more potent than PSC833 and is very specific to P-gp. (Mistry et al., 1999; Mistry et al., 2001; Walker et al., 2004) Phase I clinical trials showed that XR9576 was bioavailable

and well tolerated in healthy human subjects. (Stewart et al., 2000) Unfortunately, results from phase II trial in advance breast cancer patients with P-gp expression suggested that XR9576, given at a dose of 150 mg/kg together with anthracyclines or taxanes has only resulted in a small benefit. (Pusztai et al., 2005) Due to poor performance statuses thus discontinuations from two concurrent phase III studies in non-small cell lung cancers with treatments of vinorelbine, Paclitaxel or carboplatin; this phase II study was also discontinued earlier than expected and it was not being investigated further. (Pusztai et al., 2005)

Despite of the non-toxic nature and increased potencies from the third generation P-gp inhibitors, many of them failed to go through clinical trials. For this reason, new P-gp modulators must be developed in order to tackle this problem.

#### **1.4 Flavonoids and Their Reversal Activities in MDR Cancer Cells**

Flavonoid is a large group of polyphenolic chemicals which can be found abundantly in plants, vegetables and fruits. There are five classes of flavonoids and more than 6500 derivatives have been identified, exhibiting various beneficial effects on human health. Flavonoids act as metal ion chelator, antioxidant, anti-inflammatory agent and they also give antitumor activities. The first flavonoid derivative found to have chemosensitization properties was quercetin, which could restore the sensitivity in MDR cells to Adriamycin, inhibit ATPase activities and also preventing the binding and thus the transport of P-gp substrates such as fluorescent probe Hoechst 33342. (Boumendjel 2002; Di Pietro et al., 2002) This class of compound was also found to be inhibitors towards BCRP mediated intrinsic resistance to mitoxantrone (MTX) in breast cancer. (Zhang et al., 2004) It has

been reviewed by Morris et al. in 2006 that the P-gp inhibitory effect mediated by flavonoid may be through the direct binding of flavonoids to the NBD at C-terminus as flavonoids can directly bind to recombinant NBD2; or in second case, by inhibiting CYP43A. Having little or no adverse pharmac-interactions and cytotoxicities in animal models and possibly in the human body, synthetic and potent flavonoid modulators are being evaluated as the next in “semi-synthetic” MDR modulators.

#### **1.4.1 The synthetic flavonoid dimers as P-gp modulators**

The idea of synthetic chemicals with polyvalency was inspired by numerous biological systems demonstrating increased affinities and specificities towards their ligands-receptor bindings. These systems, for example, including interactions between multiple hemagglutinins on influenza virus and sialic acid molecules on bronchial epithelial cells; multiple bindings between antibodies, bacteria and macrophages, leading to specific recognition and triggering cell signaling for engulfment; and, polymeric DNA transcription factor gives great affinity towards the binding of DNA strand. (Mammen et al., 1998) Polymeric approach in synthetic biological molecules successfully increase their binding affinities, as well as enhancing their receptor specificities.

Polymeric biotin-avidin (Rao et al., 1998) was one of the examples with increased binding affinity by approximately 25 folds in its trivalent form. Apart from this, studies with polyvalencies towards P-gp have also been performed by using Polyethyleneglycol (PEG) ethers linker with different lengths in bivalent stipiamide. Bivalent stipiamide is a natural substrate towards P-gp that displayed dose-dependent relationships in inhibiting intracellular accumulation of bodipy-FL-prazosin. (Sauna et al., 2004)

### 1.4.2 Lead optimization of flavonoid dimers and previous work

Previous study done by Chan et al. has led to the synthesis of a series of flavonoid dimers, these dimers, were synthesized from a common monomer: apigenin (Figure 1.10). (Chan et al., 2006) The first generation compound was synthesized by linking two apigenin moieties by PEG linkers in various lengths. One of these compounds, 9d (Figure 1.11), with four PEG monomers (n=4) at the linker position; was able to give the greatest modulation activity. (Chan et al., 2006) Characterization of 9d showed that it has the ability to reverse resistance not only PTX but also other anticancer drug such as Doxorubicin and Vincristine in LCC6/MDR cells, having an  $EC_{50}$  of 900nM towards PTX. To understand the binding between 9d and P-gp, ATPase assay has been performed. Upon the binding of 9d to P-gp, ATPase was stimulated, suggesting that binding occurs at substrate-binding site and not on NBD.

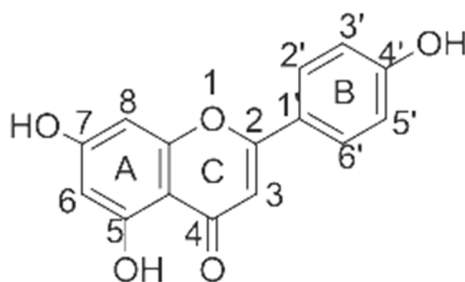


Figure 1.10 Structure of apigenin. (Chan et al., 2006)

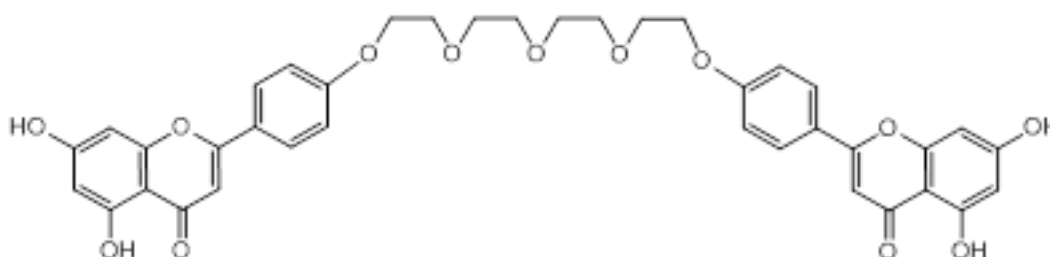


Figure 1.11 Structure of 9d. (Chan et al., 2006)

Because 9d lost its potency below  $5\mu\text{M}$ , a search for a more potent and selective modulator was started. A subsequent library was created in order to cope with such issues. (Chan et al., 2009) P-gp modulator that exerts higher lipophilicity would have a greater chance to become a good modulator. One simple approach to achieve this is by the substitution of all hydroxy groups from parent compound 9d to hydrogen. The resulted compound 1d-(5,7H) (Compound 61) (Figure 1.12) has dramatic improvement on its modulation activity. Compound 61, a 3-fold decrease in  $\text{EC}_{50}$  (360nM) against PTX compared with 9d (900nM). To further potentiate the modulation activity, more derivatives of 61 have been synthesized. The design of new compounds was based on three directions: 1) Replacing various substituent at different position on the A-ring on the flavonoid moiety; 2) changing linker position attached on B-ring and; C) making heterodimers for efficacy comparison. The replacement of different substituent had led to the development of two potent compounds: 1d-(5,7H)-7F (Compound 62) (Figure 1.13) and 1d-(5,7H)-6Me (Compound 69) (Figure 1.14), which were tested *in vivo*. (Chan et al., 2009)

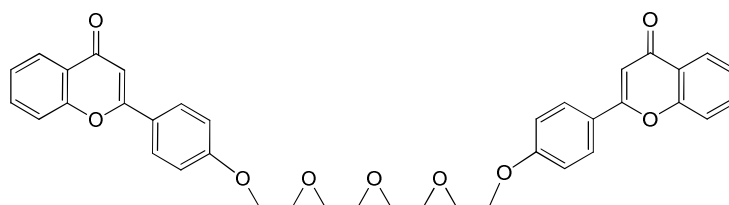


Figure 1.12 Structure of 1d-(5,7H) (Compound 61) (Chan et al., 2006)

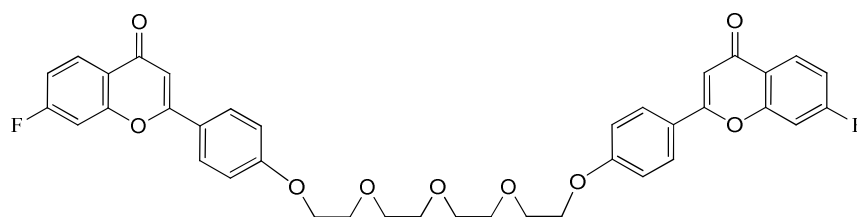


Figure 1.13 Structure of 1d-(5,7H)-7F (Compound 62) (Chan et al., 2009)

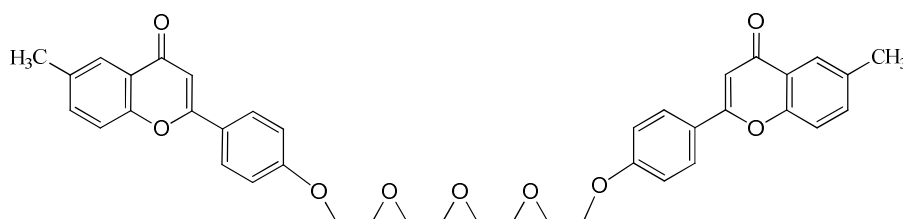


Figure 1.14 Structure of 1d-(5,7H)-6Me(Compound 69) (Chan et al., 2009)

It was found that homodimer is superior over their respective monomers or heterodimers, implying that the binding sites on P-gp was somewhat similar.

## 1.5 Objectives of this project

1. The establishment of a P-gp mediated PTX-resistant human cancer xenograft for the *in vivo* efficacy evaluation of FD18. Two human cancer xenografts, LCC6 and LCC6/MDR, were constructed as a testing platform for the evaluation of treatment efficacy between FD18 and PTX.
2. *In vitro* screening of FD18 derivatives and their *in vivo* characterizations. Preliminary data shown that FD18 is a potent P-gp substrate with acceptable aqueous solubility that may be developed for clinical use, for this, a group of FD18 derivatives have been synthesized and tested for P-gp modulating and *in vivo* toxicity. Toxicity profile of FD18 and other derivatives will be studied by short term repeated dose toxicity study, followed by histopathological evaluations on vital organs. Lead compounds with low toxicity profiles were further tested for their *in vivo* modulation activity in reversing PTX resistance in mice xenograft models.
3. Comparison study between FD18 and its metabolite, FM04, which is a potent P-gp modulator with  $EC_{50}$  at 70nM ( $EC_{50}$  of FD18 = 148 nM). Both FD18 and FM04 will be evaluated for their effect on intracellular DOX accumulation study, P-gp ATPase activity assay, intracellular accumulation and *in vivo* animal efficacy experiments.

## **Chapter 2**

### **Establishment of MDA435/LCC6,**

### **MDA435/LCC6MDR Human Breast Cancer Xenograft**

### **Models**

## 2.1 Introduction

### 2.1.1 The development of animal models for drug screening purposes

Animal models such as insects (e.g. drosophila) (Miles, 2011), aquatic animals (e.g. zebra fish) (Feitsma, 2008; Tobia, 2011) and mammals (e.g. rodents, canine) (Rivera, 2011) have been used in cancer drug discovery research for decades. Among them, mice, were widely employed in antitumor and metastasis studies during drug development.

Early efficacy studies mainly relied on spontaneous rare and difficult-to-reproduce tumor models. This led to the search on reliable animal models since the 1940s. During that period, the National Cancer Institute (NCI) began their work with murine leukemia cell line L1210 to characterize *in vivo* properties such as growth pattern and to study the *in vivo* curability with different anticancer drugs. (Law et.al., 1949) Subsequently, they have developed another ascite tumor model with murine leukemia P388, a leukemia that is more drug sensitive than L1210. The use of these animal models facilitated the cure of childhood leukemia and further expanded the use of animal models in studying cancer therapeutics. (Laszlo, 1995)

In following years, the NCI begun to study series of anticancer drug activities in the previously described ascitic tumor models and later on moved forward to solid tumor with major histotype occurring within the US territory. Subsequent to the discovery of immunodeficient athymic nude mice by SP Flanagan in 1966 (Pantelouris, 1970; Spang-Thomsen, 1976; Mecklenburg, 2005), followed by the successful transplantation of human tumors on nude mice in 1969 by Rygaard and co-workers (Rygaard, 1969), tumor models such as B16 melanoma, human breast carcinoma MX-1, human Lewis Lung

carcinoma and human Colon carcinoma (Suggitt, 2005; Teicher, 2004) had been transplanted for drug screening works in preclinical trials.

### **2.1.2 Human tumor xenograft models and their importance in anticancer drug research**

A xenograft refers to the transplantation of cultured human tumor cells or its explants into immunodeficient mice which do not reject the grafted material. (Brakebusch, 2011) Before the description of the “nude” gene (also known as the Foxn1 gene) by Flanagan in 1966 (Rygaard et al., 1969), Cattanaach’s laboratory published their observations on two hairless mutants and successfully created tumors on these mutants using human cancer cell lines in 1962. (Spang-Thomsen, 1976; Kim, 2004) Thymus dysgenesis and immunodeficient property is the major reason why nude mice can allow foreign tissue to grow on them. (Rygaard, 1969; Pantelouris, 1970; Kindred, 1971; Spang-Thomsen, 1976; Mecklenburg, 2005) Followed by the first human malignant tumor xenograft in athymic nude mice created by Rygaard in 1969 using primary tumor sample from a 74-year-old cancer patient, and the introduction of B16 melanoma xenograft model (Teicher, 2002); the use of nude mice as efficacy evaluation tool in cancer therapeutic research has gained its popularity. Another popular mouse strain for xenograft is the Severe Combined Immunodeficiency (SCID) mice, which is lacking of T and B cells. (Jacob, 2004; Shultz, 2007) Subsequently, the NCI has set up a large panel of xenografts using some major histotype of human cancer (breast, lung and colon cancer) within the US, serving as a screening and filtering system for anticancer drug already. (Suggitt et al., 2005)

Among different xenograft models available, human breast cancer is one of the most difficult tumor to be transplanted and maintained in immunodeficient mice, predominately due to its hormonal dependency, histological changes when xenografted and variable growth kinetics that are different to predict. (Bao, 1994; Kim, 200; Clarke, 1997) Kim and co-workers have conducted a survey with more than 50 current mammary tumor models. Many of these models were derived from the MCF-7 and MCF-10AT systems, possibly owing to its long history and adequate supportive information available for *in vitro* studies. The difficulties of transplantation was partially overcome by co-inoculating with extracellular-like matrix calls the Matrigel (Bao, 1994), Price et. al. also found that injection at the mammary fat pad gives a higher take rate. (Price et al., 1990) However, whether s.c. xenograft is the optimal model for drug screening that can predict clinically relevant response remains debated because tumor xenograft is not the same as human tumor, especially on its histology or growth pattern; for example, human breast cancer tumor xenografts generally have short tumor doubling times ( $T_d$ ) compared cancer patients. (Clarke, 1997) Apart from this, stromal material which is important for metastasis may not be present in xenografts. Other considerations also include the defective immune system and possible overestimation on drug response. (Kim, 2004; Rangarajan, 2003; Brakebusch, 2011; Suggitt, 2005)

Despite the above shortcomings, murine xenograft remains one of the most important tools in primary and secondary drug screening. Fiebig et al. has set up 300 human tumor xenografts and form a strong correlation between *in vivo* drug response and *in vitro* soft agar assay. (Fiebig, 2004) Apart from this, one drug that enter Phase I clinical trial usually have unknown mechanisms and have poorly defined pharmacological properties,

xenograft models at this time could provide readily accessible information such as dose-scheduling, toxic responses from combinative drug test and on efficacies, which facilitates future pharmacokinetics and pharmacodynamics studies. (Kelland, 2004) Human tumor xenografts will remain valuable in primary screen of lead anticancer compounds if careful considerations were given to experimental design, ensuring the molecular drug target is expressed and combining with principles of pharmacokinetics during investigation. (Suggitt, 200; Kelland, 2004)

## 2.2 Materials and methods

### 2.2.1 Cell lines and reagents

MDA-MB-435/LCC6 (LCC6) cell line is an estrogen receptor negative, invasive and metastatic human melanoma cell lines originated from M14 melanoma collected from the pleural effusion of a 31 years old Caucasian woman (previously thought to be derived from the MDA-MB-435 breast carcinoma) (Prasad et al., 2015). Whereas, MDA-MB-435/LCC6MDR (LCC6/MDR) was generated by retroviral transduction of human *mdr1* gene, with a constant overexpression of P-gp transporter. These two cell lines were used in this project (generous gifts from R. Clarke from Georgetown University, Washington D.C., USA). Dulbecco's Modified Eagle Medium (DMEM) was purchased in powdered form and was prepared according to the user manual. Fetal bovine serum (FBS) was purchased from Gibco. Penicillin-streptomycin solution and Trypan blue stain was purchased from HyClone. Paclitaxel (PTX) was purchased from Hubei Yuancheng Saichuang Technology Company Limited. CellTiter 96<sup>®</sup> Aqueous MTS Reagent Powder was purchased from Promega. Cell culture flasks and plates were purchased from Sterilin. Bradford solution was purchased from Bio-rad. MiliQ Water system was purchased from Merck. SuperSignal West Pico Chemiluminescent Substrate and Thermo Scientific Prestained Protein Molecular Weight Marker were purchased from Pierce. 25 gauge, 30 gauge hypodermic needles and 1cc syringe were purchased from Becton, Dickinson and Company. All other chemicals were purchased from Sigma.

### 2.2.2 Cell culturing methods and conditions

LCC6, LCC6/MDR and L929 cells were cultured in supplemented DMEM media with 10% heat inactivated FBS and 100 U/mL penicillin and 100 µg/mL of streptomycin. All cell lines were maintained at 37 °C in a humidified atmosphere with 5% CO<sub>2</sub>. The LCC6 cell lines were split constantly after a confluent monolayer has been formed.

### 2.2.3 Cell counting and trypan blue exclusion assay for viable cells

Trypsinized and PBS-washed cells from previous section were being resuspended in 1mL serum-free DMEM and pending for trypan blue exclusion assay to check the cells viabilities. Trypan blue is a diazo stain which can only be absorbed through the cell membrane by a dead cell; therefore giving these cells a distinct blue color thus excluded them from living cells. Trypan blue stain was diluted to 0.4% (w/v) with PBS and the assay performed by the addition of 50 µL stain to an equal volume of 5-fold diluted cell suspension, a development time of five minutes was allowed before loading the sample to a grid haemocytometer for cell counting. The total number of cells (cells/mL) from a sample can be mathematically computed by using the following equations.

$$\text{no. of cell per mL} = \frac{\text{no. of counted cells}}{\text{Counted Squares}} \times \text{Dilution factor} \times 10^4$$

Equation 2.1 Mathematical equation for the calculation of cell number

$$\% \text{ of viable cells} = \frac{\text{no. of unstained cells}}{\text{Total number of counted cells}} \times 100$$

Equation 2.2 Mathematical equation for calculating the percentage of viable cells

$$\text{Total number of cells} = \text{no. of cells per mL} \times \% \text{ of viable cells}$$

Equation 2.3 Mathematical equation for calculating the total number of cells within a sample

#### **2.2.4 Preparation of Drug and flavonoid dimers for cell proliferation assay**

PTX, Verapamil, PSC833 and all flavonoid dimers were dissolved in pure DMSO at a final concentration of 10 mM. Dilutions were prepared according to subsequent assay conditions and being adjusted to a final DMSO concentration of 0.05%. Doxorubicin (DOX) was dissolved in water at 4 mM.

#### **2.2.5 Cell proliferation assay (MTS assay)**

LCC6 or LCC6/MDR cells survival was checked with trypan blue exclusion assay and then seeded onto a 96-well plate (4000 cells/well) for 24-hour at 37 °C, 5% CO<sub>2</sub> in 75 µL DMEM (10% FBS, 100 U/mL penicillin and 100 µg/mL of streptomycin). Anticancer drug, Paclitaxel, was added and serial dilution in concentrations of 500, 250, 125, 62.5, 37.125, 15.625, 7.8125 and 0 nM for a final volume of 200 µL. The reaction system was then incubated at 37 °C, 5% CO<sub>2</sub> for 72-hour before the addition of MTS:PMS reagent mixture. After the incubation period, medium-drug mixture was removed from each well by vacuum suction and replaced with 100µL of unsupplied DMEM. The CellTiter 96<sup>®</sup> AQueous MTS Assay was used to measure the cell proliferation according to the manufacturer's instructions. MTS at 2mg/mL and PMS at 0.92 mg/mL were freshly prepared as a mixture in a ratio of 50:1, the mixture was then added into each well at 10 µL. The plate was again incubated at complete darkness for 2-hour at 37 °C. Cell proliferation results were checked at 490 nM and the optical density data obtained by

using an absorbance reader (Bio-Rad). Data was subsequently being converted to percentage of survival against log concentration of PTX in a sigmoidal dose response curve for finding the  $IC_{50}$  towards different modulators. (Prism 4.0) All experiments were performed in triplicate and repeated at least thrice and the results were represented as mean  $\pm$  standard error of mean.

### **2.2.6 Animal husbandry**

Balb/c nu/nu female athymic mice at 4 to 6-week old, weighing between 15-23 g, were purchased from the Laboratory Animal Unit, The University of Hong Kong, Animal and Plant Care Facilities, University of Science and Technology and Hong Kong, The Laboratory Animal Services Centre, The Chinese University of Hong Kong, Laboratory Animal Unit, The University of Hong Kong and Vital River Laboratories, Beijing, P.R.C. Animals were quarantined for 7 days before housing in a germ-free environment with a 12 hours of light and 12 hours of dark cycle. All consumables including food and water were sterilized prior for supply. Investigations were performed under the Cap 340 Animal License from the Department of Health (HKSAR Government), ethical approval from Animals Ethics Sub-committee of The Hong Kong Polytechnic University as well as Laboratory Animal Ethics Committee of The Hong Kong Polytechnic University Shenzhen Research Institute.

### **2.2.7 Establishment of LCC6 and LCC6/MDR Ascitic Model**

To allow adaptation of cultured cells in animal host, ascitic models were set up as follows: LCC6 and LCC6/MDR cells were harvested individually from monolayer culture when they reach confluences. Cells within the monolayer culture were first being trypsinized

and then centrifuged at 250 g for five minutes to collect cell pellet, the cell pellet is then being washed by warmed PBS; the above procedures were repeated thrice. Washed cells were then being resuspended in 1mL serum-free DMEM and trypan blue exclusion was performed by using equal volume of trypan blue stain to 50  $\mu$ L of 5-fold diluted cell suspension for viability check and cell counting. Cell counting was done by using a haemocytometer and the concentration of cell (cells/mL) was calculated by the equations listed in section 2.2.3.

Dilutions with cell density of  $1 \times 10^7$  cells/mL were prepared by resuspending the required volume of cells in 200  $\mu$ L of phosphate buffered saline (PBS). It was then being injected intraperitoneally (i.p.) to each quarantined Balb/c nu/nu athymic mice aged 5 to 7-week old at different concentrations of 0.8 to  $3.6 \times 10^7$  cells/injection. When ascite was being formed, the abdomen of the mouse will be swollen and a subcutaneous tumor would usually being form near the injection site. To maintain the ascite model, 50 to 100  $\mu$ L of ascite will be aspirated from the mouse and then inoculated into a new host. New ascitic cell model should be set up when ascitic passage reached its tenth.

### **2.2.8 Confirmation of PTX resistance in ascitic cells by cell proliferation assay**

Aspirated ascites of LCC6/MDR and LCC6 from section 2.2.7 was cultured in supplemented DMEM media with 10% heat inactivated FBS and 100 U/mL penicillin and 100  $\mu$ g/mL of streptomycin. After one day of cell seeding, cell culture media was removed carefully and the anchored cells were washed gently by warmed PBS to get rid of normal cells and red blood cells. Fresh supplemented DMEM media is being replaced into the washed cells to allow the formation of monolayer. When a confluence was reached, cells

were split according to section 2.2.2. Cell proliferation assay can be carried out after the third passage according to section 2.2.5.

### **2.2.9 Construction of LCC6 and LCC6/MDR xenografts from ascitic fluid**

Ascitic LCC6 and LCC6MDR cells from section 2.2.7 were maintained peritoneally in nude mice and being aspirated by a 25 gauge hypodermic injection needle during passage. Upon reaching its third passage (P<sub>3</sub>), 100 $\mu$ L of PBS diluted aspirated ascitic fluid (final concentration  $1.5 \times 10^6$  cells LCC6 or LCC6/MDR cells) is being injected subcutaneously into the rear flank of another nude mouse. A solid tumor will begin to form in approximately two weeks. When a solid tumor is formed and reached the size of 300-400 mm<sup>3</sup>, the mouse will be euthanized and surgically remove the tumor. The excised tumor will be separated into halves, followed by the removal of necrotic tissues from the core; tumor chunks of approximately 1mm<sup>3</sup> will be prepared and being transplanted subcutaneously into another nude mice. The subcutaneous xenograft will be ready for use after the third passage.

### **2.2.10 Maintenance of LCC6 and LCC6/MDR subcutaneous xenograft model**

Subsequent solid tumor model will be maintained by using a solid tumor previously generated by the injection of ascite cells harvested. The advantage of using such method is that tumor raised would have a uniformed shape with a predictable growth rate, in addition, tumor induction rate would also be enhanced. When a solid tumor is formed and reached the size of 300-400 mm<sup>3</sup>, the mouse will be euthanized and surgically remove the tumor. The excised tumor will be separated into halves, followed by the removal of necrotic tissues from the core; tumor chunks of approximately 1mm<sup>3</sup> will be prepared and

being transplanted subcutaneously into another nude mice. Animals will be monitored for their mortalities, appetites, weight changes and activity levels on every other day excluding weekends. In case of weight loss exceeding 15% from its start off body weight for three consecutive days, such mouse will be euthanized by CO<sub>2</sub> euthanasia followed by cervical dislocation.

### **2.2.11 Sample preparation for P-gp level analysis on LCC6 and LCC6/MDR ascitic cells and its solid tumor**

LCC6 or LCC6/MDR cells obtained from monolayer culture and ascitic fluid were centrifuged at 250g for five minutes to obtain cell pellets. For LCC6 and LCC6/MDR tumors, each tumor was snap frozen in liquid nitrogen and beaten by a hammer to create chunks; 0.1 g of tumor chunks was used. Cell lysis buffer was prepared by the addition of NP40 lysis buffer, 50x protease inhibitor cocktail and 50x phenylmethylsulfonyl fluoride (PMSF) to a final concentration of 1x. To each sample tubes, 200  $\mu$ L of cell lysis buffer was added, tumor samples was further mortared by a glass rod and all samples were vortexed afterwards to a suspension form and being incubated in ice for 30 minutes. Followed by the incubation period, samples were centrifuged at 500g for five minutes for the removal of cell debris; supernatants (lysate) were used and were transferred to a new sample tube. To check the total protein concentration within each sample, a portion (10  $\mu$ L) of cell lysate was being mixed into 990  $\mu$ L miliQ water for create a 100-fold diluent, 40 $\mu$ L of such diluent was then mixed with 160  $\mu$ L of Bradford solution followed by the measurement of optical absorbance at 595 nm and the protein concentration was expressed in  $\mu$ g per milliliter ( $\mu$ g/mL). The samples were subjected to western blot analysis.

### 2.2.12 P-gp expression analysis by Western Blotting

Cell lysates were loaded at 30 $\mu$ g per sample and resolved in a 9% sodium dodecyl sulfate-polyacrylamide gel electrophoresis (SDS-PAGE) and subsequently electrotransferred to a polyvinylidene fluoride (PVDF) membrane buffered in transfer buffer (25 mM Tris, 193 nM Glycine, 10% methanol) at 125V for 1 hour at 4°C. After electrical transfer, the membrane is blocked with 5% fat free milk in tween 20 tris-buffered saline (TTBS) at room temperature for 1 hour, followed by washing with TTBS at room temperature for 3 cycles at 10-minute each with gentle agitation. The membrane was then incubated with either 1:500 rabbit anti-Pgp antibody or 1:10000 mouse anti- $\beta$ -actin antibody overnight at 4°C with gentle agitation followed by washing with TTBS at room temperature for 3 cycles at 10 minutes each. Subsequently, the membrane was incubated with a secondary antibody, either 1:3000 horseradish peroxidase-conjugated goat anti-mouse antibody or 1:300 horseradish peroxidase-conjugated goat anti-rabbit antibody at room temperature for 1 hour with gentle agitation. After the secondary antibodies incubation, the membrane is washed 3 times at 10 minutes each at room temperature by TTBS. Finally, chemiluminescent substrates were added to the membrane in 1:1 manner (stable peroxide:lumini enhancer) and the western signal was detected by Bio-Rad ChemiDoc™ XRS<sup>+</sup> system.

### 2.2.13 Preparation of Drugs for PTX efficacy studies

PTX was prepared at 40 mg/mL in 50% (v/v) ethanol, 50% (v/v) Cremophor EL as follow. First, dissolve 40 mg of PTX powder in 500  $\mu$ L absolute ethanol. The suspension is then placed in 80 °C water bath for 3-minute, with subsequent agitation by a vortex until a

clear drug solution is formed. Equal volume of Cremophor EL is then added into the drug solution, vortex until it became clear. This stock solution is stable for over one month at room temperature. Prior to injection, stock solution is being diluted 1:10 by normal saline. Diluted drug solution should be consumed within 15-minute to avoid drug precipitation. Solvent of PTX is being prepared by mixing 5% (v/v) ethanol, 5% (v/v) Cremophor EL and 95% (v/v) normal saline in final volume of 1 mL.

#### **2.2.14 *In vivo* reversal activities on LCC6 and LCC6/MDR xenografts towards PTX**

Female Balb/c nu/nu mice xenografted with LCC6 or LCC6/MDR were randomized into six to eight per group for efficacy studies. Treatment began when tumor volume reached 100 to 200 mm<sup>3</sup>. Animals were divided into two treatment groups: 1) Vehicle control and 2) PTX. All animals were first administered with dimethyl sulfoxide (DMSO) intraperitoneally (i.p.) at 0-minute with an injection volume equivalent to 45 mg/kg of our flavonoid modulators, followed by an intravenous (i.v.) injection of PTX at 12 mg/kg or its solvent at equivalent volume at 60-minute on every other day in total of 4 times for 2 cycles [(q.o.d. x 4) x 2] with a 4-day drug free recovery period in between. To evaluate the therapeutic efficacy, tumor volumes, relative body weight changes, and survivals were monitored. Tumor volume and relative body weight change were being calculated by Equation 2.4 and 2.5:

$$Tumor\ volume(mm^3) = \frac{l \times w^2}{2}$$

Where,  $l$  = Longest diameter of the tumor;  $w$  = Diameter perpendicular to  $l$

Equation 2.4 Mathematical equation for the calculation of tumor volume

$$\text{Relative Body Weight Change(\%)} = \left[ 1 - \frac{\text{Body weight(Day 0)} - \text{Body weight(Treatment Day)}}{\text{Body weight (Day 0)}} \right] \times 100\%$$

Equation 2.5 Mathematical equation for the calculation of relative body weight change.

Treatment induced toxicity were defined as toxicity deaths or weight loss >15%. Treatment efficacies were analyzed in terms of % of tumor inhibition (T-C value, % T-C), and tumor doubling time ( $T_d$ ). The data were further analyzed statistically by student's t-test. The mathematical equations for %T-C and  $T_d$  were listed below:(Bissery 1991, Clarke 1997)

$$\% T - C = \left( 1 - \frac{\text{Tumor Volume}_{(Treated)}}{\text{Tumor volume}_{(Control)}} \right) \times 100 \%$$

Where,  $\text{Tumor Volume}_{(Treated)}$  = Averaged tumor volume from drug treatment group on termination day;  $\text{Tumor volume}_{(Control)}$  = Averaged tumor volume from solvent control group on termination day

Equation 2.6 Mathematical equations for the calculation of percentage of tumor inhibition (%T-C)

$$\text{Tumor doubling time}(T_d) = (t_2 - t_1) \frac{\log(2)}{\log(\text{tumor vlume } 2) - \log(\text{tumor volume } 1)}$$

Where,  $t_2$  = Final day;  $t_1$  = Initial day;  $\text{tumor volume } 2$  = tumor volume at  $t_2$ ;  
 $\text{tumor volume } 1$  = tumor volume at  $t_1$

Equation 2.7 Mathematical equations for the calculation of tumor doubling time ( $T_d$ )

## **2.3 Results**

### **2.3.1 Establishment of LCC6 and LCC6/MDR Ascitic Model**

Various concentrations of MDA435/LCC6 or MDA435/LCC6MDR cell ( $0.08 - 2 \times 10^8$ ) has been injected to female Balb/c nude mice to investigate the probability for the induction of ascite as described in section 2.2.7. Animals received either cell injection intraperitoneally has an uptake rate greater than ninety-five percent. Cell concentration per animal, ascite formation and their survival status were summarized in Table 2.1.

Table 2.1 Summary of ascitic model with LCC6 and LCC6/MDR cell line.

Cell line	Number of passage (n=1, unless stated)	Number of Cell injected	Ascite formation	Days of death post passage
MDA435/LCC6	P <sub>0</sub> *	0.8 x 10 <sup>7</sup>	Yes	ND <sup>#</sup>
	P <sub>0</sub> *	1.5 x 10 <sup>7</sup>	Yes	ND <sup>#</sup>
	P <sub>1</sub>	~ 1 x 10 <sup>7</sup>	Yes	ND <sup>#</sup>
	P <sub>2</sub>	~ 1 x 10 <sup>7</sup>	Yes	ND <sup>#</sup>
	P <sub>3</sub>	~ 1 x 10 <sup>7</sup>	Yes	ND <sup>#</sup>
MDA435/LCC6MDR	P <sub>0</sub> *	0.1 x 10 <sup>7</sup>	Yes	ND <sup>#</sup>
	P <sub>0</sub> * (n=2)	0.5 x 10 <sup>7</sup>	Yes	ND <sup>#</sup>
	P <sub>0</sub> *	1 x 10 <sup>7</sup>	Yes	ND <sup>#</sup>
	P <sub>1</sub>	1.5 x 10 <sup>7</sup>	Yes	64
	P <sub>2</sub> (n=2)	3x 10 <sup>7</sup>	Yes	34 and 38
	P <sub>3</sub>	3.6 x 10 <sup>7</sup>	Yes	46
	P <sub>4</sub>	2.3 x 10 <sup>8</sup>	Yes	31
	P <sub>5</sub>	3.8 x 10 <sup>7</sup>	Yes	33
P <sub>6</sub>	2 x 10 <sup>7</sup>	Yes	40	

\* P<sub>0</sub>; Passage from cell culture to animal.

# ND = Not determined.

Various cell numbers of LCC6 and LCC6/MDR were injected intraperitoneally in 5 – 7 weeks old female athymic nude mice. Time was allowed for the development of ascites and was subsequently aspirated for the next passage for the maintenance of model and construction of solid tumor xenografts.

### 2.3.2 Confirmation of PTX resistance in ascitic LCC6/MDR cancer cells

To confirm the resistance towards PTX in ascitic cells prior to the construction of the mouse xenograft, LCC6/MDR ascite was aspirated from the animal and transferred back into cell medium for MTS assays according to section 2.2.9. The  $IC_{50}$  obtained towards PTX in ascitic cell was  $139 \pm 2.1$  nM versus Paclitaxel + DMSO control  $115.8 \pm 19.8$  nM (mean  $\pm$  SEM, Figure 2.1), which was comparable to the  $IC_{50}$  from cultured cells (148nM).

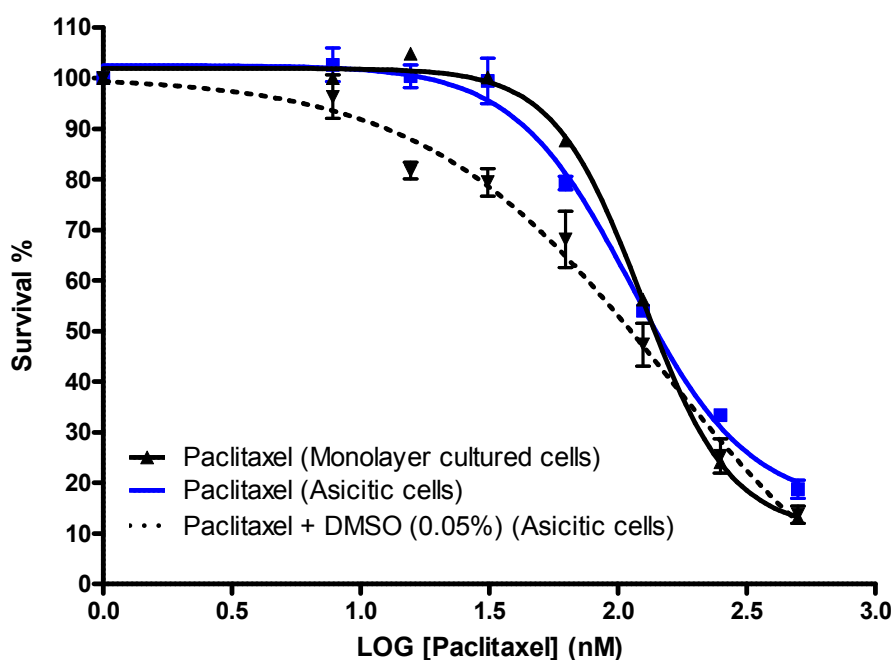


Figure 2.1 Confirmation of PTX resistance in ascitic LCC6/MDR cancer cells. Aspirated ascites of LCC6/MDR was cultured in cell medium. After the third passage, cytotoxicity assay (n=4) were performed with various concentrations of PTX and modulator vehicle. LCC6/MDR cells was seeded at 2000 cell per well, PTX or DMSO were added 24 hours after in a final volume of 200  $\mu$ L with subsequent incubation of 72 hours. To measure the cell proliferation, the CellTiter 96® AQueous MTS Assay was employed.  $IC_{50}$  values were calculated from the dose-response curves of MTS assays. All experiments were performed in quadruplicate and the results were presented in mean  $\pm$  SEM.

### **2.3.3 P-glycoprotein (P-gp) expression analysis on LCC6 and LCC6/MDR ascitic cells and their solid tumors**

P-gp expression level was confirmed by using western blotting. Lysates of LCC6 and LCC6/MDR cells, ascitic fluids and tumors were collected and prepared for the analysis. No detectable P-gp was found in wild type or ascite LCC6 cells. In contrast, higher level of P-gp was observed in MDR1 samples. (Figure 2.2A and B)

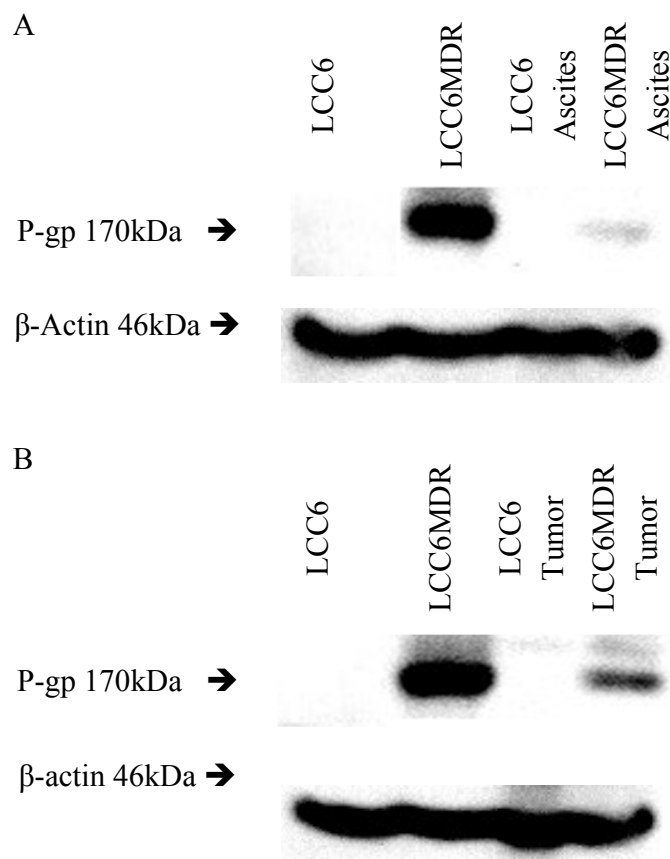
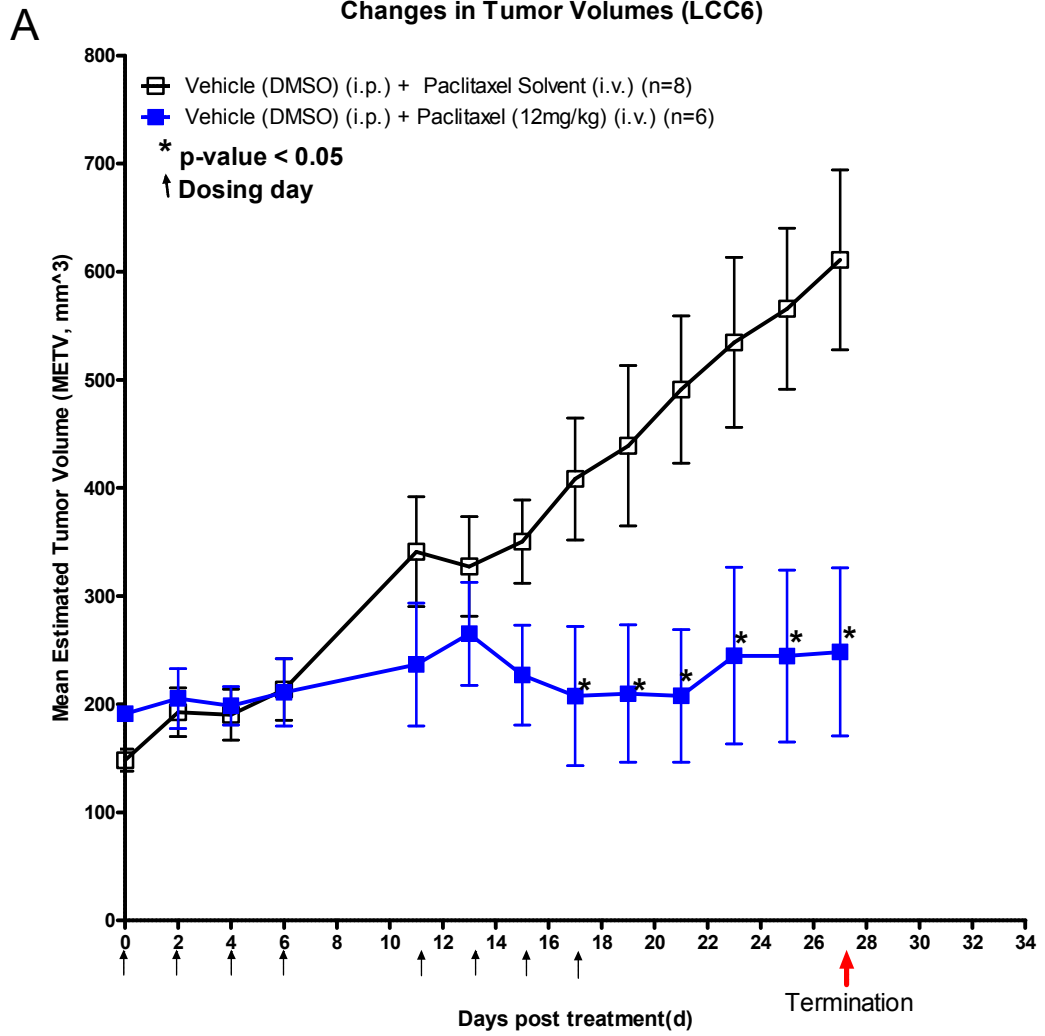


Figure 2.2 P-glycoprotein (P-gp) expression analyses by western blotting. A) P-gp levels comparing between cell lysates from monolayer culture and lysates obtained from peritoneal ascites. B) P-gp levels comparing between cell lysates from monolayer culture and lysates obtained from subcutaneous tumor. (Loading amount: 30 $\mu$ g, rabbit anti-P-gp antibody: 1:500, mouse anti-  $\beta$ -actin antibody: 1:10000)

### 2.3.4 Efficacy of LCC6 and LCC6/MDR tumor model towards PTX treatment

We determined a dose regimen that is safe and produce no or modest antitumor effects when PTX was used alone. Female athymic nude mice implanted with LCC6 or LCC6/MDR tumor xenografts were randomized for the assessment of PTX efficacy according to section 2.2.14.

Twelve mg/kg PTX resulted in a maintenance effects to LCC6 tumors (Figure 2.3A) from  $190 \pm 7 \text{ mm}^3$  on Day 0 to  $248 \pm 78 \text{ mm}^3$  on Day 27. On the other hand, 4-fold increase in average tumor size was observed in solvent control group. In LCC6/MDR xenografts, tumors from both treated and control group have similar growth rate. No therapeutic response was found in PTX-treated group. Tumor inhibition (%T-C) for sensitive and resistant xenografts were 49% and 16% respectively. (Figure 3.3B) We can conclude that intravenous injection of Paclitaxel at 12 mg/kg resulted in moderate efficacy in sensitive model and no effects towards treating resistant tumors. In addition, no animal deaths were observed during and post treatment, further suggesting the present treatment design is safe and suitable for further efficacy study.



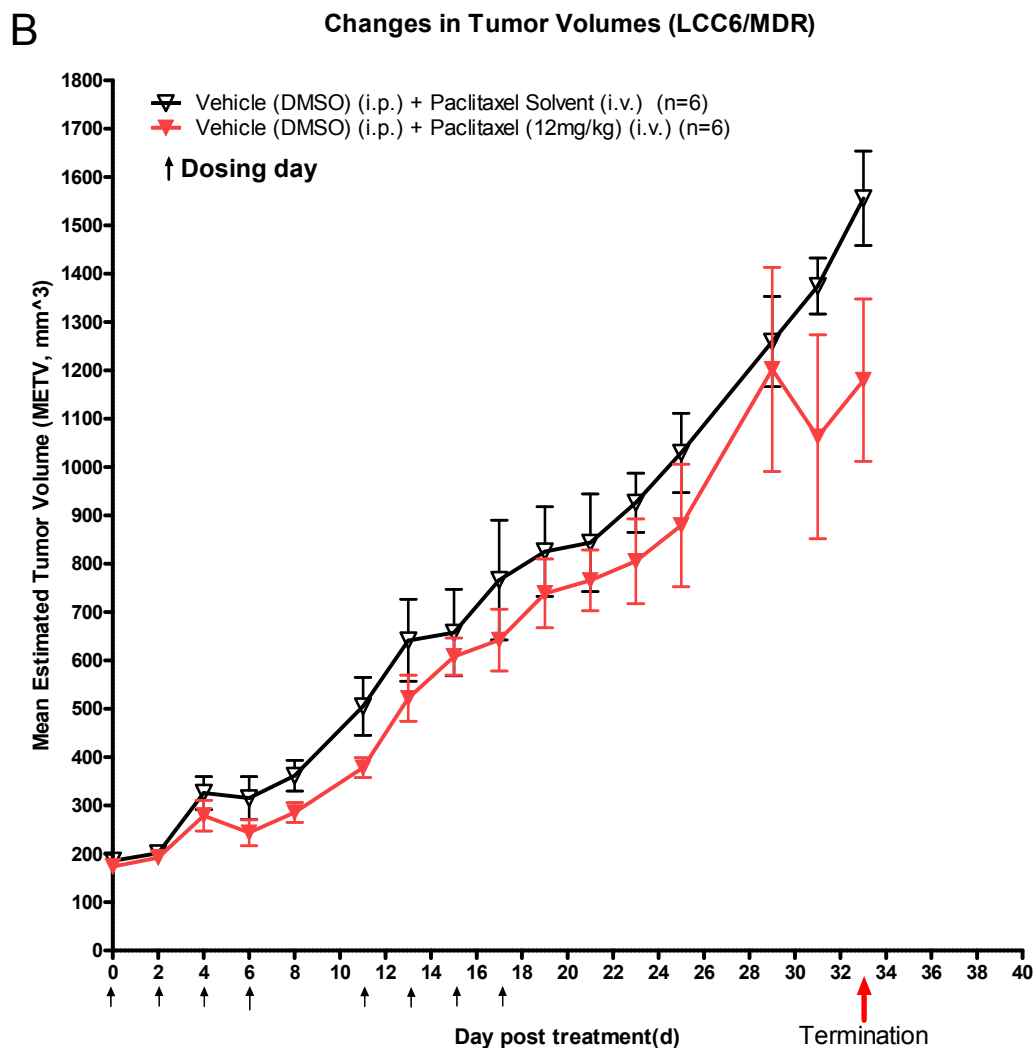


Figure 2.3 Tumor response curve for LCC6 and LCC6/MDR human cancer xenograft. A) LCC6 xenografts were treated with DMSO (Empty Square) or DMSO + PTX (12 mg/kg) (Filled Square). B) LCC6/MDR xenografts were treated with DMSO (Empty Triangle) or DMSO + PTX (12 mg/kg) (Filled Triangle). All animals were treated under a schedule of q.o.d x 4 for two cycles with a four days drug free holiday. Tumor volumes were measured on treatment days and animals were monitored for any abnormal behaviors or deaths. Statistical analysis was performed by one-way-ANOVA. (\* $p < 0.05$ ).

## 2.4 Discussion

In this chapter, two human tumor xenografts LCC6 and LCC6/MDR have been developed for subsequent *in vivo* efficacy evaluation between PTX and synthetic flavonoid dimers. Validations of model P-gp resistances have been conducted to confirm their usefulness and consistencies.

In previous study done by the laboratory of R. Clarke, LCC6 and LCC6/MDR ascite models were highly reproducible, with an induction rate of 100% and a median survival at 30 days. Apart from this, the origin of these ascitic cells as human cells was confirmed by karyotyping analysis; none of these cells have been contaminated with other murine cells. (Leonessa et.al., 1996) We have reproduced both ascite models through the injection of monolayer culture into mice peritoneum. The only difference was a prolonged survival (40 days) in the MDR model, even after an injection of a large amount of cells ( $>10^7$ ). Such phenomenon was possibly due to strain differences between Balb/c nu/nu mice (inbred) in here and NCr nu/nu mice (Outbreed) in Clarke's group, as well as changes in husbandry condition. (Leonessa et.al., 1996)

MTS assay and western blotting analysis were performed to see if aspirated ascitic cells were capable of conferring PTX resistance and maintaining the expression of P-gp. Since ascitic fluid is a mixture of blood cells, normal epithelial cells and malignant cells, therefore, it was essential to isolate targeted malignant cells from other unwanted cells by growing back into growth medium before these *in vitro* assays. (Easty et. al., 1957; Leonessa et.al., 1996) Results from cytotoxicity assay suggested these isolated ascitic LCC6/MDR cells can maintain their resistance toward PTX with an  $IC_{50}$  result of 139 nM,

comparable to previous data. (Chan et al., 2006) Notable decrease of P-gp level from ascitic LCC6/MDR cells was observed and expected possibly due to the samples were freshly obtained from animal without prior isolation *in vitro*. As mentioned previously, ascite is a mixture of cells, the presence of other normal cells would likely dilute the population of MDR1 overexpressed malignant cells from the loaded sample. Nevertheless, enrichment of P-gp from solid tumor sample was monitored, indicating the expression of P-gp did not forfeit during animal passage and the model is valid to be utilized.

Paclitaxel was chosen in this project because it is an effective chemotherapeutic agent for treating various human solid tumors and it is a substrate for P-gp transporter. (Rowinsky and Donehower, 1993, Jang et al., 2001) From the drug development's point of view, safety is the most important issue, therefore, an effective yet least toxic dose and schedule is preferred. As the maximum tolerated dose (MTD) of a single intravenous injection on PTX with Cremophor EL formulation was found to be at 20 mg/kg, for repeated dosage, there is a need to adjust either the dose concentration or the treatment frequency to avoid possible toxicity. (Kim et al., 2001) With reference to a few studies working on P-gp modulators with repeated treatments of PTX, the dose regimen was compromised at 12 mg/kg for 8 times in total with a drug free recovery period as a preliminary scheme. (Dantzig, 1996, Jin, 2005, Mistry, 2001, Rose, 1992) Preliminary antitumor study demonstrated that the present dose regimen design was efficacious only in LCC6 xenografts and were safe for all animals. Further investigation of antitumor effects in combinatory treatments with PTX will be performed. Optimization of treatment regimens and dosing frequency will be performed and discussed in chapter 3.

## **Chapter 3**

# **Pharmacokinetics, toxicity and efficacy studies of FD18 and its derivatives**

### 3.1 Introduction

Due to previous successful approach in synthesizing potent flavonoid dimers 9d then 61, 62 and 69. (Table 4.1; compound 2 - 4) More derivatives with different linker positions has been synthesized for characterizations. The amendment of linker positions from C4' to C2' and C3' on B-ring resulted in a lowered potency, suggesting linker at C4' position is still being optimal. Further to this, another batch of compounds with linkers attached other than C4', 2' and 3' position were synthesized and will be tested in follow section within this chapter.

Compounds those were highly hydrophobic often associated with poor aqueous solubility. Despite of their brilliant P-gp modulation feature, were difficult to proceed further. Such phenomenon has been observed with preliminary *in vivo* dose finding assays, the injection of 1d-(5,7H) (Compound 61), 1d-(5,7H)-7F (Compound 62) or 1d-(5,7H)-6Me (Compound 69) have resulted in precipitation within the peritoneal cavities of treated animals (data not shown). This urged the development of compounds that possess a higher aqueous solubility yet not losing their potencies. With the use of compound 61 as parent compound, subsequent introduction of an amine group within the PEG linker allowed the creation of another new library with series of amine linked dimers. (Chan et al., 2012) *In vitro* cytotoxicity screening suggested that 1d-(5,7H)-NBn (FD18) and its parent 1d-(5,7H)-NH (Table 4.1; compound 13 and 14) were the best compounds from this series. These compounds have improved hydrophilicity and having even higher reversing activities. 1d-(5,7H)-NH was being abandoned eventually as for its cell killing effects in normal fibroblasts. An extensive mechanistic study has been done to understand the working mechanism of FD18. Findings suggested that FD18 behave at a competitive

inhibitor to other P-gp substrates and binding directly to the substrate binding site. The solubility and potency of FD18 allowed it to take one step further for *in vivo* characterization. In this chapter, *in vivo* characterization of FD18 and its derivatives will be performed.

## 3.2 Materials and methods

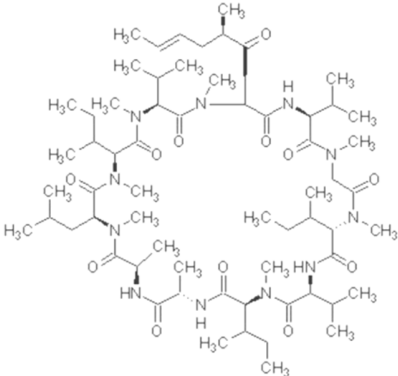
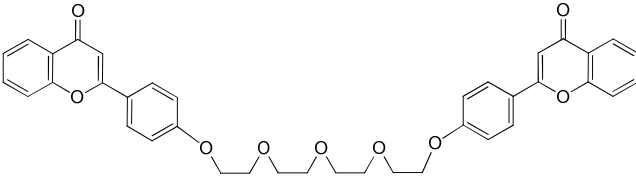
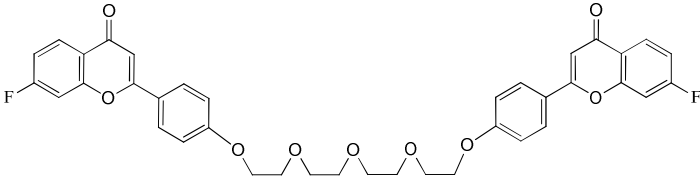
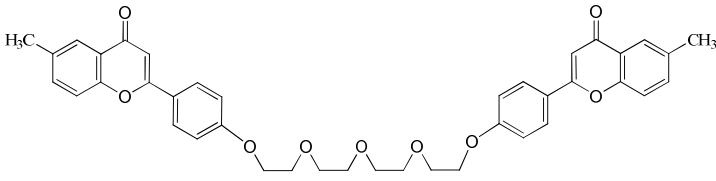
### 3.2.1 *In vitro* P-gp reversing activities towards PTX

A few flavonoid homodimers were synthesized and being listed in Table 3.1. To measure their reversing activities in LCC6/MDR cells towards PTX, MTS assay was performed as follow.

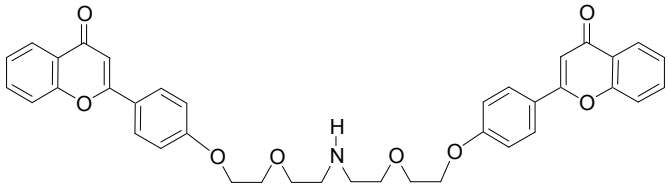
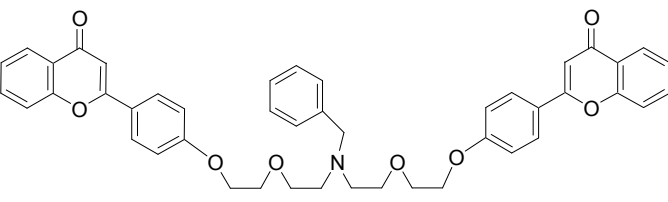
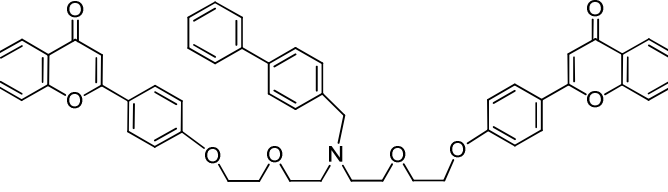
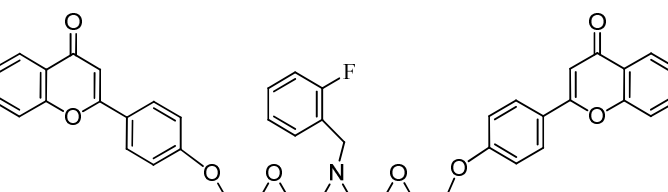
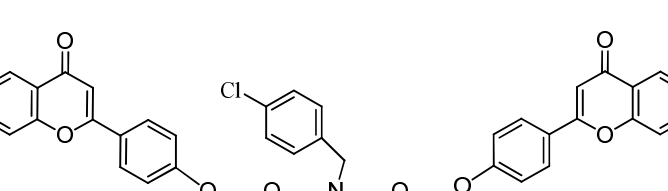
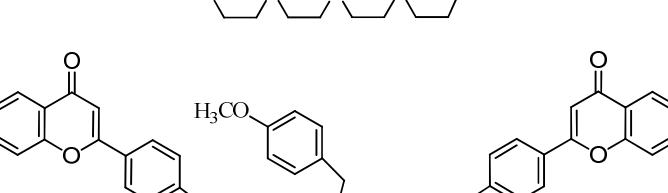
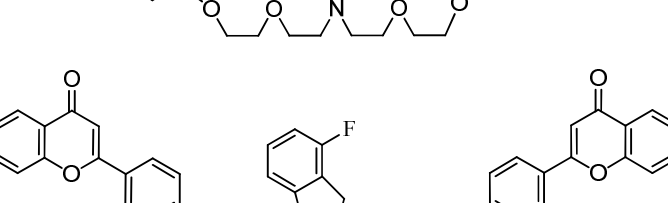
LCC6 or LCC6/MDR cells survival was checked with trypan blue exclusion assay and then seeded onto a 96-well plate (4000 cells/well) for 24-hour at 37 °C, 5% CO<sub>2</sub> in 75 µL DMEM (10% FBS, 100 U/mL penicillin and 100 µg/mL of streptomycin). Anticancer drug, Paclitaxel, was added and serial dilution in concentrations of 500, 250, 125, 62.5, 37.125, 15.625, 7.8125 and 0 nM for a final volume of 200 µL. The reaction system was then incubated at 37 °C, 5% CO<sub>2</sub> for 72-hour before the addition of MTS:PMS reagent mixture. After the incubation period, medium-drug mixture was removed from each well by vacuum suction and replaced with 100µL of unsupplied DMEM. The CellTiter 96® AQueous MTS Assay was used to measure the cell proliferation according to the manufacturer's instructions. MTS at 2mg/mL and PMS at 0.92 mg/mL were freshly prepared as a mixture in a ratio of 50:1, the mixture was then added into each well at 10 µL. The plate was again incubated at complete darkness for 2-hour at 37 °C. Cell proliferation results were checked at 490 nM and the optical density data obtained by

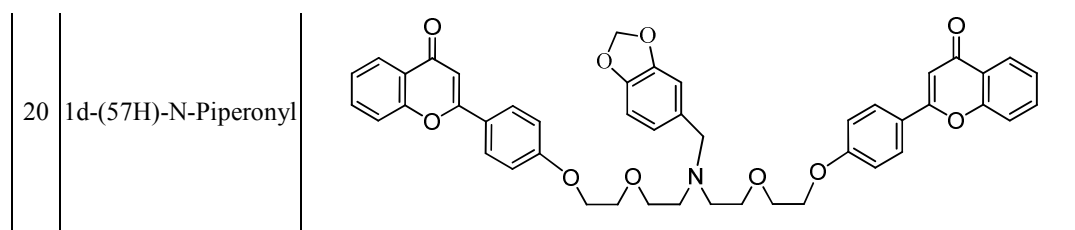
using an absorbance reader (Bio-Rad). Data was subsequently being converted to percentage of survival against log concentration of PTX in a sigmoidal dose response curve for finding the  $IC_{50}$  and  $EC_{50}$  (Half maximal effective concentration; a concentration for each modulator required to demonstrate its half maximal activity) that towards different modulators. (Prism 4.0) All experiments were performed in triplicate and repeated at least thrice and the results were represented as mean  $\pm$  standard error of mean.

Table 3.1 Structures of modulators.

ID	Compound	Structures
1	PSC 833	
2	1d-(57H) (61) #	
3	1d-(57H)-7F (62) #	
4	1d-(57H)-6Me (69) #	

5	2'-1d-(57H) #	
6	3-1d-(57H) #	
7	3'-1d-(57H) #	
8	5-1d-(57H)	
9	7-1d-(57H)	
10	1d-(5,7H)-linker 2NMe	
11	1d-(57H)-linker NMs	
12	1d-(57H)-linker NTs	

13	1d-(57H)-NH <sup>^§</sup>	
14	1d-(57H)-N-Bn <sup>^§</sup>	
15	1d-(57H)-N-(4PhBn)	
16	1d-(57H)-N-(2FBn)	
17	1d-(5,7H)-N-(4ClBn)	
18	1d-(57H)-N-(4MeOBn)	
19	1d(5,7H)-N-(2-,6-diFBn)	



Three series of flavonoid dimers have been synthesized. Compound 3 – 9 were synthesized based on compound 2, differed in linker positions. Compound 10 – 12 and 14 were synthesized based on 13, with an amine linker and various functional groups substituted. Compound 15 – 20 were synthesized by adding different functional group from their parent compound, 14. (Published data: <sup>#</sup>(Chan et al., 2009), <sup>^</sup>(Chan et al., 2012), <sup>§</sup>(Yan et al., 2016))

### 3.2.2 Cytotoxicities of flavonoid modulators

*In vitro* toxicity of flavonoid dimers were determined by using L929 murine fibroblast cell line. Cells were first seeded in a 96-well plate with 100  $\mu$ L growth medium for 24-hours at a cell concentration of 10000 cells/well. A concentration range of dimers were added into the cell suspension with a final concentration of 200  $\mu$ L. To determine the percentage of survivors, MTS assay was carried out as described in Chapter 2 at section 2.2.5.

### 3.2.3 Drug preparation for animal experiments

PTX was prepared at 40 mg/mL in 50% (v/v) ethanol, 50% (v/v) Cremophor EL as follow. First, dissolve 40 mg of PTX powder in 500  $\mu$ L absolute ethanol. The suspension is then placed in 80 °C water bath for 3-minute, with subsequent agitation by a vortex until a clear drug solution is formed. Equal volume of Cremophor EL is then added into the drug solution, vortex until it became clear. This stock solution is stable for over one month at room temperature. Prior to injection, stock solution is being diluted 1:10 by normal saline. Diluted drug solution should be consumed within 15-minute to avoid drug precipitation.

Solvent of PTX is being prepared by mixing 5% (v/v) ethanol, 5% (v/v) Cremophor EL and 95% (v/v) normal saline in final volume of 1 mL. PSC833 solution is made up of cremophor:ethanol (65:35 v/v) and formulated at 10 mg/mL. Stock solution of flavonoid dimers 1d-(5,7H)-N-BnHCl (FD18), 1d-(5,7H)-N-(4MeOBn)HCl (4MeO), 1d-(5,7H)-N-(4ClBn)HCl (4Cl), 1d-(5,7H)-N-2,6-diFBn (diF), 1d-(5,7H)-N-4PhBnHCl (4Ph), 1d-(5,7H)-N-2FBnHCl (2F) and 1d-(5,7H)-N-Piperronyl (N-Pip) stock solutions were formulated in 13.6% cremophor EL, 13.6% Ethanol and 72.8% physiological saline (0.9%; w/v) at 4mg/mL (or 3 mg/mL for 4Ph, 2F and N-Pip) and prepared as follow. Weight and dissolve 4 mg flavonoid powder (3 mg for 4Ph, 2F and N-Pip) into 136  $\mu$ L of physiological saline (0.9%; w/v), heat up to 80 °C in a water bath for 5-minute, with subsequent agitation by a vortex until the suspension became milky. The milky solution was brought to room temperature, 136  $\mu$ L of Cremophor EL and 136  $\mu$ L Ethanol were added with continuous agitation until a clear viscous solution is formed. Finally, top up this solution to 1 mL with 592  $\mu$ L of 0.9% (w/v) saline, vortex until a uniform clear solution is formed. Solvent of the above modulators is being prepared by simple mixing of 13.6% cremophor EL, 13.6% Ethanol and 72.8% physiological saline (0.9%; w/v) in final volume of 1 mL. All modulator solutions were freshly prepared on the day of injection.

#### **3.2.4 Pharmacokinetic study of FD18**

The preparation of FD18 was described in previous section of 3.2.3. FD18 at 45 mg/kg were administered to female Balb/c mice through i.p. injection. At various time points (10, 30, 60, 120, 240, 420, 840, 720 and 960-minute), blood samples were collected in a heparinized eppendorf tube via cardiac puncture after deep anesthesia by ethyl ether. The

samples were centrifuged at 16100 g for 10-minute immediately for the separation of blood plasma. Plasma sample collected was transferred to a new eppendorf tube and stored at -20°C until analysis. Pharmacokinetics data analysis was done by utilizing a non-compartmental model. Area under the plasma concentration-time curve (AUC), half-life for elimination ( $t_{1/2\beta}$ ), half-life for absorption ( $t_{1/2\alpha}$ ), clearance (CL), maximum plasma concentration ( $C_{\max}$ ) and time to maximum plasma concentration ( $T_{\max}$ ) were calculated by PK Solutions 2.0 (Summit Research Service, Ashland, U.S.A). (Yan et al., 2016; appendix 1)

### 3.2.5 *In vivo* short term toxicity study

The objective of this study is to determine whether the designed treatment dose and schedule is usable thus safe to animals. Flavonoid modulators listed in section 3.2.1 were tested for their *in vivo* toxicities. Due to the maximum solubility of FD18 and the injection limit; FD18 was dosed at a maximum usable dosage (MUD) of 45 mg/kg. A lower dose of 30 mg/kg were included as a safety net. The rest of the modulators were tested at 45 mg/kg similar to FD18. Treatment schedule of these modulators were set on every other day in total of 12 injections (q.o.d. x 12). Under all settings, modulators were tested with either PTX at 12 mg/kg or 8 mg/kg or its solvent (equivalent volume to 12 mg/kg). PSC833, a more potent P-gp modulator compared to FD18 *in vitro*, were tested in various concentrations (10, 5, 2.5, 1.6 mg/kg) with or without PTX at 8 or 4 mg/kg. Treatment schedule of PSC833 is eight injections in 17 days (q.o.d. x 4 for 2 cycles, with 4 days drug free period between each cycle). The following parameters were used to indicate whether drug related toxicity during or post-treatment (10 days after dosing cycle) have occurred. A) Mortality. B) Weight changes. A more stringent definition herein applied. Weight loss

should not exceed 15% (normally 20%) compared to day 0 of treatment for more than 3 or more consecutive days. C) Other observable parameters. Reduced or loss of activity levels, abnormal posture and loco moments, reduced or loss of appetites, hypothermia, skin abnormalities such as inflammation or rashes and so on will be monitored closely. Animal with the above symptoms were euthanized.

### **3.2.6 Tissue processing and embedding for histopathological studies**

All animals were sacrificed after the short-term toxicology studies by overdose of CO<sub>2</sub> and then by cervical dislocation for necropsy. Vital organs (liver, heart, kidneys and spleen) were collected, weighed, gross checked and then fixed in 10% neutral buffered formalin (NBF) for 8 to 10 hours. The organs were further trimmed into cubes with a thickness of 3mm. These trimmed tissues were fixed under NBF for another 2-hour, then processed in an automatic tissue processor (Leica ASP 200) and embedded in paraffin. Tissue blocks were sectioned by a rotary microtome to give 3-micron-thick cut sections. They were mounted onto clean slides and then stained with Gill's 3 hematoxylin for 45minutes and 1% eosin Y in 1% calcium chloride (CaCl<sub>2</sub>) for 10 minutes followed by microscopic morphological investigations.

### **3.2.7 Histopathological evaluation of selected flavonoid modulators**

Pathological grading was evaluated by a registered pathologist. Symptoms such as polymorphism of cells, degenerative features, and disappearance of nucleus were examined under a light microscope of 100x. A scoring system of 0 to 5 was applied, where 5 indicated severe condition and 0 represented negative incidence. Scoring of condition was based on comparison to treatment controls. To quantify, samples were observed under

a high power field (400x) with a light microscope, 10 random fields within hot spot areas (areas that most likely observed to have adverse changes) were selected and manually counted for the number of abnormal cells. Evaluations were done based on the following criteria listed in Table 3.2.

Table 3.2 Histopathological grading criteria.

Organ	Assessment Criteria
Liver	1) Hepatitis 2) Polymorphism of nucleus 3) Regenerative hepatocytes 4) Necrosis 5) Infiltration of white blood cells
Kidney	1) Changes in glomerulus, proximal and distal convoluted tubule structures 2) Necrosis
Heart	1) Necrosis 2) Regenerative cardiac cells
Spleen	1) Splenic atrophy on white and red pulp

Vital organs obtained from autopsy were fixed and process, then perform H&E staining. Pathological evaluation was done by a registered pathologist based on the above criteria.

### 3.2.8 *In vivo* modulating activity towards PTX in LCC6/MDR xenografts

LCC6/MDR xenograft models were setup as described previously in Chapter 2 at section 2.2.10. Treatment of LCC6/MDR-xenografted Balb/c female nu/nu mice begin when tumor volume reached about 100-150 mm<sup>3</sup>. Animals were randomized into groups of 7 to 11. Treatment dosage and schedule were selected from the toxicity study according to section 3.2.5. Detailed study plan is being described below in Table 3.3. Animals were assessed for treatment efficacies, survivals and toxicities according to sections 3.2.5 and

3.2.9. Upon termination on day 32, animals will be dissected for postmortem studies. Gross checking of vital organs was conducted. Statistical analysis on tumor volumes between control and treatment group was performed by using one-way ANOVA with Bonferroni post test.

Table 3.3 Treatment groups and schedules.

A	Group	n	Dosing schedule	Treatment
	1	8		Solvent Control
	2	9	q.o.d. x 12	FD18 (45 mg/kg; i.p.) + PTX solvent
	3	8		FD18 solvent + PTX (12 mg/kg; i.v.)
	4	11		FD18 (45 mg/kg; i.p.) + PTX (12 mg/kg; i.v.)
	5	7	Day 0, 2, 4, 6 and 11, 13, 15, 17	PSC 833 (2.5 mg/kg; i.p.) + PTX (8 mg/kg; i.v.)

B	Group	n	Dosing schedule	Treatment
	1	8		Solvent control
	2	8	q.o.d. x 12	Modulator solvent + PTX (12 mg/kg; i.v.)
	3	8		4MeO (45 mg/kg; i.p.) + PTX solvent
	4	8		4Cl (45 mg/kg; i.p.) + PTX solvent
	5	7		N-Pip (45 mg/kg; i.p.) + PTX solvent
	6	8		4MeO (45 mg/kg; i.p.) + PTX (12 mg/kg; i.v.)
	7	7		4Cl (45 mg/kg; i.p.) + PTX (12 mg/kg; i.v.)
	8	8		N-Pip (45 mg/kg; i.p.) + PTX (12 mg/kg; i.v.)

Two separated experiments have been conducted. (A) *In vivo* modulation activity study in LCC6/MDR xenografts towards PTX. FD18, together with PTX at 12 mg/kg (group 4) or its solvent (group 2); were compared to solvent control (group 1) and PTX control (group 3). A positive control of PSC833 at 2.5 mg/kg was included (group 5) and treatment at a less frequent schedule of 8 injections in a 17-day treatment period. (B) *In vivo* modulation study towards PTX. Another batch of LCC6/MDR xenograft was created for the study of FD 18 derivatives. Same dosing and scheduling strategy were employed with reference to (A). All groups consisted of 7 – 11 animals (n=7-11). Tumor volumes, weight changes and survival were constantly monitored during and after treatment. Tumor volume data obtained were statistically analyzed by one-way ANOVA.

### 3.2.9 Evaluation of treatment efficacy

To evaluate the therapeutic efficacy, tumor volumes, relative body weight changes, and survivals were monitored. Tumor volume and relative body weight change were being calculated as referred to Chapter 2, section 2.2.14, equations 2.4 and 2.5:

The indication of treatment induced toxicity were listed in Chapter 2, section 2.2.13. Treatment efficacies were analyzed in terms of % of tumor inhibition (T-C value, % T-C), and tumor doubling time ( $T_d$ ). The data were further analyzed statistically by one-way-ANOVA with Bonferroni post test. The mathematical equations for %T-C and  $T_d$  were listed in Chapter 2, section 2.2.14, equations 2.6 to 2.7. (Bissery et al. 1991, Clarke 1997)

### 3.2.10 *In vivo* Paclitaxel accumulation study

LCC6/MDR xenograft models were setup as described previously. Experiment was conducted when tumors reached 100 -120 mm<sup>3</sup>. FD18 injection (45 mg/kg; i.p.) was made at 0-hour followed by PTX treatment (40 mg/kg; i.v.) 1-hour after. Tumor samples were collected 7-hour post-PTX administration.

### 3.2.11 Extraction of PTX from LCC6/MDR tumors for HPLC analysis

Tumor samples were homogenized with 1 mL of water with the addition of 50  $\mu$ L docetaxel at 60  $\mu$ g/mL as an internal standard. The homogenate was extracted thrice for PTX by using 3 mL of diethyl ether, vortexed then centrifuged at 2,700 g for 5-minute. Supernatant was collected and dried at 80°C. The extracted PTX samples were stored at -20°C until HPLC analysis. Prior to HPLC analysis, the samples were reconstituted by

adding 50  $\mu$ L acetonitrile, followed by the removal of unwanted debris by filtering the samples through a 0.2  $\mu$ m nylon filter. HPLC analysis was performed subsequently according to previous published methods. (Yan et al., 2016; appendix 1)

### **3.2.12 Dose optimization of FD18 in reversing P-gp mediated PTX resistance in LCC6/MDR xenografts**

A higher dosage of FD18 (90 mg/kg) was tested as described section 3.2.8 Table 3.3A (Group 1 - 4) to see if modulating effects could be potentiated. Due to the previous mentioned MUD for FD18; it was administrated via two injections at 45 mg/kg at 0 and 9-hour on the same day. Formulation of FD18, evaluation and assessment guidelines can be referred to sections 3.2.3, 3.2.5 and 3.2.9 respectively.

## **3.3 Results**

### **3.3.1 *In vitro* screening of flavonoid dimers for their P-gp modulating activities towards PTX**

Three series of flavonoid dimers were examined as listed in section 3.2.1. The first series was derived from parent compound 1d-(5,7H) (compound 2), having four polyethylene glycol (PEG) molecules as linker at C4 position. Based on this compound, derivatives were synthesized with PEG linker at different positions. Previous published data suggested that compounds 2 - 4 were the most potent compounds (Chan et al., 2009), therefore, they were used to compared to the newly synthesized compounds. (Table 3.4, compound 5-9) Linker positioned at C5 ( $IC_{50}$  of 42.8 nM) weakened the activity, whereas, linker at C2', C3, C3' and C7 enhanced it ( $IC_{50}$  of  $19.3 \pm 3.2$ , 16.5,  $20.13 \pm 5.1$  and 10.6

respectively). Therefore, linker at C4 position (i.e. compound 2) is still the best modulator from this series.

Although compounds 2 – 4 were potent, they have poor aqueous solubility. To increase aqueous solubility, a nitrogen-containing PEG linker was used. Protonation of nitrogen can increase aqueous solubility (Table 3.4; compound 10 – 14) Among these amine-linked compounds, 13 and 14 were the most potent ( $IC_{50} = 1.1$ )  $EC_{50}$  of compound 13 was 219 nM, almost the same as the parent compound 2 (222 nM). Compound 13 was relatively toxic to normal fibroblasts ( $IC_{50} = 6 \mu M$ ), Compound 14, has an  $EC_{50}$  of 148 nM, and was non-toxic to fibroblast ( $IC_{50}$  towards L929 cells at 85  $\mu M$ ), different dimers were created. Further structural substitution of various functional groups on the benzyl ring at linker can maintain their efficacies. (Table 3.4; compound 15 - 20) They were active within a nanomolar range without significant toxicities to fibroblast. Among all compounds, 4Ph has highest selective index of >962 whereas diF was the lowest at >422. FD18, the lead compound, has 574. (Table 3.5) These compounds were subsequently further characterized by *in vivo* through pharmacokinetic, toxicity and *in vivo* efficacy study.

Table 3.4 Summary of P-go modulating activities of flavonoid dimers towards PTX.

ID	Compound	Linker position	Modulation activities on LCC6/MDR			EC <sub>50</sub> towards PTX (nM ± SEM)	Cytotoxicity to L929 cells (IC <sub>50</sub> ; μM ± SEM)
			[Compound]	IC <sub>50</sub> towards PTX (nM ± SEM)	RF		
	Control		-	126.2 ± 6.1	1.0	-	-
	DMSO Control		0.05%	127.0 ± 4.4	1.0	-	-
	Cremophor EL Control		0.08%	104.3	1.2	-	-
1	PSC 833		1 μM	2.6 ± 0.4	48.8	2.3 ± 0.5	>100
2	1d-(57H) #	4	1 μM	8.9 ± 2.6	14.3	222 ± 71	>100
3	1d-(57H)-7F #	4	1 μM	10.6 ± 4.9	11.6	ND	ND
4	1d-(57H)-6Me #	4	1 μM	4.9 ± 2.1	25.9	ND	ND
5	2'-1d-(57H) #	2'	1 μM	19.3 ± 3.2	6.5	ND	ND
6	3-1d-(57H) #	3	1 μM	16.5	12.1	ND	ND
7	3'-1d-(57H) #	3'	1 μM	20.1 ± 5.1	6.3	ND	ND
8	5-1d-(57H)	5	1 μM	42.8	2.9	ND	ND
9	7-1d-(57H)	7	1 μM	10.1	12.5	ND	ND
10	1d-(5,7H)-linker 2NMe		1 μM	29.1 ± 10.0	4.3	ND	ND
11	1d-(57H)-linker NMs		1 μM	16.3 ± 1.9	7.8	ND	ND

12	1d-(57H)-linker NTs		1 $\mu$ M	7.6 $\pm$ 1.6	16.7	ND	ND
13	1d-(57H)-NH <sup>^</sup> <sup>§</sup>		1 $\mu$ M	1.1 $\pm$ 0.1	115.5	219 $\pm$ 53	6 $\pm$ 1
14	1d-(57H)-N-Bn <sup>^</sup> <sup>§</sup>		1 $\mu$ M	1.1 $\pm$ 0.1	115.5	148 $\pm$ 18	85 $\pm$ 5.0
15	1d-(57H)-N-(4PhBn)		1 $\mu$ M	4.8 $\pm$ 0.5	26.5	72 $\pm$ 21	>69.3
16	1d-(57H)-N-(2FBn)		1 $\mu$ M	1.5 $\pm$ 0.2	84.7	179 $\pm$ 44	>100
17	1d-(5,7H)-N-(4ClBn)		1 $\mu$ M	4.4 $\pm$ 0.6	28.9	177 $\pm$ 14	>78.2
18	1d-(57H)-N-(4MeOBn)		1 $\mu$ M	1.3 $\pm$ 0.0	32.6	104 $\pm$ 7.0	>100
19	1d(5,7H)-N-(2-,6-diFBn)		1 $\mu$ M	1.7 $\pm$ 0.3	74.7	237 $\pm$ 91	>100
20	1d-(57H)-N-Piperonyl		1 $\mu$ M	3.4 $\pm$ 0.1	37.4	204 $\pm$ 20	>100

Series of flavonoid dimers were tested for their *in vitro* P-gp modulating activities towards PTX. Compound ID 2-4 were lead compounds previously established. ID 5-9 were differed in linker positions. Modulators 10-14 were linked with different linkers to enhance their aqueous solubility. The lead amine linked compound, 14, was modified further to compounds 15 -20, with different functional groups substituted on the amine linker group. All modulators were tested at 1 $\mu$ M and were compared to PSC833 as positive control. Apart from the determination of IC<sub>50</sub> (nM) on PTX, some of these modulators with high relative fold (RF) (ratio of IC<sub>50</sub> of LCC6MDR cells without modulator to LCC6MDR cells with modulator) values suggesting they have higher sensitivities to PTX. They were taken into further investigations for their EC<sub>50</sub> (nM) on PTX (a dose of modulator that gives its half maximal effects towards PTX) and cytotoxicity towards normal cells (L929; murine fibroblasts). ND; Not determined. (Published data: <sup>#</sup>(Chan et al., 2009), <sup>^</sup>(Chan et al., 2012), <sup>§</sup>(Yan et al., 2016))

Table 3.5 Selective indices for selected modulators.

ID	Compound	Selective Index
14	1d-(57H)- N-Bn (FD18)	574
15	1d-(57H)-N-(4PhBn) (4Ph)	> 962
16	1d-(57H)-N-(2FBn) (2F)	> 559
17	1d-(5,7H)-N-(4ClBn) (4Cl)	> 442
18	1d-(57H)-N-(4MeOBn) (4MeO)	> 961
19	1d(5,7H)-N-(2-,6-diFBn) (diF)	> 422
20	1d-(57H)-N-Piperonyl (N-Pip)	> 490

Selective index is ratio defined by the IC<sub>50</sub> towards fibroblast L929 divided by the EC<sub>50</sub> for reversing PTX resistance. The higher the value, the more potent and less toxic it is.

### 3.3.2 Pharmacokinetic study of FD18

Results obtained from this section were performed by Kan from Chow's group. (Kan, PhD thesis, 2015; Yan et al., 2016) Since FD18 was the first candidate synthesized among other modulators listed in Table 3.5, it was treated as a model for pharmacokinetic study. The pharmacokinetic properties of FD18 were summarized as follows. When FD18 was administered to mice through i.p. injection at 45 mg/kg, and monitored for 16 hours. (Figure 3.1), it exhibited a rapid absorption phase and reached a C<sub>max</sub> of 2350 ng/mL at 120-minute (T<sub>max</sub>). FD18 was also able to maintained at a plasma concentration above its EC<sub>50</sub> (148nM; 107 ng/mL) for more than 10 hours.

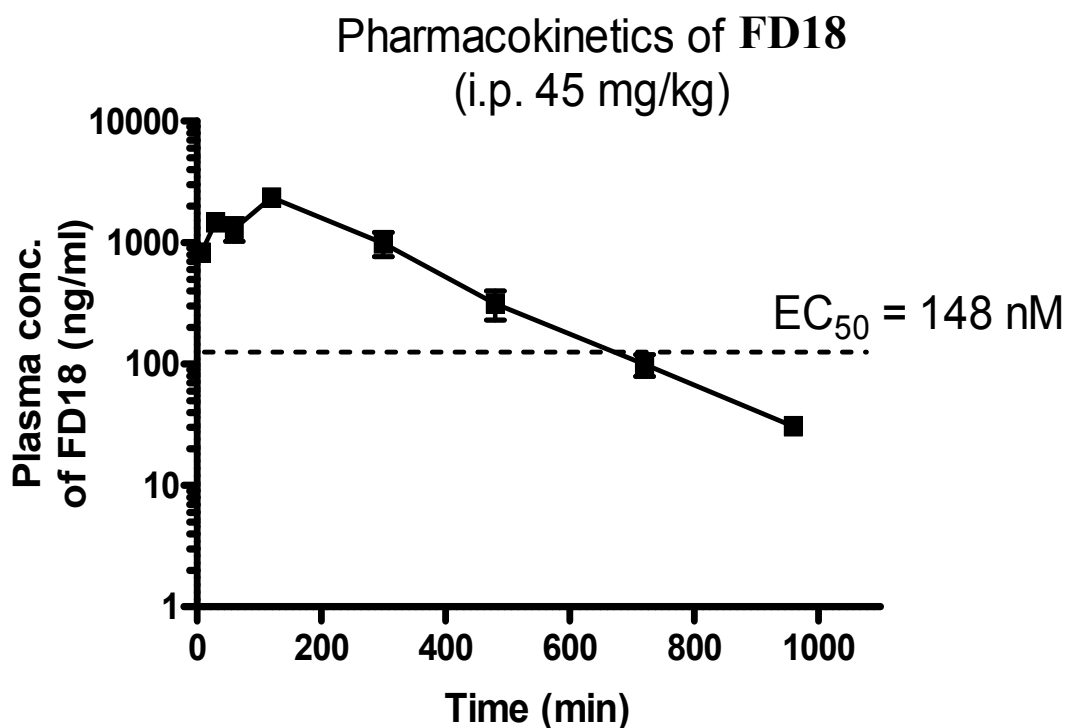


Figure 3.1 Plasma concentration of FD18 against time. FD18 was injected intraperitoneally to mice and was monitored from 0 to 16 hours. The dotted line at 107 ng/mL represents the EC<sub>50</sub> of FD18 at 148 nM. (Yan, 2016)

Oral bioavailability of FD18 was also studied in rat, C<sub>max</sub> from oral feeding was half of that of i.p. injection with a low bioavailability (F) of 2.4% (by calculating from the AUCs arisen from i.v. injection, data not shown). In view of this, subsequent studies of FD18 was prepared using i.p. route.

### 3.3.3 Evaluation of *in vivo* short-term toxicity of selected dimers

Pharmacokinetics studies showed that i.p. injection of FD18 can enter the systemic circulation and maintain at a level above its EC<sub>50</sub> for a reasonable period. Modulators

listed in Table 3.5 were tested for their *in vivo* toxicities. These modulators were tested at 30 and/or 45 mg/kg (i.p.) in combination of PTX at 12 mg/kg (i.v.). A new treatment protocol was implemented here with 12 injections (q.o.d. x 12) instead of 8. Data from this study were summarized and shown in Table 3.6. FD18, when used alone or with PTX at either 30 and 45 mg/kg, causes no toxicity. Nevertheless, derivatives of FD18 (diF, 4Ph and 2F), caused toxicities in mice as reflected by their weight loss. Interestingly, 4Ph and 2F treated mice were observed with auricular chondritis (Figure 3.2), leading to the loss or damage of ear pinna (Figure 3.2) PSC 833, served as a positive control, was tested from 1.6 to 10 mg/kg with PTX at 8 or 4 mg/kg for 8 treatments. Results suggested that the toxic symptoms potentiate when dose concentration increases, therefore it should be kept below 2.5 mg/kg. Current results led to the selection of FD18 and its derivatives (4MeO, 4Cl and N-Pip) for further *in vivo* efficacy study in section 3.3.5.

Table 3.6 Summary of toxicity data.

Group	n	Treatment		No. of death(s)	Weight loss >15%	Other observation(s) (if stated)
		Schedule	Dosage			
1	5		Modulator vehicle (eqv. to 3 mg/mL stock) + PTX vehicle	0/5	0/5	
2	5		Modulator vehicle (eqv. to 4 mg/mL stock) + PTX vehicle	0/5	0/5	
3	5		FD18 (30 mg/kg; i.p.) + PTX vehicle	0/5	0/5	
4	5		FD18 (30 mg/kg; i.p.) + PTX (12 mg/kg; i.v.)	0/5	0/5	
5	5		FD18 (30 mg/kg; i.p.) + PTX (8 mg/kg; i.v.)	0/5	0/5	
6	5		FD18 (45 mg/kg; i.p.) + PTX vehicle	0/5	0/5	
7	5		FD18 (45 mg/kg; i.p.) + PTX (12 mg/kg; i.v.)	0/5	0/5	
8	5		FD18 (45 mg/kg; i.p.) + Paclitaxel (8 mg/kg; i.v.)	0/5	0/5	
9	5	q.o.d. x 12	diF (45 mg/kg; i.p.) + PTX (12 mg/kg; i.v.)	0/5	1/5	
10	5		4Ph (45 mg/kg; i.p.) + PTX (12 mg/kg; i.v.)	0/5	1/5	Auricular chondritis
11	5		2F (45 mg/kg; i.p.) + PTX (12 mg/kg; i.v.)	0/5	2/5	Auricular chondritis
12	5		4MeO (45 mg/kg; i.p.) + PTX (12 mg/kg; i.v.)	0/5	0/5	
13	5		4Cl (45 mg/kg; i.p.) + PTX (12 mg/kg; i.v.)	0/5	0/5	
14	5		N-Pip (45 mg/kg; i.p.) + PTX (12 mg/kg; i.v.)	0/5	0/5	
15	2		PSC 833 (1.6 mg/kg; i.p.) + PTX (8 mg/kg; i.v.)	0/2	0/2	
16	2	Day 0, 2, 4, 6	PSC 833 (1.6 mg/kg; i.p.) + PTX (4 mg/kg; i.v.)	0/2	0/2	
17	2		PSC 833 (2.5 mg/kg; i.p.) + PTX (8 mg/kg; i.v.)	0/2	0/2	
28	2	and	PSC 833 (2.5 mg/kg; i.p.) + PTX (4 mg/kg; i.v.)	0/2	1/2	
29	2		PSC 833 (5 mg/kg; i.p.) + PTX (8 mg/kg; i.v.)	0/2	2/2	
20	2	11, 13, 15, 17	PSC 833 (5 mg/kg; i.p.) + PTX (4 mg/kg; i.v.)	0/2	2/2	
21	2		PSC 833 (10 mg/kg; i.p.) + PTX (8 mg/kg; i.v.)	1/2	2/2	
22	2		PSC 833 (10 mg/kg; i.p.) + PTX (4 mg/kg; i.v.)	2/2	2/2	

Mice in groups of 5 (or 2 for PSC833) were tested for the toxicities from different modulators at 45 mg/kg with or without PTX. FD18, the lead compound was test for another dosage of 30 mg/kg. Treatment induced toxicity was evaluated by observations of deaths and weight loss >15% for three more consecutive days.

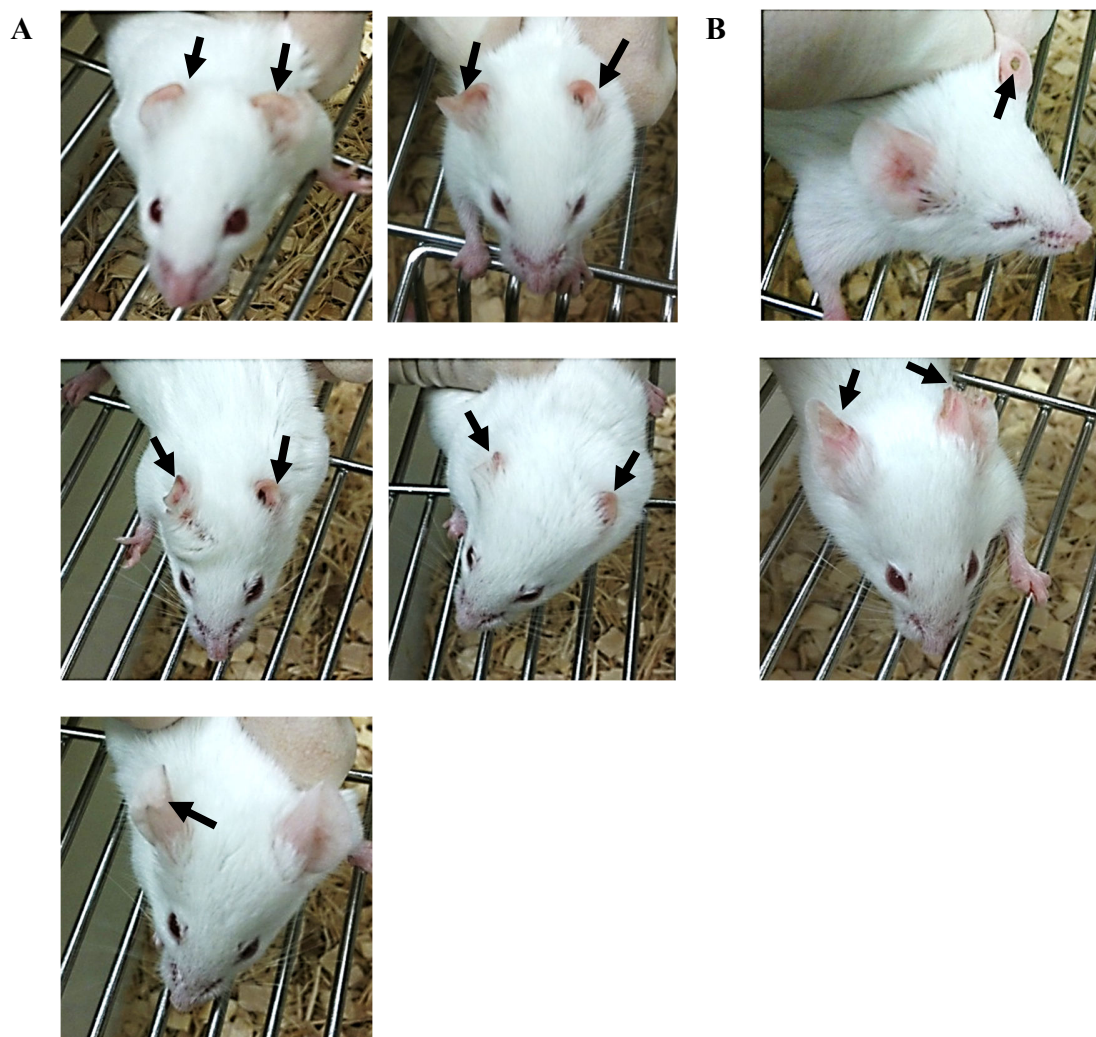


Figure 3.2 Images of animals with auricular chondritis (arrows). A) Treatment of 4Ph; B) Treatment of 2F. Ear pinnae of mice were lost or damaged.

### 3.3.4 Histopathological study of FD18, 4MeO, 4Cl and N-Pip

Histopathological effects of modulators on vital organs were evaluated (Table 3.7 and Figure 3.4 A to C). One common toxicity-induced observation was regeneration of cells, characterized by hyperplasia and polymorphism. This serves to compensate for the loss of cells due to toxicity. PTX was found to increase the number of regenerative cells in

cardiac and hepatic tissues. (Table 3.7) Surprisingly, co-treatment of PTX and selected modulators displayed protective effects. (Table 3.7, column 5 - 8) PTX also caused necrosis in hepatocytes and modulation offered protective effect. In addition, structural distortions of glomerulus, proximal and distal convoluted tubules and necrosis in renal tissue were also seen within the same treatment group. On the other hand, whilst PTX caused the loosening or shrinkage of glomerulus, co-treatment with 4Cl and N-Pip was protective. (Table 3.7)

Table 3.7 Summary of histopathological grading.

Organ	Abnormity	Control	PTX	FD18 + PTX	4MeO + PTX	4Cl + PTX	N-Pip + PTX
		Scoring 0 (negative incidence) → 5 (severe)					
Liver	Necrosis	0	2 - 3	1 - 1.5	0 - 1	0	0 - 2
	Regeneration	0	3 - 4	1 - 3	1 - 2	0 - 1	2
Heart	Regeneration	0	2	1 - 2	1	1 - 2	1 - 1.5
Kidney	Distortion of glomerulus structure	0	2	1 - 2	0 - 2	0 - 0.5	0.5 - 1

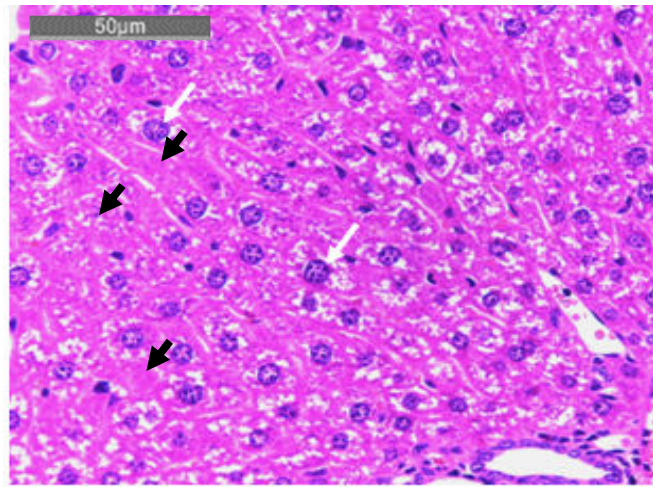
Scoring from 0 to 5 was assigned. Vital organs from each group were compared individually to their controls. (Control versus PTX and PTX versus various modulator groups). Independent experiments N=2.

To quantify these findings, tissues were observed at 400x magnification. Ten random hot spots of incidence (necrosis, binucleated cells and hyperplastic cells) were observed. PTX slightly increased necrosis in hepatic tissue. (Figure 3.3A I) Co-treatment with modulators slightly exacerbated it, although not significant except N-Pip. Regenerative features of hepatocytes were classified into binucleation (Figure 3.3A III) and hyperplasia (Figure 3.3A IV). PTX treatment provoked the incidence of binucleated cells, but has no effect on the enlargement of hepatocytes. Similar degree of binucleation cells were found after treatment with 4MeO and N-Pip, indicating that such observation was purely due to PTX treatment. Interestingly, co-administration of FD18 ( $p = 0.06$ ) and 4Cl resulted in protective effect on hepatocytes. Number of hyperplastic cells was increased. Treatment of N-Pip was the most severe followed by FD18 ( $p = 0.07$ ). Other modulators gave comparable results as control or PTX-treated groups.

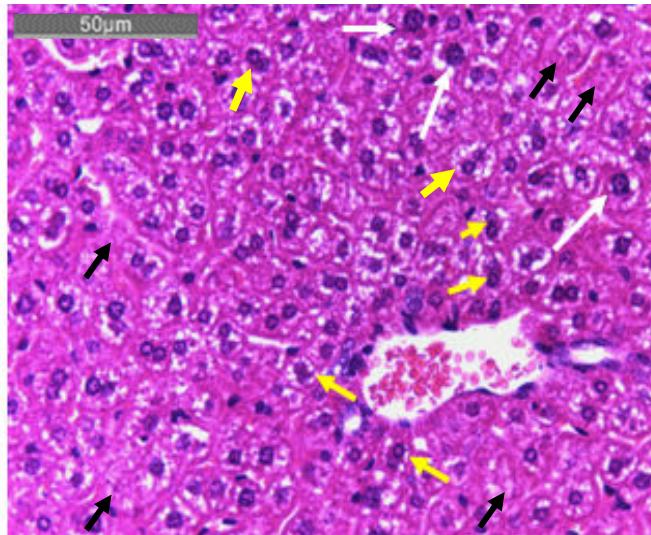
Effect on cardiac tissues were displayed in Figure 3.3B I, with white arrows representing regenerative cells. Regenerative cells were significantly increased after PTX treatment,

but selected modulators gave significant protection to cardiac cells. (Figure 3.3B II) Changes in renal structures were often found if any drugs or their metabolites were toxic upon clearance. Since systemic blood flow enters from afferent arteriole, the first site that encounter these chemicals would be the glomerulus. It was shown in Figure 3.3C I and II that PTX treatment, but not with any modulators, has promoted (although not significant) structural changes of glomerulus. Other observations such as widening of proximal and distal convoluted tubules were not found in any of the tissue samples. In summary, histopathological evaluation of organ samples obtained from previous toxicity studies supported the safe use of selected modulators. Any of the adverse effects shown at present were most likely due to PTX treatment that was not harmful to the animals. As a result, the present dose regimens and schedule would be used in efficacy studies in the next section.

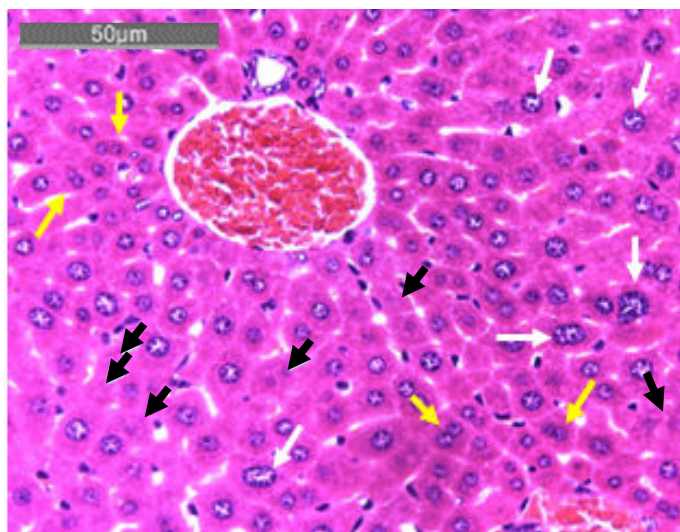
A I



Control, 400x



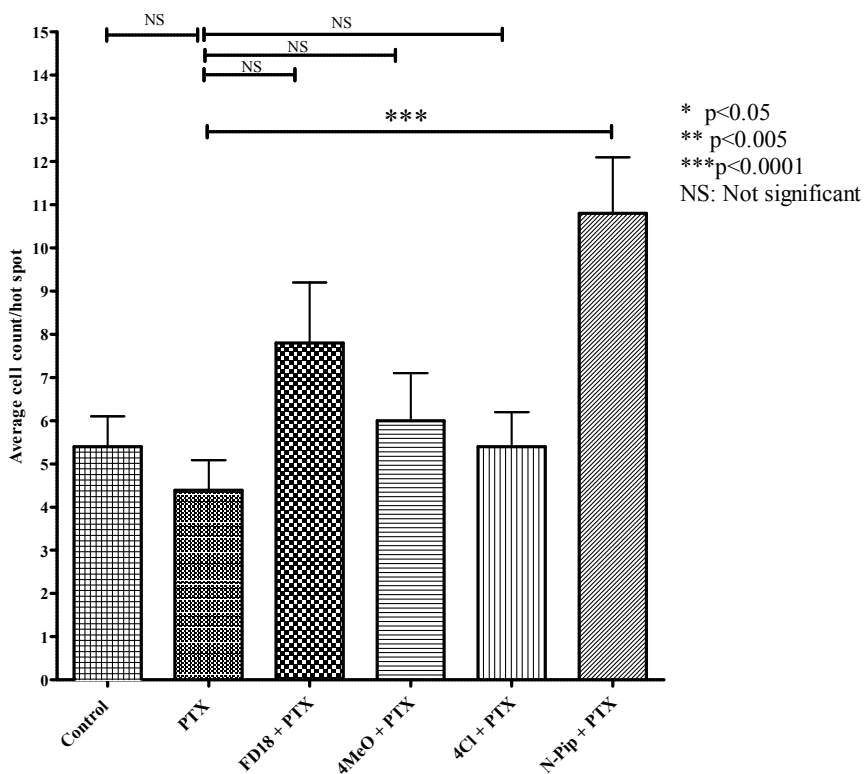
PTX, 400x



FD18 + PTX, 400x

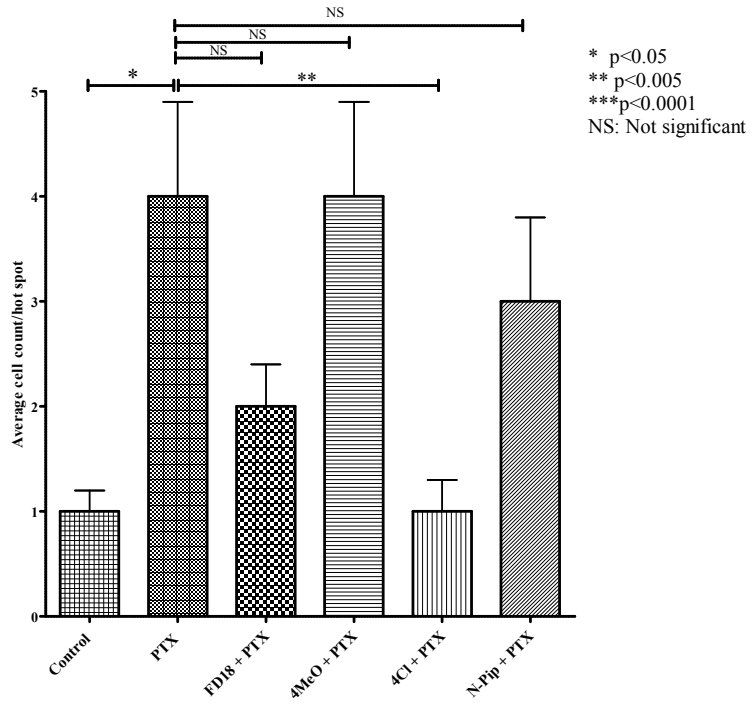
A II

Liver (Necrotic cells)



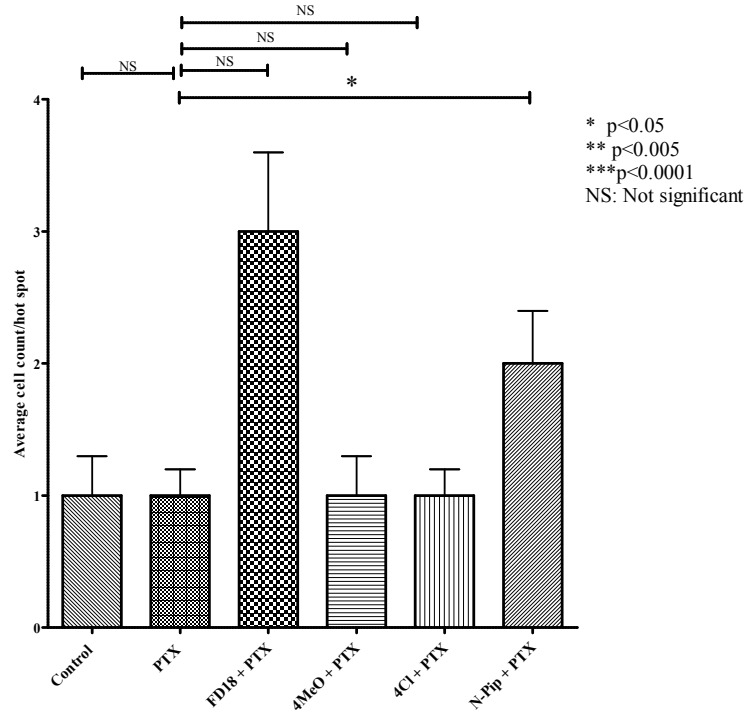
A III

Liver (Regenerative features A: Binucleated cells)

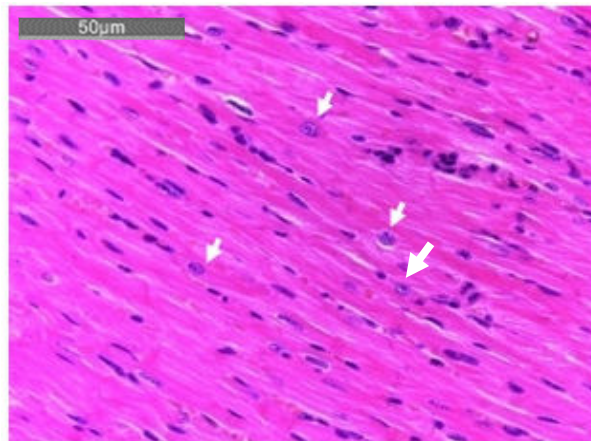


A IV

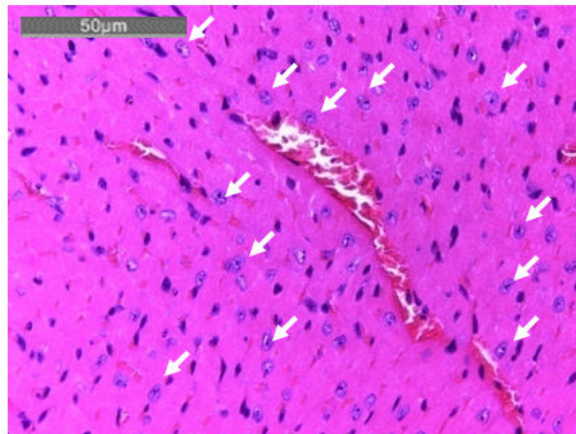
Liver (Regenerative features B: Hyperplastic cells)



BI

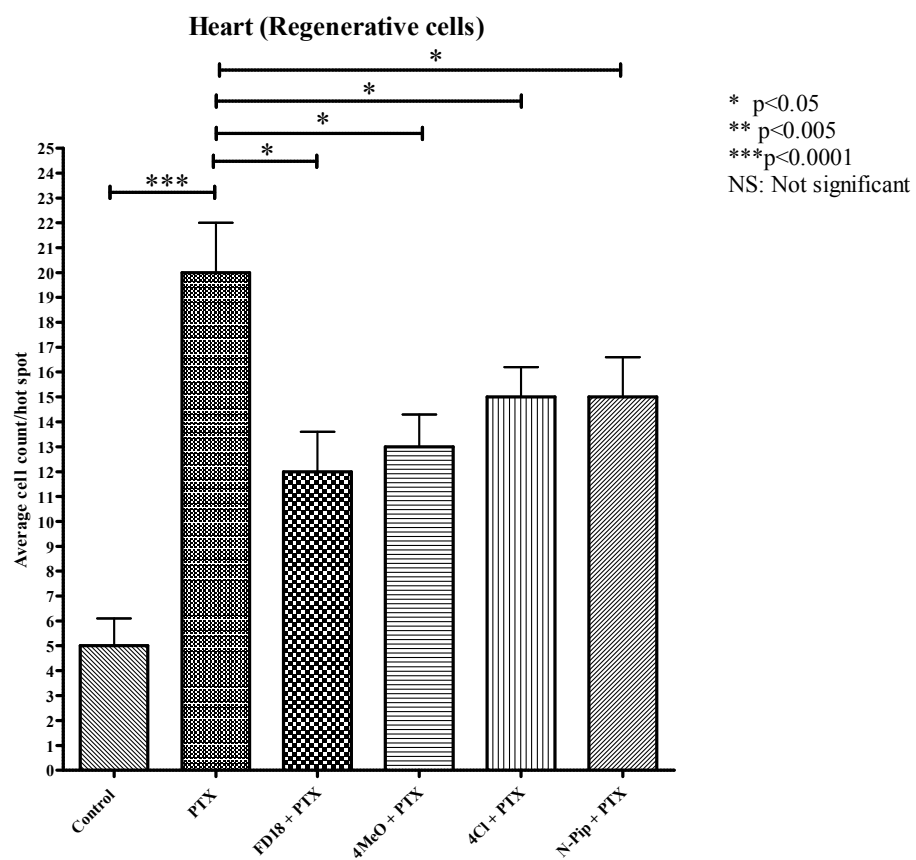


Control, 400x

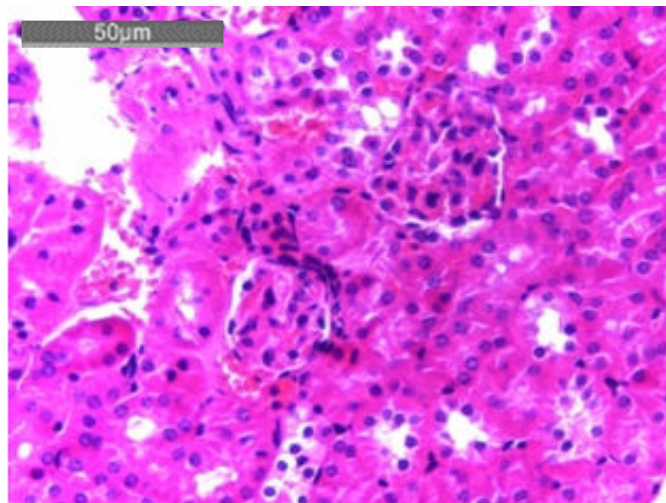


PTX, 400x

B II



CI



Control, 400x



PTX, 400x

C II

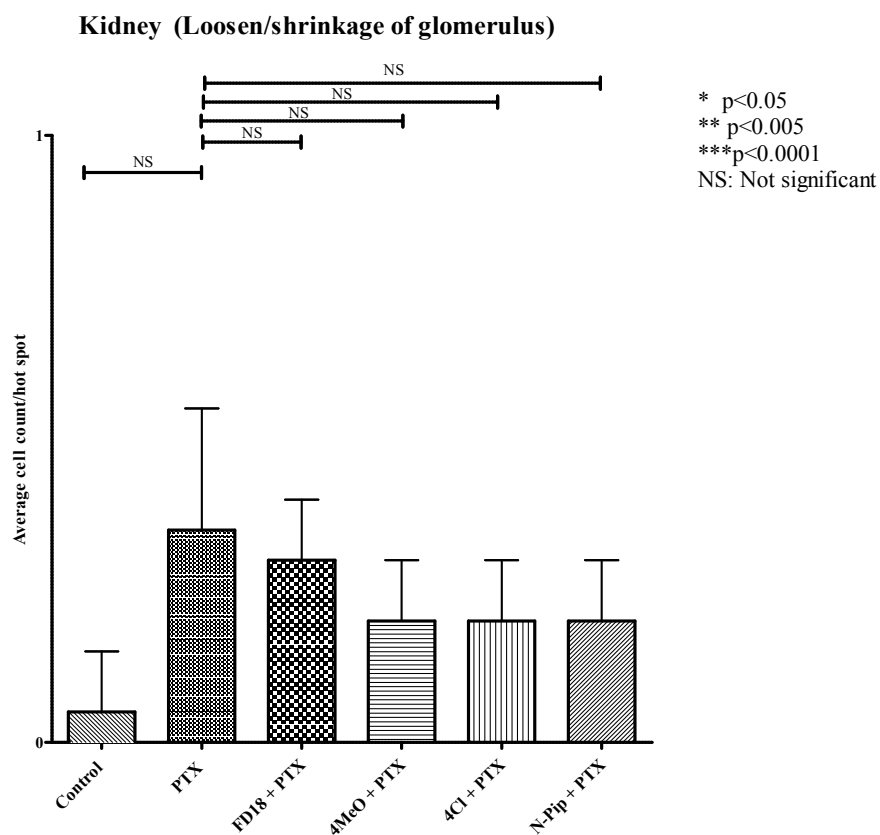


Figure 3.3 Histopathological evaluations of vital organs. Results obtained from examination of liver (A), heart (B) and kidney (C) were presented accordingly. Abnormalities of hepatocytes were found to be as monocellular necrosis (AI; black arrows) and regenerative features (binucleation of cells (A I; yellow arrows) and hyperplasia (AI; white arrows)). In cardiac tissue, regenerative cells were the only abnormalities being found (BI; white arrows). Structural distortion on glomerulus was the predominant feature being found in abnormal renal tissue (CI; black circle). Total counts of these abnormal features were analyzed in bar charts. ((A) II – IV, (B) II and (C) II)

### 3.3.5 *In vivo* modulating activity of FD18 towards P-gp mediated PTX resistance

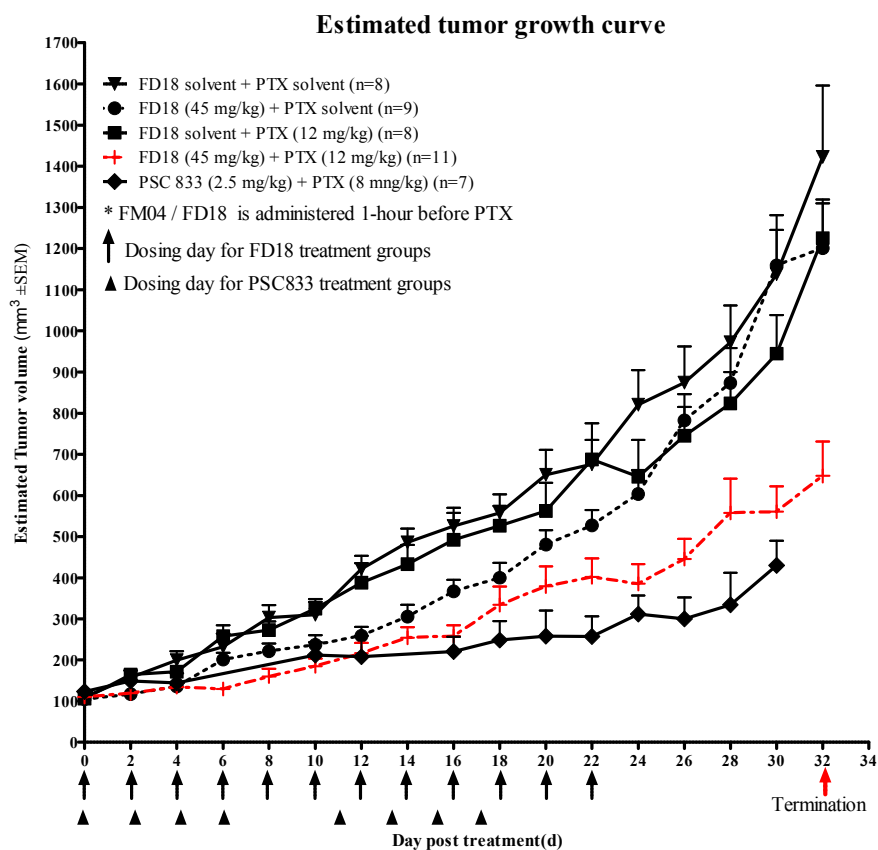
Two separate experiments have been conducted to compare the efficacy between FD18, 4MeO, 4Cl and N-Pip. (Figure 3.4A and B, Table 3.8 and 3.9) In efficacy study of FD18, treatment of FD18 or PTX alone did not cause any inhibitory effects when compared to solvent control. Dosing FD18 at 45 mg/kg 1-hour before PTX was able to resensitize LCC6/MDR tumors towards PTX resistance. Tumor volumes obtained on day 32 was  $648 \pm 84$ , compared to solvent treated tumors at  $1422 \pm 174$ ; giving a tumor inhibitory percentage of 54% ( $p < 0.01$ ).

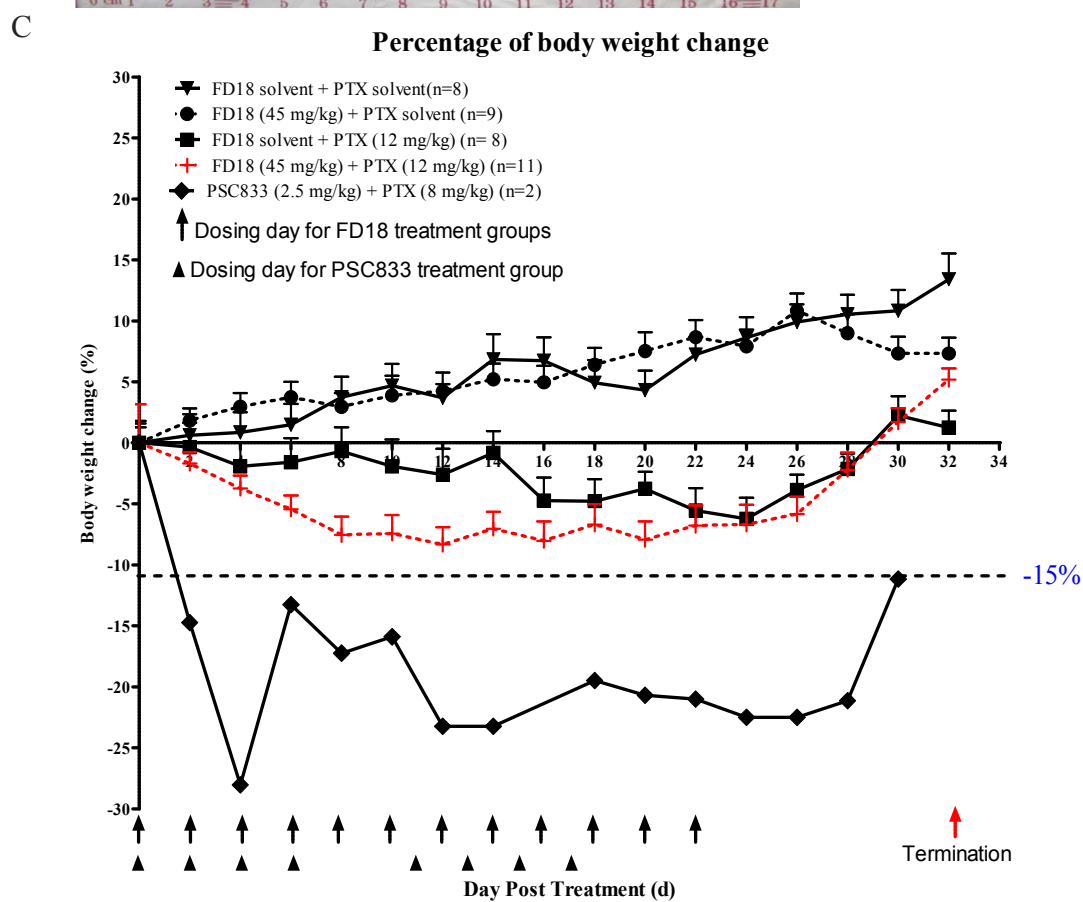
Apart from tumor volume, treatment of FD18 + PTX also significantly prolonged the tumor doubling time from 9 (PTX control) to 13 days ( $p < 0.01$ ). (Table 3.8) No animal death or weight loss greater than 15% was observed during the whole treatment and post-treatment period for PTX alone, FD18 alone or FD18 + PTX group. (Figure 3.4C) The death incidence from FD18 control on day 30 was probably due to tumor burden from the animal per se. (Figure 3.4D) At postmortem study, the wet weight of vital organs in all treated animals were similar to that of control. (Figure 3.4E)

As a positive control, PSC833 was used at a much lower dosage of 2.5 mg/kg with reduced PTX dosage of 8 mg/kg. Previous experimental data suggested that PSC833 is quite toxic compared to FD18 (data not shown), therefore, instead of dosing the animals for 12 times on every other day, a less frequent treatment protocol was employed (q.o.d. x 4 for 2 cycles with 4 days recovery period in between). Tumor volume of  $430 \pm 60$  was obtained on day 30. However, severe toxicity was observed. Animals experienced weight loss at 15% right after the first injection and were further worsen to 30% on next measurement

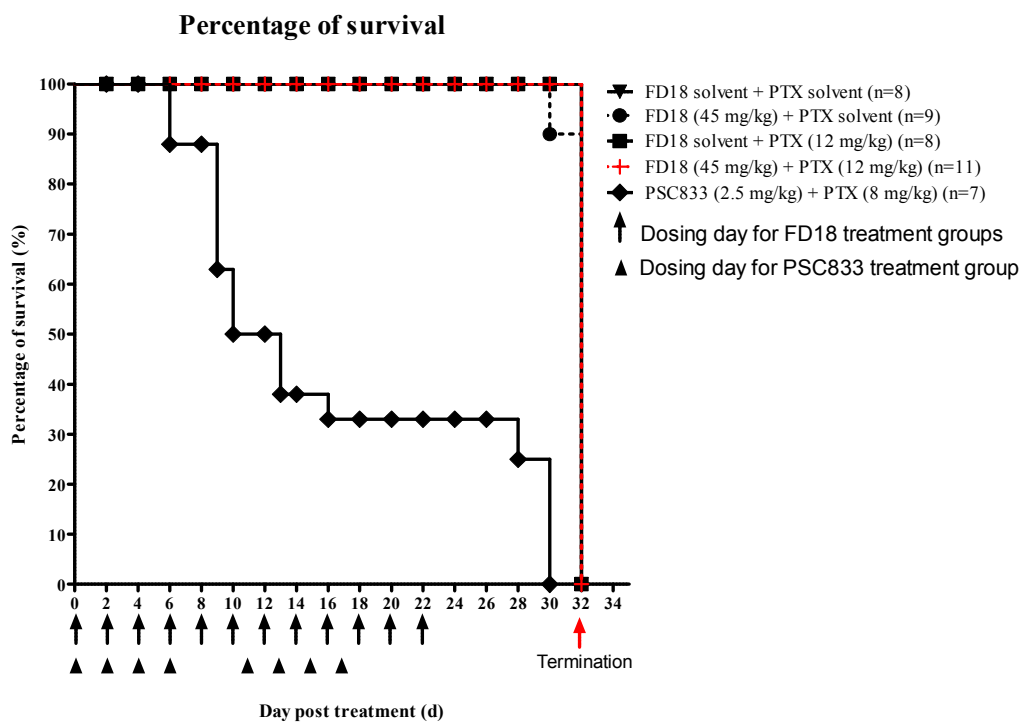
day. Although toxic effects were reduced in the end of treatment period, its toxic level reached at nearly 25%. (Figure 3.4C) Treatment related deaths were also being noted (5 out of 7 died) constantly during and after treatment. (Figure 3.4D) These findings suggested that the combinatorial use of PSC833 with PTX, even at a low dose, is not feasible and should be avoided. *In vivo* modulating activity by FD18 is summarized in Table 3.8.

A





D



E

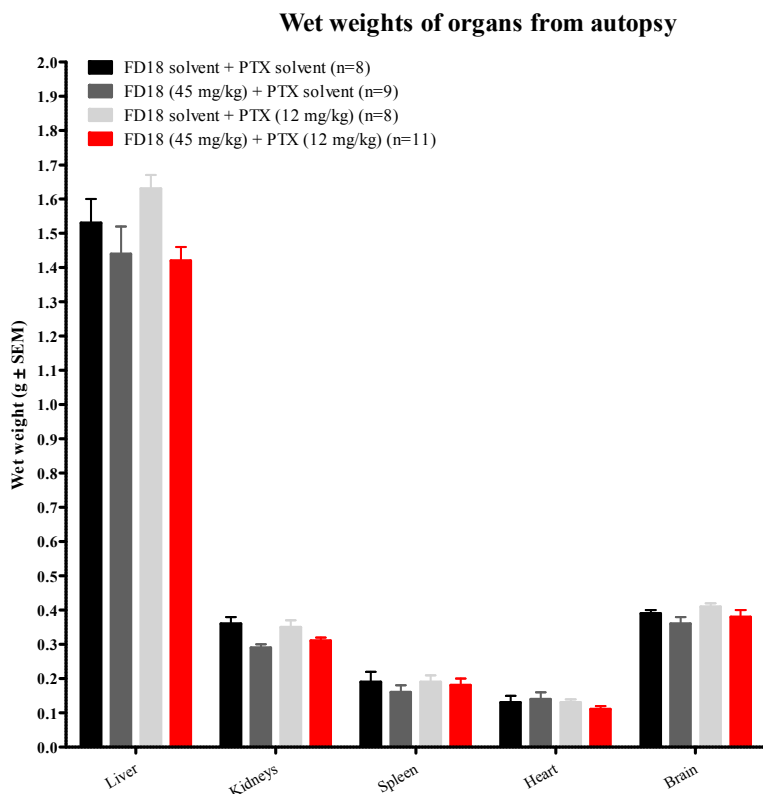


Figure 3.4 *In vivo* modulating activity of FD18 towards P-gp mediated PTX resistance. (A) Estimated tumor volume curve. Tumor volumes were being measured on every other day and data obtained was plotted against day post treatment of tumor growth trend analysis. (B) Tumor image. Tumors obtained on day 32 after termination were aligned according to their sizes and photographed. (C) Percentage of body weight change. Weight of each animal was monitored on every other day, change of weight were expressed in percentage and plotted against days. (D) Survival curve. Survival of animals were monitored every day, expressed in survival percentage and analyzed by plotting against days. (E) Wet weight of organs. Upon autopsy, vital organs were grossed checked and weighted. They were compared individually to control groups to see if there are any treatment related adverse effects.

Table 3.8 Summary of *in vivo* modulating activity of FD18.

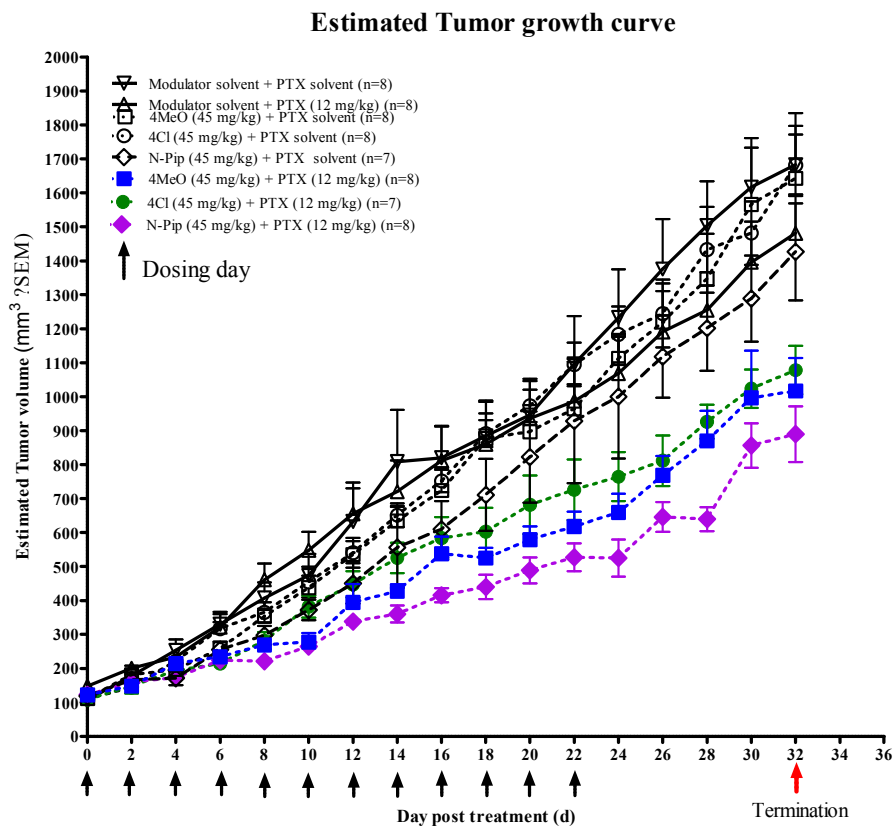
Treatment	Tumor volume (mm <sup>3</sup> ± SEM)	Tumor doubling time (T <sub>d</sub> ) (days ± SEM)	Tumor inhibition (%) (VS solvent control)
FD18 solvent + PTX solvent	1422 ± 174	9 ± 0.5	-
FD18 (45 mg/kg) + PTX solvent	1225 ± 84	10 ± 0.4	14
FD18 solvent + PTX (12 mg/kg)	1201 ± 118	9 ± 0.3	16
FD18 (45 mg/kg) + PTX (12mg/kg)	648 ± 84 ]**	13 ± 0.7 ]**	54
PSC833 (2.5 mg/kg) + PTX (8 mg/kg)	430 ± 60 <sup>a</sup>	ND	ND

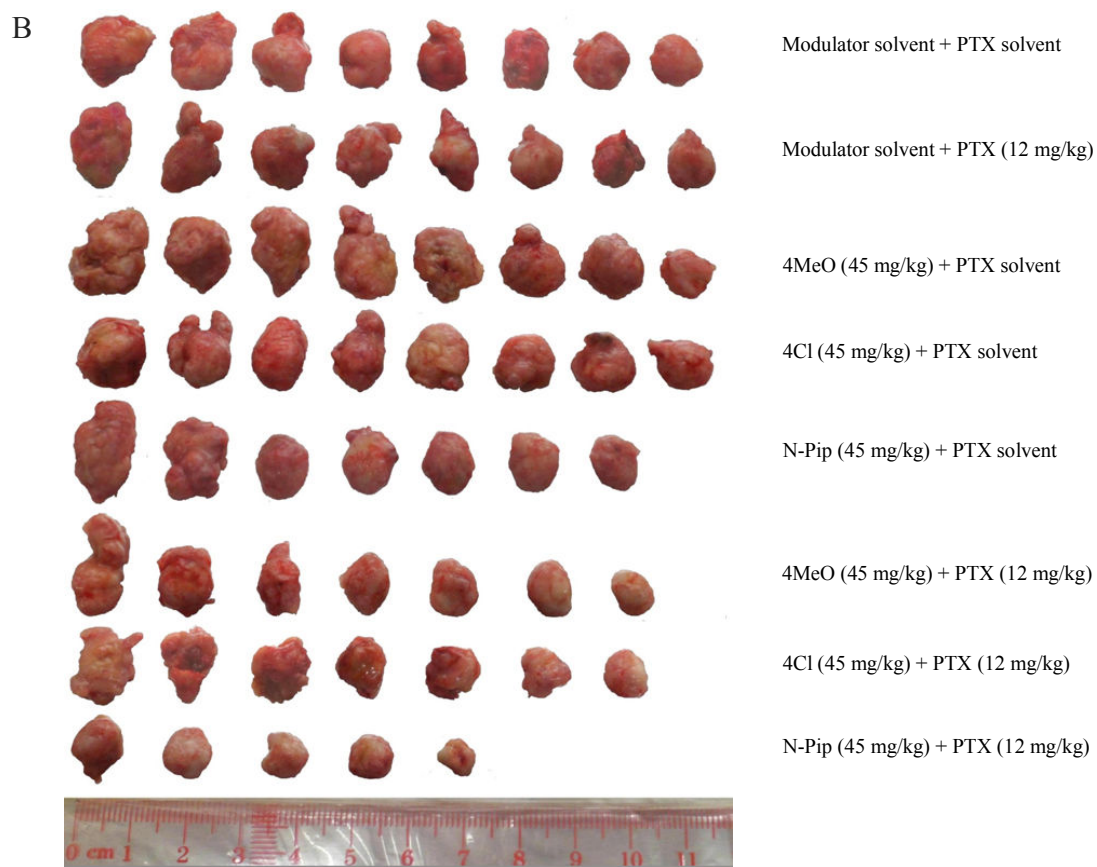
Data obtained from Figure 4.5 were summarized and statistically compared in terms of tumor volumes, tumor doubling days. %T-C was calculated to evaluate treatment efficacies. <sup>a</sup>Data obtained from the survivors. (n=2) (\*\* p<0.01)

The same experimental approach was used to study other FD18 derivatives in modulating PTX resistance caused by P-gp expression. 4MeO, 4Cl and N-Pip were administrated alone at 45 mg/kg or with together with PTX at 12 mg/kg. (Figure 3.5A) Treatment of PTX (12 mg/kg) or modulators alone did not cause any significant inhibitory effects when compared to solvent control group. When xenografts were being treated with 4MeO, 4Cl or N-Pip in the presence of PTX (12 mg/kg); tumor volume was reduced by 40% (4MeO + PTX; 1017 ± 98), 36% (4Cl + PTX; 1078 ± 71) and 47% (N-Pip + PTX; 890 ± 82) respectively (Table 4.9). Co-treatment with FD18 derivatives and PTX, however caused treatment related weight loss (Figure 3.5C) and deaths (Figure 3.5D). The trend of weight changes in these combination group were very similar. Initial treatments caused weight loss in all animals, although not to a toxic level. However, when it approached to the mid-course, the weight loss exceeded 15%; with the greatest weight loss for 4MeO at 25%, 4Cl at 30% and N-Pip at 35% compared to day 0. Weight loss stabilized after day 22 and animals slowly regain their body weights. At the end, only 4MeO + PTX treated animals, but not the other two groups, was able to restore their body weights back to the non-toxic level before termination. Drug induced toxicity from these modulators were also reflected

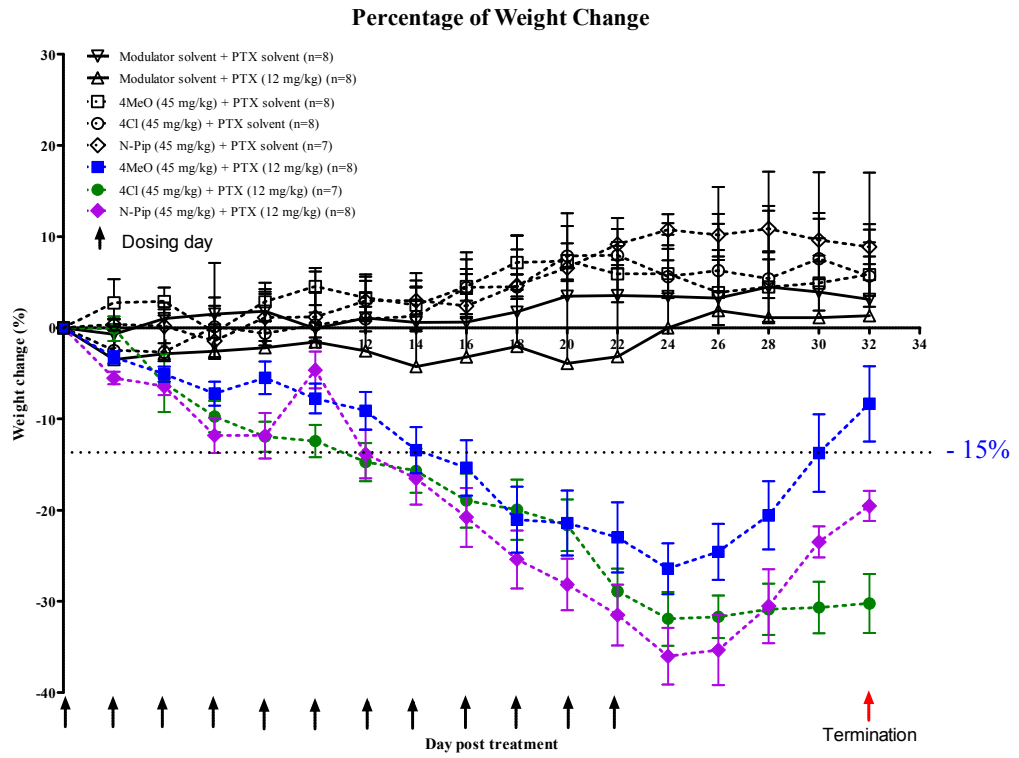
by toxic deaths in 4MeO + PTX and N-Pip + PTX treatment groups. In summary, FD18 has similar *in vivo* efficacy as other derivatives but the former is much safer to use *in vivo*.

A





C



D

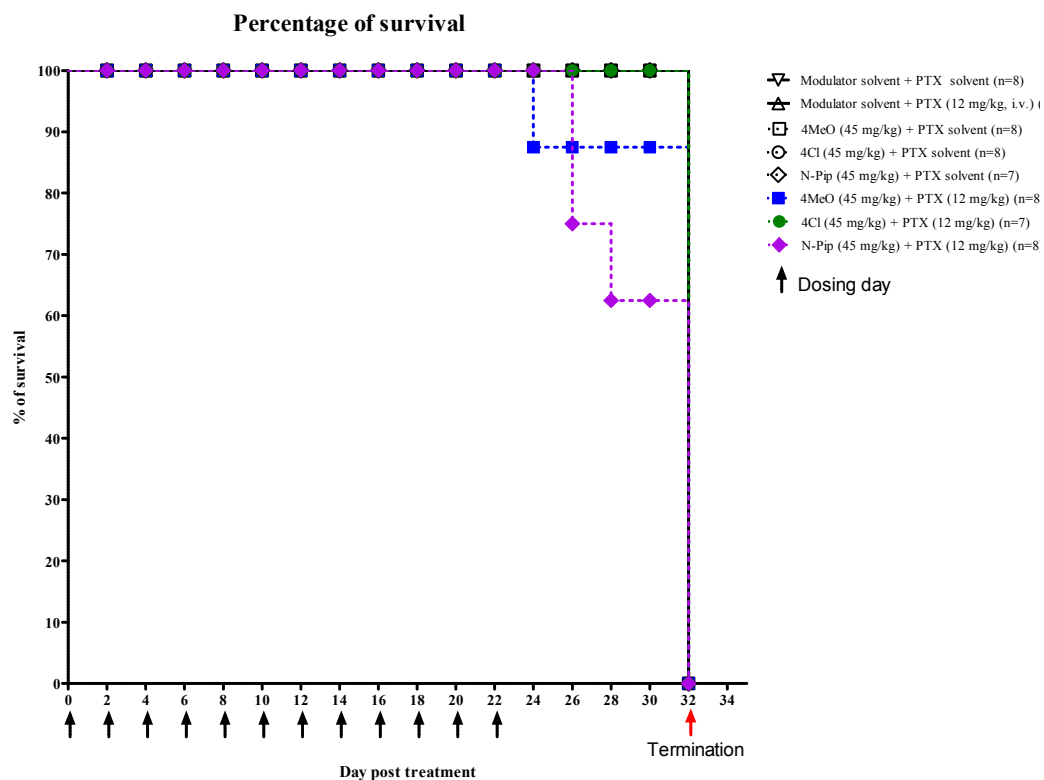


Figure 3.5 *In vivo* modulating activities of FD18 derivatives towards P-gp mediated PTX resistance. (A) Estimated tumor volume curve. Tumor volumes were measured on every other day. (B) Tumor image. Tumors obtained on day 32 after termination were arranged according to their sizes. (C) Weight changes curve. Weight of each animals were monitored on every other day, change of weight were expressed in percentage and plotted. (D) Survival curve. Survival of animals were monitored on every day, expressed in survival percentage and analysed plotting. (E) Wet weight of organs. Upon autopsy, vital organs were grossly checked and weighted. They were compared individually to control groups to see if there are any treatment related adverse effects.

Table 3.9 Summary of *in vivo* modulating activity of FD18 derivatives.

Treatment	Tumor volume (mm <sup>3</sup> ± SEM)	Tumor doubling time (T <sub>d</sub> ) (days ± SEM)	Tumor inhibition (%) (VS solvent control)
Modulator solvent + PTX solvent	1683 ± 151	8.5 ± 0.3	-
Modulator solvent + PTX (12 mg/kg)	1481 ± 115	9.8 ± 0.3	12
4MeO (45 mg/kg) + PTX solvent	1643 ± 155	8.6 ± 0.3	2
4Cl (45 mg/kg) + PTX solvent	1682 ± 90	8.4 ± 0.2	0
N-Pip (45 mg/kg) + PTX solvent	1427 ± 143	9 ± 0.4	15
4MeO (45 mg/kg) + PTX (12 mg/kg)	1017 ± 98	10.9 ± 0.6	40
4Cl (45 mg/kg) + PTX (12 mg/kg)	1078 ± 71	9.9 ± 0.5	36
N-Pip (45 mg/kg) + PTX (12 mg/kg)	890 ± 82	11.8 ± 1.2	47

Data obtained from Figure 4.5 were summarized and statistically compared in terms of tumor volumes, tumor doubling days. %T-C was calculated to evaluate treatment efficacies.

### 3.3.6 *In vivo* accumulation of PTX in LCC6/MDR tumors

Results obtained with the assistance of Chong from Chow's group. The possible working mechanism for FD18 in reversing PTX resistance in P-gp mediated tumors *in vitro* has been demonstrated in previous studies. (Chan et al., 2009) Flavonoid dimers resensitized P-gp mediated resistance through inhibiting P-gp transport of drugs. To further study this proposed mechanism, an *in vivo* PTX accumulation study was performed. LCC6/MDR xenografts were pretreated with 45 mg/kg FD18 in 0-hour followed by treatment of PTX at 40 mg/kg at 1-hour. A relatively higher amount of PTX was used to ensure a detectable level of PTX in the tumor within a short period of time. Animals were terminated and tumors were excised at 7-hour. Excised tumors were homogenized and extracted for PTX for HPLC measurements. Treatment with PTX alone, PTX + FD18 solvent and PTX + FD18 resulted in 4347 ± 398, 3847 ± 720 and 7861 ± 701 (ng PTX/g of tissue ± SEM) respectively. (Figure 3.6)

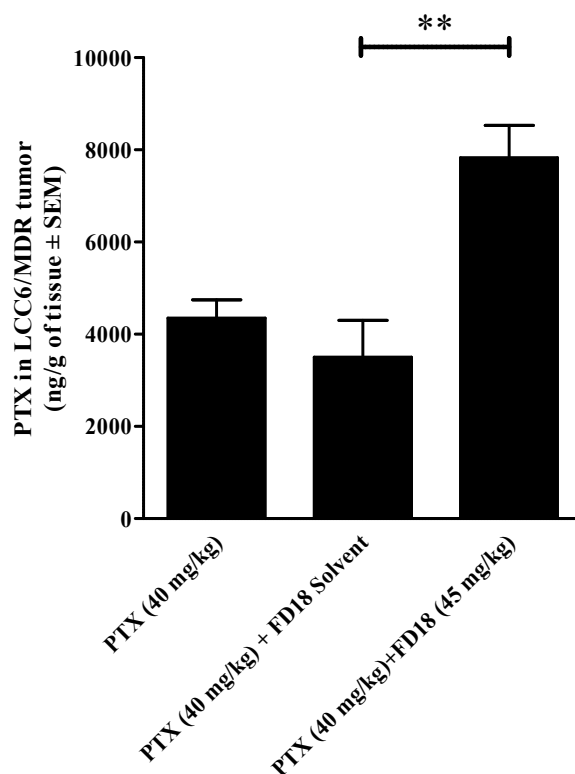


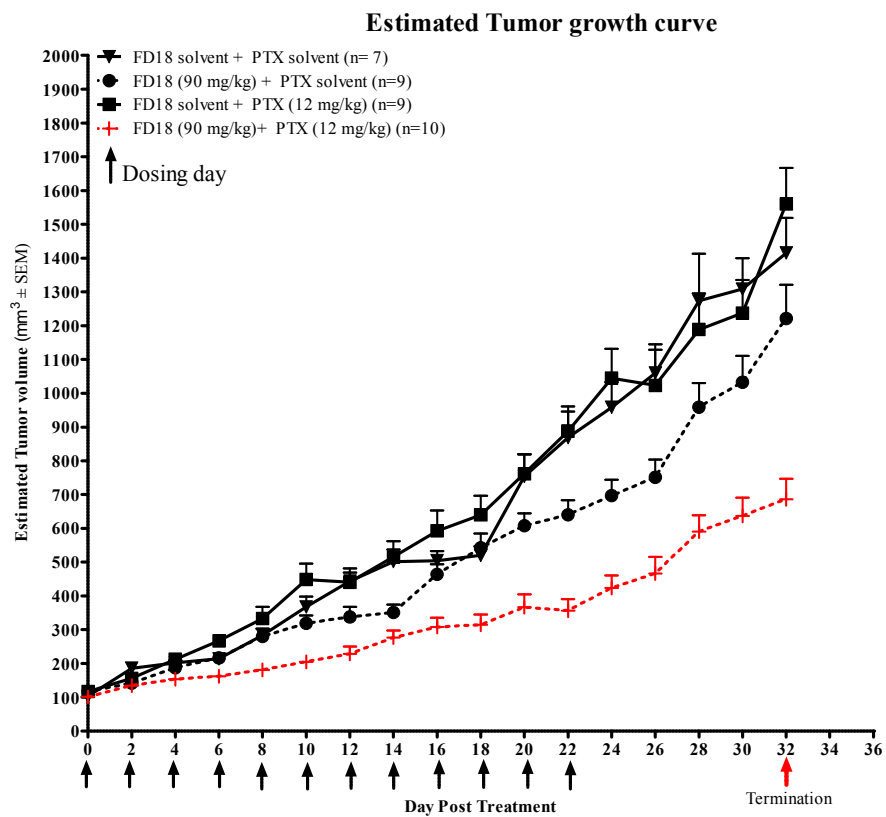
Figure 3.6 *In vivo* PTX accumulation in tumor after FD18 treatment. PTX (40 mg/kg), together with FD18 solvent or FD18 at 45 mg/kg were administered to LCC6/MDR tumor bearing mice at 0 and 1-hour respectively. Mice were sacrificed and tumors were excised for PTX level measurement through HPLC analysis. Independent experiment N=3.

### 3.3.7 Dose optimization of FD18 in reversing P-gp mediated PTX resistance in LCC6/MDR xenografts

A dose escalation of FD18 was performed using 90 mg/kg administered twice. (Figure 3.7 and Table 3.10) Treatment of solvent, FD18 and PTX alone has no significant modulating effect with tumor volumes on day 32 at  $1415 \pm 104$ ,  $1221 \pm 99$  and  $1560 \pm 106 \text{ mm}^3$  respectively. Tumor doubling times from these controls were about 9 days. On

the contrary, when LCC6/MDR tumors were treated with FD18 at 90 mg/kg together with PTX at 12 mg/kg, tumor growth on day 32 was significantly reduced to  $686 \pm 60\text{mm}^3$  ( $p < 0.01$ ). Tumor doubling time was also from 9 to 12 days. (Figure 3.7A, Table 4.10) %T-C value of FD18 (90 mg/kg) + PTX treatment group was 51% (Table 3.10), which was highly comparable FD18 (45 mg/kg) + PTX (Table 3.8) (%T-C = 54%). In addition, treatment of FD18 at 90 mg/kg induced toxicity. Although body weight changes were not affected (Figure 3.7C); two out of ten animals died on day 12 and 14 accordingly. (Figure 3.7D) Results in here implied that, FD18, even though acting as a safe and promising P-gp inhibitor; should not be used at such a high dose. Besides, with only a slight improvement in treatment outcome, the usage of FD18 at 45 mg/kg but not 90 mg/kg in combination of PTX 12 mg/kg seemed to be optimal under current setting.

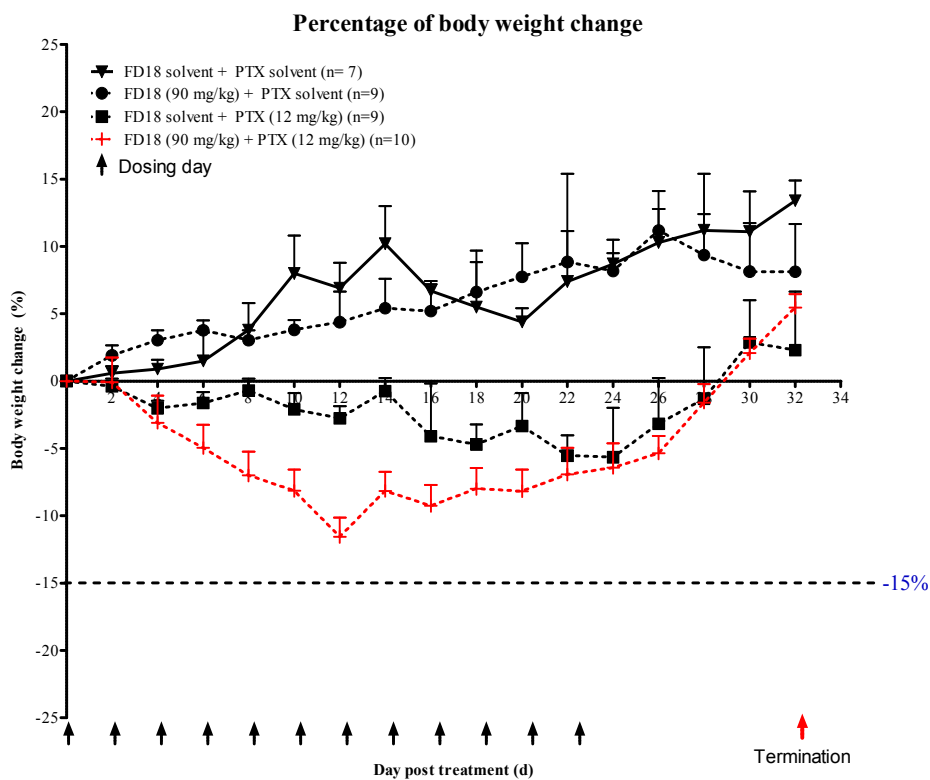
A



B



C



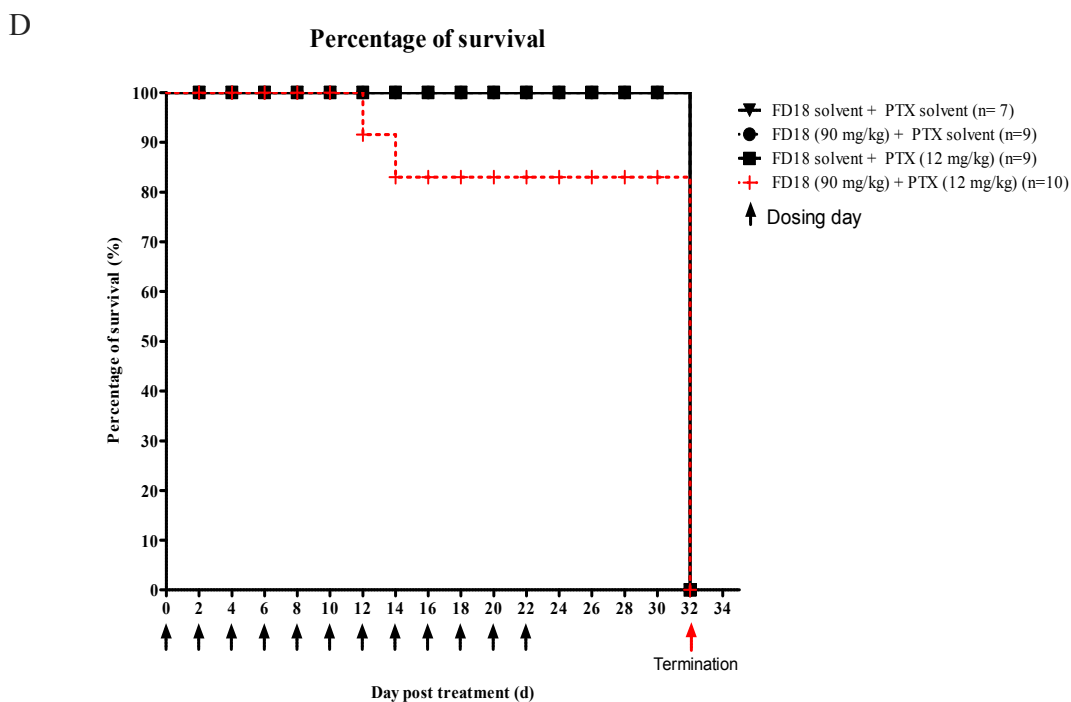


Figure 3.7 Dose optimization of FD18 in treating LCC6/MDR xenografts towards PTX. (A) Estimated tumor volume curve. Tumor volumes were measured on every other day. (B) Tumor image. Tumors obtained on day 32 after termination were arranged according to their sizes. (C) Percentage of body weight change. Weight of each animal was monitored on every other day and expressed in percentage. (D) Survival curve. Survival of animals were monitored every day and expressed in survival percentage.

Table 3.10 Summary of dose optimization of FD18 in treating LCC6/MDR towards PTX.

Treatment	Tumor volume (mm <sup>3</sup> ± SEM)	Tumor doubling time(T <sub>d</sub> ) (days ± SEM)	Tumor inhibition (%) (VS solvent control)
FD18 solvent + PTX solvent	1415 ± 104	9 ± 0.4	-
FD18 (90 mg/kg) + PTX solvent	1221 ± 99	9 ± 0.4	14
FD18 solvent + PTX (12 mg/kg)	1560 ± 106	9 ± 0.3	ND
FD18 (90 mg/kg) + PTX (12mg/kg)	686 ± 60	12 ± 0.5	51

Data obtained from Figure 4.8 were summarized and statistically compared in terms of tumor volumes, tumor doubling days. %T-C was calculated to evaluate treatment efficacies. (\*\* p<0.01), ND: Not determine

### 3.4 Discussion

Extensive flavonoid homodimer candidate screening process and lead optimization work have been done by Chow's laboratory previously. (Chan et al., 2006; Chan et al., 2009; Chan et al., 2012) An obstacle from the original selected compounds (compound 2 – 4) is their poor aqueous solubility; this resulted in precipitation *in vivo* (data not shown). In here, the lead compound, FD18, together with its derivatives; had great improvements towards solubility. Such improvement was done by the introduction of amine group to the PEG linker. These newly-synthesized compounds were first compared for their *in vitro* reversing activities and their toxicities. Derivatives of FD18, unlike other tested modulators, were able to maintain their activities on P-gp inhibition. In addition, it has been reported that a good P-gp inhibitor should possess a higher hydrophobicity. (Pe´rez-Victoria et al., 1999) The benzyl group attached on the amine group in FD18 is very hydrophobic, yet not too bulky, making it ideal as a desirable P-gp inhibitor.

Pharmacokinetics study was one of the approaches to study the pharmacological properties of these dimers using FD18 as a model. After an i.p. injection of 45 mg/kg; it was found to be bioavailable. Plasma concentration of FD18 exceeded its EC<sub>50</sub> level (148 nM) for almost 10-hour. The toxicity of FD18 and its derivatives were evaluated through short term toxicity study and histopathological study. Modulators at 45 mg/kg together with PTX treatment at 12 mg/kg, did not cause severe toxicities in general. Nevertheless, modulators 4Ph, diF and 2F showed toxic responses as revealed by weight loss greater than 15% for three or more consecutive days. Interestingly, the 4Ph and 2F were found causing auricular chondritis in treated animals. Auricular chondritis is associated with clinical symptoms of redness and swelling of ear cartilage and sometimes causing pain to

animals. Such condition would ultimately lead to the deformation of both ear pinnae. Studies have shown that this pathological condition could occur spontaneously in mice or rats due to nearby metal ion release from metal ear tags or arouse from autoimmune disease. (Kitagaki and Hirota, 2007; Meingassner, 1991; Prieur et al., 1984; Cremer et al., 1981) Since metal ear tags were not used in all animal studies and the study of drug treatment leading to any autoimmune responses was beyond the scope of study. The only observation could be noted in here was the attachment of a phenyl group at C4 position or a fluoride group at C2 position on the benzyl ring at the linker resulted in such observation. Present toxicological results suggested 4Ph, diF and 2F are too toxic for further studies.

Paclitaxel, although acting as a potent anticancer agent; was known to be associated with animal toxicities including cardiotoxicity, manifested by hypotension and arrhythmias (Menna et al., 2008); nephrotoxicity, resulting in atrophy at glomerulus and surrounding tubular structures (Rabah, 2009); and hepatotoxicity such as hepatitis, polymorphism of hepatocytes and necrosis of cells. (Ermolaeva et al., 2008) Some of these toxicological features may only be revealed by studying the histological changes on cells from organ tissue samples. For this, histological studies of vital organs were performed. Treatment of PTX induced some histological changes to liver, heart and kidney, yet not to a severe extent. Additional treatments by selected modulators did not potentiate these effects, but providing an overall protection to these organs, reflecting these flavonoid dimers were safe to be used.

Herein, *in vivo* P-gp modulation activities of selected modulators have been compared. FD18, being the most potent candidate among these flavonoid dimers, was very safe to

animals even under such frequent dosing schedule. Contrary to its derivatives which gave comparable activities, all of them shown either toxicity weight loss or deaths. It was surprising that these treatment-induced toxicity symptoms were not shown in non-tumor bearing mice; however, xenografted animals had become more sensitive to treatments. Same phenomenon was also observed in PSC833 treated animals, with a little toxicity in non-tumor bearing mice but then a severe toxicity has been developed in xenografted mice.

Because *in vitro* study suggested that the working mechanism of FD18 was through competitive inhibition to P-gp, leading to intracellular accumulation of anticancer drugs and thus exerts killing effects. (Chan et al., 2012) To explore if FD18 would share the same mode of action, an *in vivo* tumor accumulation study was conducted. It was observed that FD18 co-treatment also increase PTX accumulation in tumor. FD18 enters the systemic circulation and traveled to tumor site, modulated these P-gp overexpressed tumor cells and caused intracellular deposition of PTX, resulted in tumor growth inhibition.

Having shown that FD18 at 45 mg/kg treated with PTX has given promising results, an attempt of using FD18 at double dose was applied. It was initially expected that a better treatment response would be observed under such dose regimen. Unfortunately, overall treatment improvement was only modest, together with the induction of toxicity responses, making such idea not feasible.

In comparison to other P-gp inhibitors, such as XR9576 (Tariquidar) (Martin et al., 1999) and LY335979 (Zosuquidar) (Dantzig et al., 2001); FD18 exerts similar modulating

activity. Tariquidar was used to treat MDR overexpressed human ovarian carcinoma at 10 mg/kg (i.v.) and PTX at 15 mg/kg in three injections; with an inhibitory effect of tumor growth at approximately 50%. Zosuquidar, being used at 30 mg/kg (i.p.) together with 20 mg/kg PTX in 5 days treatment, has produced a less potent inhibitory effect of 40% towards MDR resistance human non-small cell lung cancer. FD18, administered at 45 mg/kg (i.p.) with a decreased amount of PTX (12 mg/kg) for twelve injections, was effective in treating LCC6/MDR tumors, within a tumor inhibition percentage of 54%. It was debatable that the results obtained from FD18 was only at a moderate level when compared to these two modulators, however, clinical studies revealed that there were rooms left for the development of FD18. Zosuquidar was once being tested in Acute Myeloid Leukemia (AML) and recurrent breast cancer patients, unfortunately clinical study showed no improvements on disease progression. (Cripe et al., 2010, Ruff et al., 2009) Tariquidar, also displays limited ability in treating breast cancer which failed to give treatment response with anthracyclines or taxanes. (Puztai et al., 2005) By and large, FD18 is a safe, bioavailable and a promising novel P-gp modulator when it was used at 45 mg/kg with PTX.

## **Chapter 4**

### **Activity characterization of FD18 metabolite, FM04**

## 4.1 Introduction

Understanding the *in vivo* properties of potential drug candidates is essential in drug discovery and development prior to clinical trials. These properties, including absorption, distribution, metabolism and excretion (ADME), were equally important as potency. Drug candidates involved in clinical trials often failed or delayed for commercialization due to poor efficacy, toxicity and inadequate characterizations of drug metabolism and pharmacokinetics (DMPK). (White, 2000) Therefore, the study of ADME, in particular DMPK would provide important information in selection of lead compounds for clinical trials.

Metabolism is the mechanism of elimination of foreign and undesirable compounds from the body and the control of levels of desirable compounds in the body (Gunaratna, 2001) It governed the performance and safety of a drug by modifying the physicochemical, pharmacological, physiological and toxicological properties, resulting in drug metabolites became either activated (in the case of prodrug) or deactivated, toxification or detoxified. (Kirchmair et al., 2015) The process of drug metabolism involved two steps, phase I and II. In phase I metabolic reactions, drug molecules will undergo modifications such as oxidation, reduction and hydrolysis, aiming to increase aqueous solubility of a drug for the ease of elimination. These modifications usually require a number of catalytic enzymes such the cytochrome P450 (CYP) and flavin-containing monooxygenases (FMOs) (Baranczewski et al. 2006) Phase II metabolic reactions referred to the addition of functional groups by conjugation for example glucuronidation, sulfation, the conjugation with amino acid or glutathione. The conjugation process usually further

enhance the aqueous solubility thus facilitate the excretion process via urination and bile production. (Gunaratna, 2000) By understanding the metabolic properties of a drug, it can help to optimize the stability thus affect the *in vivo* risk-benefit ratio. (Kirchmair et al., 2015)

#### 4.1.1 *In vitro* working mechanism of FD18 and its metabolic study

In chapter 4, FD18 was proven to give effective P-gp modulations *in vivo* towards PTX resistant xenografts. Toxicological and histopathological studies also supported that FD18 is a safe P-gp inhibitor suitable for further investigations. Subsequent studies of possible working mechanism and metabolism of FD18 have been conducted understand further. (Chan et al., 2012; Kan, PhD thesis, 2015)

First, FD18 was tested for its P-gp ATPase activity. It was hypothesized that if FD18 is binding to the substrate recognition site of P-gp, ATPase would be stimulated. In the contrary, if it binds to the NBD, ATPase activity would be diminished. Result showed that FD18 was able to stimulate P-gp ATPase activity, suggesting FD18 is binding to the substrate recognition site. (Chan et al., 2012) In subsequent kinetic assays, FD18 was demonstrated as a competitive inhibitor to DOX with a  $K_i$  of  $0.3\mu\text{M}$ . Further to this, FD18 was also able to inhibit DOX transport through intracellular DOX accumulation assay. Intracellular accumulation of FD18, however, resulted in the retention in LCC6 cells but not LCC6MDR, suggesting the expression of P-gp can eliminate the accumulated FD18; supporting FD18 as a substrate to P-gp. (Chan et al., 2012)

Metabolic study of FD18 was conducted by incubation in rat and human liver microsomes in the presence of NADPH followed by mass spectrometry analysis. The metabolic

pathway of FD18 has resulted in three metabolites namely, 14a, FM327 and FM04. (Figure 4.1)

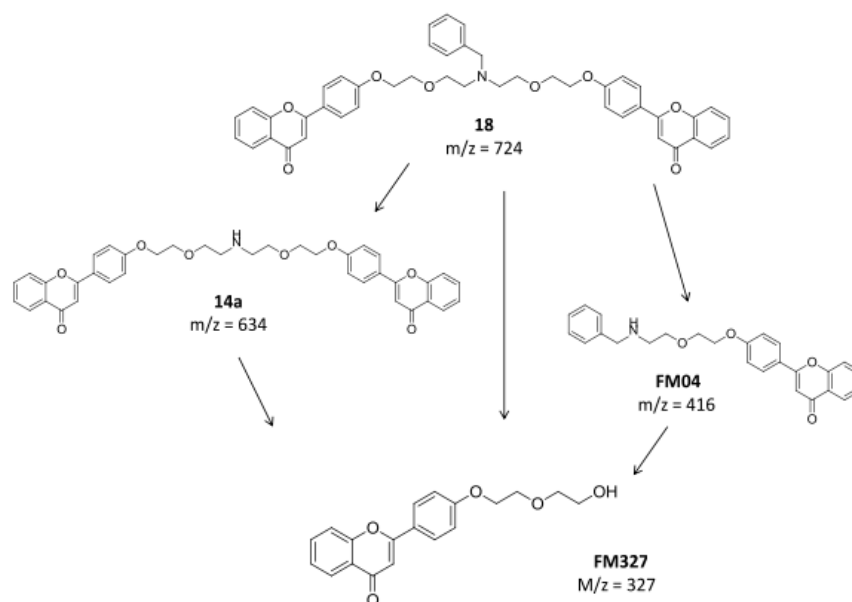


Figure 4.1 A proposed metabolic pathway for FD18. (Kan, PhD thesis, 2015)

The three metabolites were tested for their *in vitro* P-gp modulating potencies and cytotoxicities towards a series of anticancer drugs. A summary of results is shown in Table 4.1. with the metabolite 14a has an  $EC_{50}$  towards PTX at  $305 \pm 35$  nM, which is less active than the parent compound FD18. (Chan et al., 2012) Another metabolite, FM327 was also found to be inactive in reversing PTX resistance in LCC6/MDR cells therefore was not investigated further. It was surprising that the third metabolite, FM04, was more potent with an  $EC_{50}$  of  $70 \pm 26$  nM compared to the parent compound FD18 ( $148 \pm 18$  nM). Apart from this, cytotoxicity study in L929 fibroblast also suggests FM04 is less toxic than FD18. This led to a greater selective index of  $>471$ , compared to FD18

(574). It is possible that FD18 exerts dual effects can either modulates P-gp directly, and or after metabolism in the hepatic system, became metabolized to FM04 and continue to modulate P-gp., FM04 may once again enters the blood circulation and modulate P-gp. Having a wider therapeutic window with enhanced aqueous solubility, FM04 was being investigated further for its PK properties here.

Table 4.1 Summary table for *in vitro* P-gp modulation activity studies of FD18 and its metabolites.

Compound	EC <sub>50</sub> in reversing resistance of LCC6/MDR towards various anticancer drugs (nM ± SEM)						Cytotoxicity in L929 cells (μM ± SEM)	Selective Index
	PTX	VBL	VCR	DOX	DNR	MTX		
FD18	148 ± 18	173 ± 27	179 ± 32	131 ± 13	95 ± 25	90 ± 20	85 ± 5	574.3
14a	305 ± 35	ND	ND	ND	ND	ND	5.9 ± 0.6	19.3
FM327	>1000	ND	ND	ND	ND	ND	ND	ND
FM04	70 ± 26	61 ± 13	83 ± 11	153 ± 39	88 ± 52	64 ± 27	> 33	>471

FD18 and its metabolites were tested at 1 μM for its *in vitro* reversal activities in LCC6/MDR human cancer cells with a selection of anticancer drugs. Cytotoxicity of each compound was tested in L929 murine fibroblasts. Selective index was determined by the ratio between the IC<sub>50</sub> of L929/EC<sub>50</sub> of LCC6/MDR towards PTX. Independent experiment of N=1-7; ND; Not determined.

#### 4.1.2 Pharmacokinetic properties of FM04

Herein, the pharmacokinetic properties of FM04 were studied with the use of Balb/c mice model. (Figure 4.2) Intraperitoneal injection of FM04 at 28 mg/kg (identical molar concentration as FD18 at 45 mg/kg) resulted in a  $C_{max}$  of 3400 ng/mL at 5-minute ( $T_{max}$ ). Plasma level exceeds its  $EC_{50}$  of 76nM (32ng/mL) for about 4 hours. Bioavailability of i.p. injection of FM04 was 24.3%. In view of the enhanced aqueous solubility, FM04 was able to formulate in aqueous solution (5% ethanol, 95% saline; v/v), which favored both injection and oral gavage. Oral dosing of FM04 at 100 mg/kg in mice was found to be absorbable and bioavailable, resulted in a  $C_{max}$  of 1500 ng/mL at 30-minute ( $T_{max}$ ) and a bioavailability of 5.3%. Similarly, it was also found to have plasma concentration exceeding the  $EC_{50}$  of FM04 for more than 10 hours. A notable delay of  $T_{max}$  was probably due to the CYP450 metabolism in gastrointestinal tract. (Kan, PhD thesis, 2015)

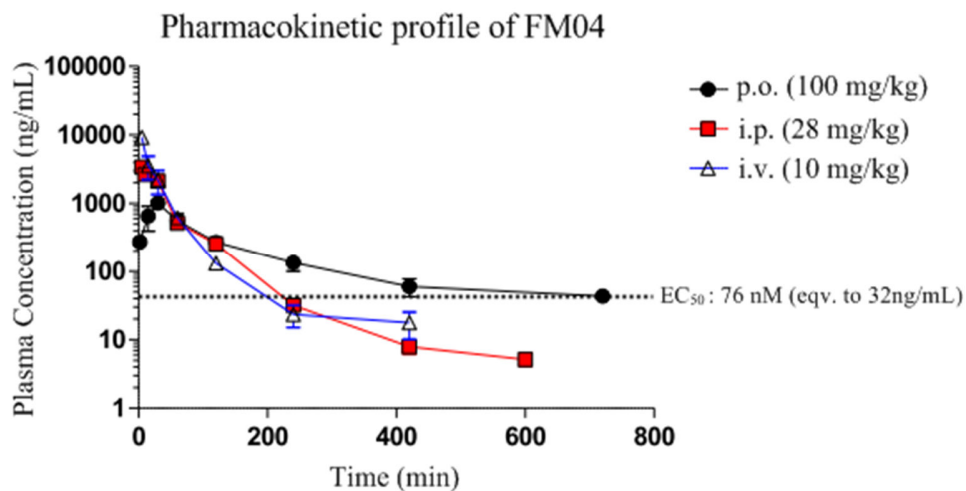


Figure 4.2 Pharmacokinetic profile of FM04. FM04 was administered via oral (100 mg/kg), intraperitoneal (28 mg/kg) and intravenous (10 mg/kg) route into Balb/c mice. At each time point, blood samples were obtained through cardiac puncture followed by mass spectrometry analysis with deuterium-FM04 as internal standard. Data on the plot were expressed in mean  $\pm$  SEM; independent experiments N=4-7. (Kan, PhD thesis, 2015)

In comparison with i.p. administration of FD18 at 45 mg/kg, the same molar concentration of FM04 at 28 mg/kg generated an even higher  $C_{max}$  compared to FD18 (2354 ng/mL). Although the retention time for the plasma concentration exceeding  $EC_{50}$  for FM04 is shorter than FD18 at 600 minutes, the greatly-improved *in vitro* P-gp modulation activities and increased aqueous solubility would compensate for the shorter half-life.

## 4.2 Materials and methods

### 4.2.1 *In vitro* P-gp ATPase activity study

P-gp ATPase activity was measured with the P-gp Glo assay system (Promega) with human P-gp membrane, the experimental procedures and conditions were carried out according to manufacturer's protocol. Briefly, recombinant human P-gp (25  $\mu$ g) was

incubated in the presence of 5 mM MgATP with various treatments: (1) No treatment control, (2) 100  $\mu$ M Na<sub>3</sub>VO<sub>4</sub> (3) 1% DMSO (4) 200  $\mu$ M Verapamil (5) - (8) 20 to 80  $\mu$ M FD18 and (9) – (12) 20 to 80  $\mu$ M FM04 at 37 °C for 40-minute. After the incubation period, the reaction was quenched and the remaining level of unmetabolized ATP reacted was by the addition of ATP detection reagent followed by an additional 20-minute incubation time at room temperature. The luminescence signal was subsequently measured with CLARIOstar multimode microplate reader (BMG Labtech). ATPase activity was presented as a difference in luminescence of samples compared to that treated with sodium vanadate and expressed in relative luminescence unit (RLU). A net increase or decrease of luminescence signal indicates the stimulation and inhibition of P-gp ATPase respectively.

#### **4.2.2 Effect of FD18 and FM04 on intracellular DOX accumulation in LCC6/MDR cells**

In a 6-well plate, 1 x10<sup>5</sup> cells of LCC6 or LCC6/MDR cells were seeded in each well in 2 mL with DMEM medium with 10% FBS. After 24-hour, medium from each well was removed and 2 mL of fresh DMEM medium (without FBS) with various concentrations of FM04 or FD18 were added. The cells were then incubated for 30-minute at 37 °C. A final concentration of 20  $\mu$ M DOX and various concentrations of flavonoid dimer (final concentration 0.015 to 10  $\mu$ M) were then added and incubated for 2-hour at 37°C. The cells were then harvested by trypsinization. Trypsinized cells were transferred to a 2 mL eppendorf tubes wrapped by foil and washed thrice with ice cold PBS. Cell lysis was performed by using 450  $\mu$ L of 0.3 M HCl in 50% ethanol and vortexed for 30 to 60-second. To remove any cell debris, each lysed samples were centrifuged at 6000g for 3

min, followed by preserving the supernatant for fluorescence measurement of DOX using a spectrofluorometer with an excitation wavelength ( $\lambda_{\text{excite}}$ ) of 470nm and an emission wavelength ( $\lambda_{\text{emit}}$ ) of 585 nm.

#### **4.2.3 Intracellular accumulation of FM04**

In an eppendorf tube,  $1 \times 10^6$  cells of LCC6 or LCC6/MDR were suspended in 1 mL DMEM medium with 10% FBS together with 1, 2.5, 5, 7.5, 10, 25 and (or) 50  $\mu\text{M}$  of FM04 followed by an incubation period of 2-hour at 37 °C with agitation. After incubation, cells were harvested and washed thrice by ice cold-PBS. Cell lysis was performed by repeated freeze and thaw cycles. To remove cell debris, the sample was centrifuged at 16000 g for 10-minute. Supernatant was transferred to a new eppendorf and stored at -20 °C until analysis. Samples were brought to mass spectrometry (LC-MS triple quadrupole) analysis for FM04 concentrations.

#### **4.2.4 Drug preparation for animal studies**

PTX was prepared at 40 mg/mL in 50% (v/v) ethanol, 50% (v/v) Cremophor EL as follow. First, dissolve 40 mg of PTX powder in 500  $\mu\text{L}$  absolute ethanol. The suspension is then placed in 80 °C water bath for 3-minute, with subsequent agitation by a vortex until a clear drug solution is formed. Equal volume of Cremophor EL is then added into the drug solution, vortex until it became clear. This stock solution is stable for over one month at room temperature. Prior to injection, stock solution is being diluted 1:10 by normal saline. Diluted drug solution should be consumed within 15-minute to avoid drug precipitation. Solvent of PTX is being prepared by mixing 5% (v/v) ethanol, 5% (v/v) Cremophor EL and 95% (v/v) normal saline in final volume of 1 mL. Stock solution of FD18, was

formulated in 13.6% cremophor EL, 13.6% Ethanol and 72.8% physiological saline (0.9%; w/v) at 4mg/mL. Solvent of FD18 was being prepared by simple mixing of 13.6% cremophor EL, 13.6% Ethanol and 72.8% physiological saline (0.9%; w/v) in final volume of 1 mL. FM04 was formulated in 5% Ethanol and 95% physiological saline (0.9%; w/v) at 4 mg/mL. Solvent of FM04 was prepared by mixing 5% Ethanol with 95% physiological saline (0.9%; w/v) in 1 mL. All modulator solutions were freshly prepared on the day of injection.

#### **4.2.5 Comparison study of FD18 and FM04 *in vivo* modulation activity**

FM04, metabolite from FD18, was compared to FD18 for *in vivo* modulation activity in LCC6/MDR xenografts. FD18 at 45 mg/kg and FM04 at 28 mg/kg were used in this study. FM04 was used at 28 mg/kg as identical molar concentration as FD18 at 45 mg/kg. (Molar mass of FD18 = 724 g/mol; FM04 = 416 g/mol) Treatment schedule, assessment criteria were identical as described in chapter 3.

## 4.3 Results

### 4.3.1 *In vitro* P-gp ATPase activity assay

The P-gp ATPase activity study was performed first in order to examine if FM04 is a substrate of P-gp. If FM04 behave similarly to FD18 and acting as a substrate to P-gp, it shall stimulate ATPase activity by binding itself towards the substrate recognition site at the substrate binding region on the transmembrane helices. Conversely, P-gp ATPase activity would be inhibited if FM04 binds to the ATPase at the NBD region. The effects of FM04 and FD18 towards P-gp ATPase is shown in Figure 4.3, with Verapamil at 200  $\mu$ M as positive control and 1% DMSO as solvent control. In previous report, FD18 acted as a stimulator to P-gp ATPase (Chan et al., 2012), the stimulatory effect of FD18 in here was reproducible. (Figure 4.3) FM04; is less potent than FD18 in stimulating P-gp ATPase. This result implies that FM04 may bind to the substrate binding site of P-gp and similar to FD18. FM04 is therefore very likely to be a substrate of P-gp.

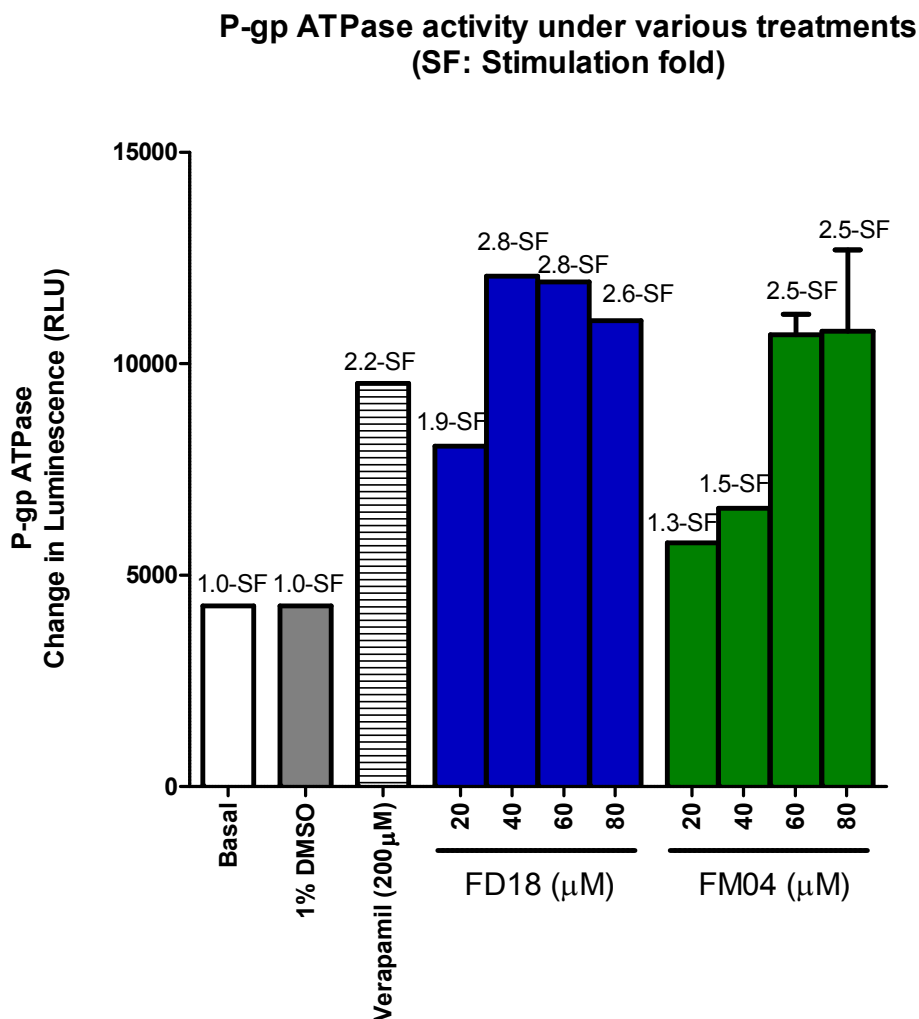


Figure 4.3 *In vitro* P-gp ATPase activity study of FM04 and FD18. Microsomes containing recombinant human P-gp were incubated for 2-hour at 37 °C under a series of FD18 or FM04 concentration, with Verapamil at 200 μM and 1% DMSO as positive and solvent control respectively. Subsequent to incubation, the level of the remaining ATP within the reaction system was measure through luminescence changes. Changes in signals represents either a stimulatory (positive gain) or an inhibitory (negative loss) actions to P-gp ATPase. Results were normalized to the basal activity and presented as stimulation fold (SF). Data expressed in mean ± SEM; N = 1-2 independent experiments.

### 4.3.2 Effect of FD18 and FM04 on intracellular DOX accumulation in LCC6/MDR cells

Effect of FM04 on intracellular DOX accumulation assay was investigated. (Figure 4.4) LCC6 cells accumulated 2.3-fold more DOX than LCC6/MDR cells. Co-treatment with VER, FD18 or FM04 can increase DOX accumulation in LCC/MDR in a dose dependent manner. (Figure 4.4) This comparable to previous study of FD18.

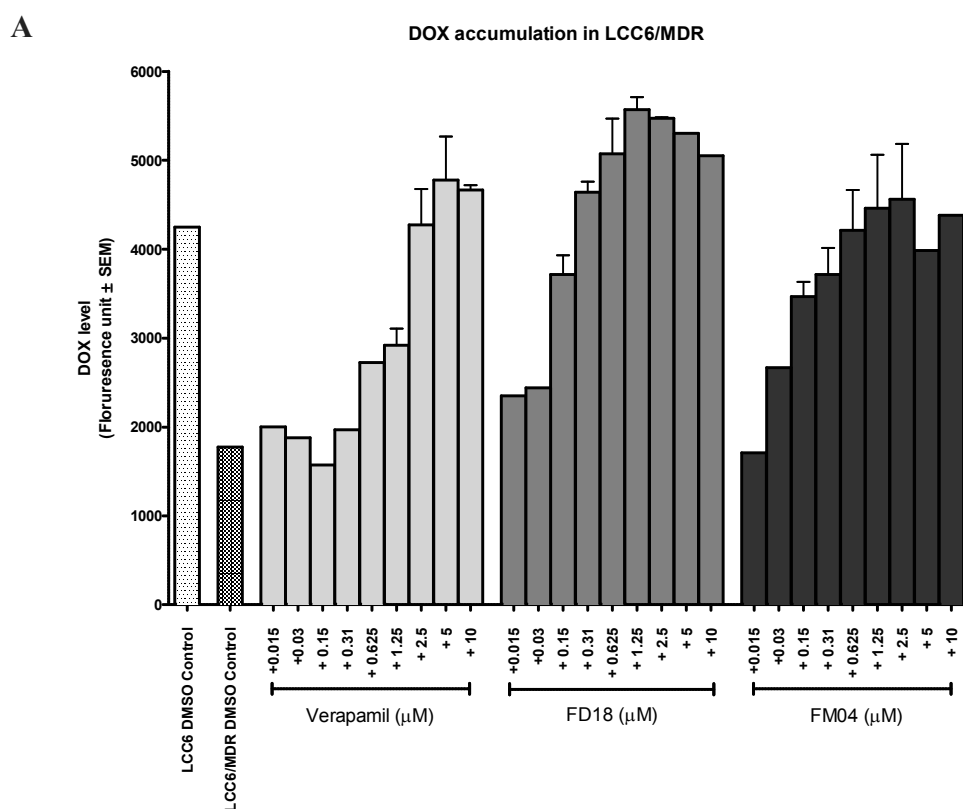


Figure 4.4 Effect of FD18 and FM04 on intracellular DOX accumulation in LCC6/MDR cells. LCC6/MDR cells were incubated under various concentrations of FD18, FM04 or Verapamil (VER) for 2 hours in the presence of 20  $\mu$ M DOX. Cells were washed and lysed after the incubation period. Supernatant after cell lysis was collected for the measurement of DOX level. All modulators were dissolved in 1% DMSO. DMSO (1%) was served as negative control. DOX level were expressed in fluorescence  $\pm$  SEM; independent experiments N=2-3.

### 4.3.3 Intracellular accumulation of FM04

It would be ideal that FM04 is not effluxed by P-gp, thereby allowing it to accumulate to exert its inhibitory effect. It was found that FM04 accumulated at a higher level in both LCC6 and LCC6/MDR cells (Figure 4.5), suggesting that FM04 is not effluxed by P-gp.

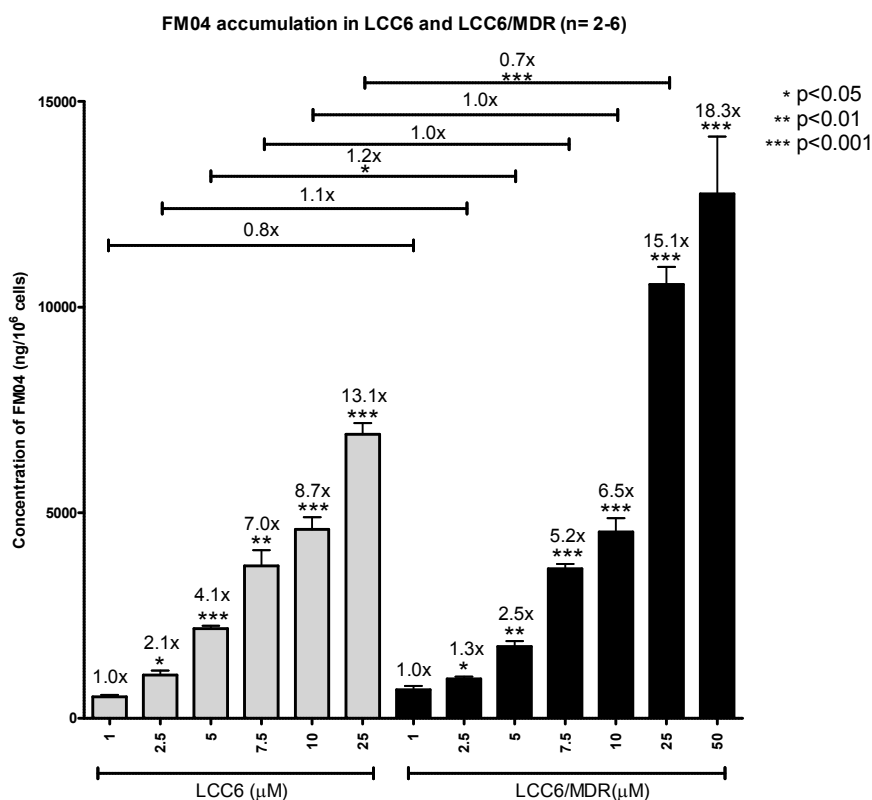


Figure 4.5 Intracellular accumulation of FM04 in LCC6 and LCC6/MDR cells. LCC6 or LCC6/MDR cells were incubated with a series of concentration of FM04 for 2-hour at 37 °C. Subsequent to incubation, cells were washed and lysed. The concentration of FM04 from the supernatant was measured by mass spectrometry and expressed in ng/10<sup>6</sup> cells. Fold changes of each sample was calculated by dividing the concentration of FM04 measured in treated samples to the concentration of FM04 measured from sample treated with 1 μM of FM04. Fold change between LCC6 and LCC6/MDR under the same treated concentration was also being calculated by dividing the concentration of FM04 in LCC6 cells by the concentration of FM04 in LCC6/MDR cells. Data expressed in mean ± SEM; N=2-6 independent experiments. Statistical analysis was done by using Student's t-test, \* p<0.05; \*\* p<0.01; \*\*\* p<0.001.

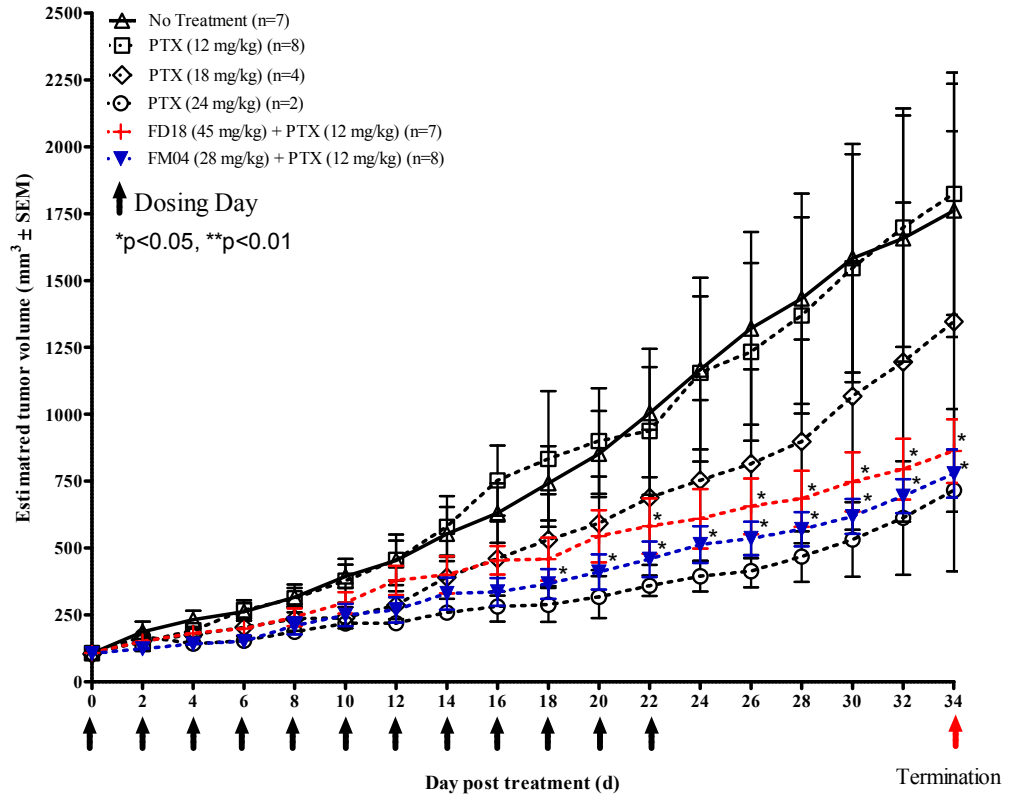
#### 4.3.4 *In vivo* comparison study of FD18 and FM04 in treating PTX resistance tumor bearing mice

*In vivo* efficacy of FM04 was measured. (Figure 4.6 A to D) Untreated tumor size reached  $1761 \pm 443 \text{ mm}^3$  on the day of termination (day 34). Treatments with 12 or 18 mg/kg of PTX resulted in tumor sizes of  $1824 \pm 453 \text{ mm}^3$  and  $1347 \pm 503 \text{ mm}^3$  respectively, indicating PTX under these dose regimens were relatively ineffective. Animals treated at higher dosages of PTX (24 mg/kg) resulting in tumor volume of  $716 \pm 151 \text{ mm}^3$  at the end of experiment. Co-treatment with FM04 or FD18 with PTX at 12 mg/kg resulted in a significant tumor growth inhibition with tumor volume of  $778 \pm 91 \text{ mm}^3$  and  $863 \pm 112 \text{ mm}^3$  on day 34. Tumor doubling time were also extended from 10 days (in PTX 12 mg/kg group) to 12 days. (Table 4.2) Comparing the efficacy between FM04 and FD18, the %T-C from FM04 treatment was calculated as 57%, which is 4% higher than FD18 treatment. In summary, FM04 at the same molar concentration to FD18, is demonstrating a slightly better potency.

No significant weight loss (Figure 4C) or animal deaths (Figure 4D) was recorded for FD18 + PTX or FM04 + PTX groups. Current results suggested that PTX, even up to the MTD level, could not overcome the PTX resistance arisen from LCC6/MDR tumors and causes toxicity in the animals. In contrast, treatments comprised of same molar concentration of FD18 (45 mg/kg) or FM04 (28 mg/kg) together with PTX as low as 12 mg/kg has successfully demonstrated promising outcomes. PTX resistant tumors were resensitized towards PTX treatment without causing any treatment related toxicities. This result suggests that both FD18 and FM04 are effective *in vivo* with no noticeable toxicity effect. FM04 would be better than FD18, in term of its solubility and dosing amount.

A

Estimated tumor growth curve



B



No Treatment

PTX (12 mg/kg)

PTX (18 mg/kg)

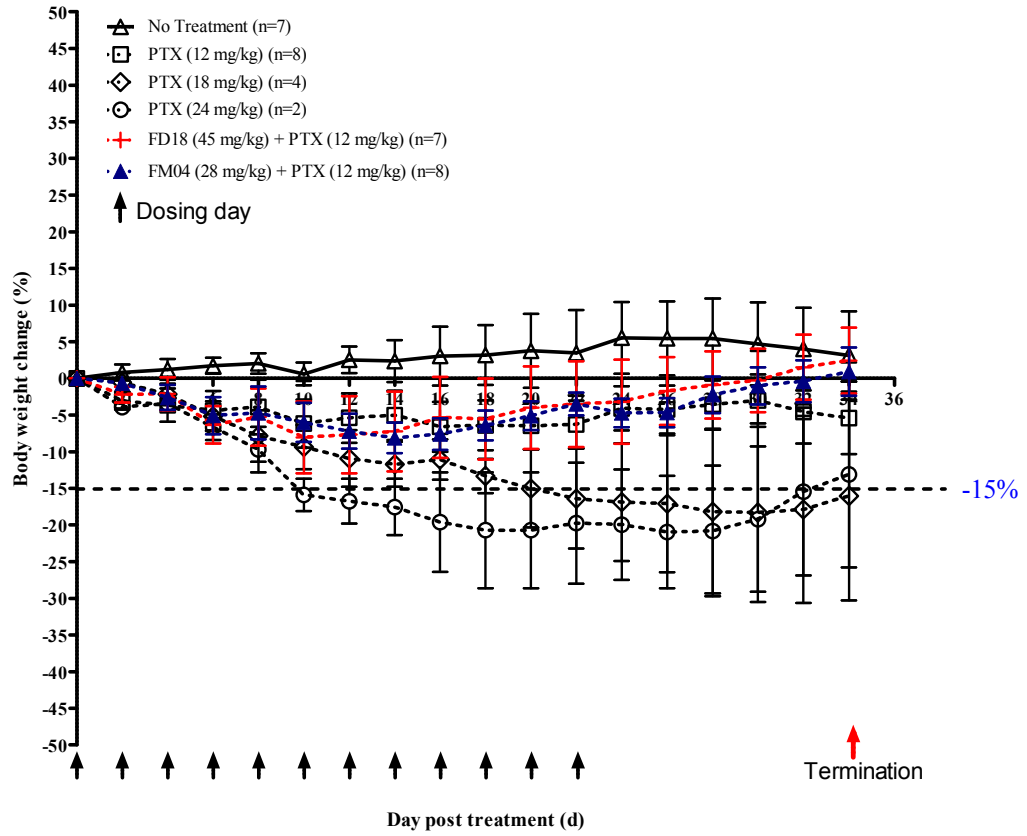
PTX (24 mg/kg)

FD18 (45 mg/kg) +PTX (12 mg/kg)

FM04 (28 mg/kg) + PTX (12 mg/kg)

C

Percentage of body weight change



D

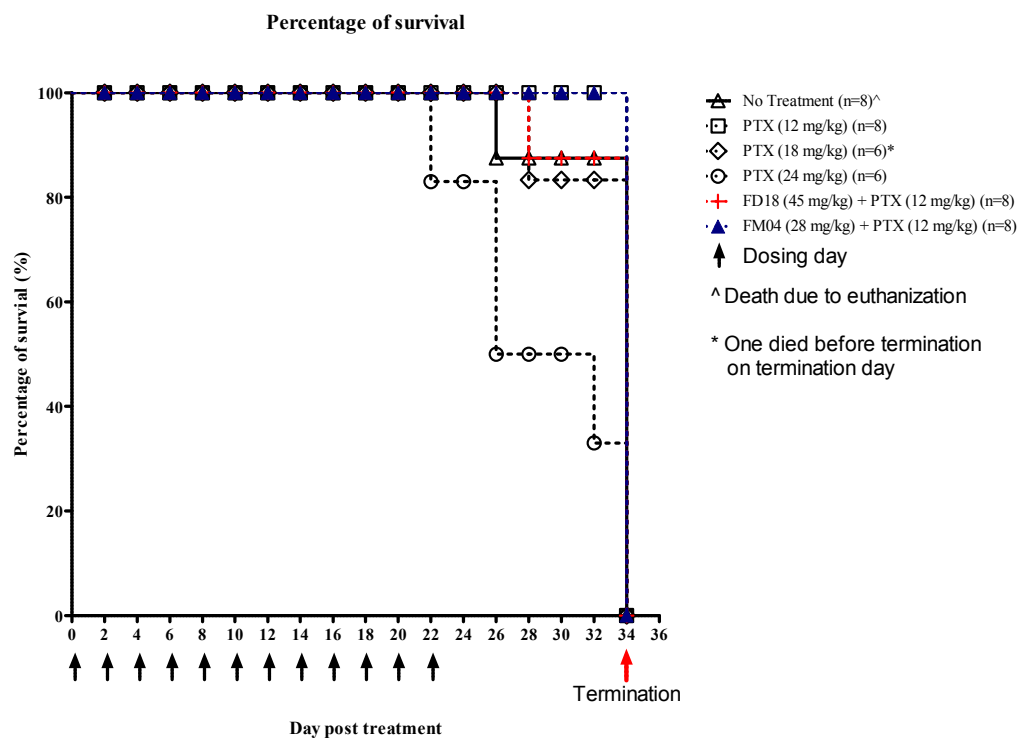


Figure 4.6 *In vivo* modulating activity of FM04 towards P-gp mediated PTX resistance. (A) Estimated tumor volume curve. Tumor volumes were measured on every other day. (B) Tumor image. Tumors obtained on day 32 after termination were aligned according to their sizes. (C) Percentage of body weight change. Weight of each animal was monitored on every other day, change of weight were expressed in percentage and plotted against days. (D) Survival curve. Survival of animals were monitored every day, expressed in survival percentage. Data expressed in mean  $\pm$  SEM. N=6-8 per treatment group.

Table 4.2 Summary of *in vivo* modulating activity of FM04.

Treatment	Tumor volume (mm <sup>3</sup> ± SEM)	Tumor doubling time (T <sub>d</sub> ) (days ± SEM)	Tumor inhibition (%) (VS no treatment)
No Treatment	1761 ± 443	9 ± 0.7	-
PTX 12 mg/kg	1824 ± 453	10 ± 0.9	-
PTX 18 mg/kg	1347 ± 503	12 ± 0.5	24
PTX 24 mg/kg	716	14	ND
FD18 45 mg/kg+ PTX 12 mg/kg	863 ± 112	12 ± 0.8	53
FM04 28 mg/kg + PTX 12 mg/kg	778 ± 91	12 ± 0.8	56

Data obtained from Figure 4.5A were summarized and statistically compared in terms of tumor volumes, tumor doubling days. %T-C was calculated to evaluate treatment efficacies. Statistical analysis was done by one-way-ANOVA \*p<0.05, NS; Not significant, ND; Not Determine.

#### 4.4 Discussion

ADME properties of a novel drug candidate can provide information to predict its safety profile. Metabolites may be either inactive with increased hydrophilicity which promotes excretion through urination (phase I reactions) or became conjugated for bile or urine elimination (phase II reaction). In some cases, drug metabolites might have different pharmacological properties compared to its parental compound. They may become a new and less toxic drug. (Gunaratna, 2000)

FD18 is metabolized into 14a, FM327 and FM04. (Kan, PhD thesis, 2015) These metabolites have decreased hydrophobicity and manifested distinct pharmacological attributes. Compound 14a was a direct metabolite of FD18 (Chan et al., 2012) with reduced P-gp activity and displayed cellular toxicity in L929 fibroblasts. Metabolite FM327 has a poor pharmacological efficacy when compared to FD18. Interestingly, metabolite FM04 was more potent and water soluble.

In this chapter, FM04 was studied in more details. FM04 is likely to be a substrate of P-gp because it can stimulate P-gp ATPase and was able to inhibit the transport of DOX in LCC6/MDR cells. FM04 accumulated to the same level in both LCC6 and LCC6/MDR cells. Base on this result, FM04 appears to be a substrate of P-gp yet cannot be pumped. In a separate study done by Kan from Chow's laboratory in searching how FM04 may influence cellular uptake of PTX in transwell assay over 120 minutes (data not shown); it was observed that FM04 was able to be uptaken rapidly (> 80%) from apical side. On the other hand, only a small percentage (< 25%) of FM04 was being absorbed by the Caco-2 cells from basal side and only about 5% of it was effluxed back into the apical side. Results from this study support the notion that FM04 cannot be pumped by P-gp once it has been uptaken. In addition, it was previously illustrated by Clark's research team that cellular confinement of small molecules in P-gp substrate binding side can cause constant stimulation of P-gp ATPase. (Loo et al., 2003) As a result, it is possible for FM04 may be trapped in LCC6/MDR cells and continuously stimulate P-gp ATPase.

FM04 produced a slightly better *in vivo* efficacy in reversing PTX resistance compared to its parent compound (FD18). In addition, animals from FM04 + PTX treatment group were as healthy as in FD18 + PTX treatment group as reflected by animal body weight changes and animal survival. Animals receiving co-treatment of either FM04 or FD18 with PTX resulted in comparable efficacies to that of PTX treatment at 24 mg/kg. Nonetheless, the latter caused severe toxicities with marked weight loss of greater than 15% during treatment period and a death incidence of nearly 65%. This result illustrates the safety advantage of using co-treatment of FD18 or FM04 + PTX over higher doses of PTX. FM04 has several advantages, namely improved potency and metabolic stability

and increased hydrophilicity, allowing FM04 to become water soluble (in 5% ethanol) and the use of CreEL is not necessary.

To investigate the druggability of FM04 and FD18, one can use the popular Lipinski's rules of 5 (Ro5). (Lipinski et al., 1997) A lead chemical which is has a potential to become a drug relies on the following: (1) Molecular weight (MW) is smaller than 500; (2) A calculated logarithm of the octanol–water partition coefficient ( $clogP$ ) is smaller than 5; (3) Less than 5 hydrogen bond (H-bond) donor (expressed in –OHs and –NHs) and (4) Less than 10 H-bond acceptors (expressed in –Os and –Ns). (Lipinski et al., 1997) With reference to these guidelines, FM04, which has a MW of 416 g/mol (724 g/mol for FD18);  $clogP$  at 4.06 (7.07 for FD18); only 1 H-bond donor (same as FD18) and 5 H-bond acceptors (9 for FD18) (Kan, PhD thesis, 2015), FM04 seemed to be more druggable than FD18. Kan has demonstrated the inhibition of GI tract P-gp through p.o. administration of FM04. This resulted in a 7-fold increase of PTX absorption through Balb/c mice GI tract and giving therapeutic responses to wild type LCC6 nude mice xenografts. (Kan, PhD thesis, 2015)

The current findings suggested that FM04 can be used in the form of injections, targeting P-gp overexpressing tumors directly and resensitize it towards certain anticancer drugs (PTX in our case); or to be administered orally as an inhibitor to GI tract P-gp, leading to the absorption of drug that were previously not bioavailable through oral dosing. Together with the non-toxic and water soluble nature of FM04, it has high potential to be further developed.

## **Chapter 5**

### **Conclusion and future perspectives**

## 5.1 Summary of work

The major obstacle in cancer treatment is the emergence of MDR mediated by P-gp especially in recurrent tumors. Lots of efforts have been spent in searching for solutions to overcome such phenomenon but to no avail. Some P-gp inhibitors had excellent preclinical potency however failed in subsequent clinical trials thus dashing hope in the community. (Cripe et al., 2010; Pusztai et al. 2005; Planting et al., 2004; Kuppens et al., 2007; Ruffet al., 2009) The aim of current study is an extension to previous work in searching for a new class of P-gp inhibitor based on synthetic flavonoid dimer. (Chan et al., 2006; Chan et al., 2009; Chan et al., 2012)

Because of the pseudodimeric structure of P-gp (Aller et al., 2009), libraries of flavonoid dimers have been synthesized with the goal of improving its potency and specificity. Not only can these dimers reverse MDR mediated by P-gp in human cancer cells, they also have anti-leishmanial activities. (Wong et al., 2012; Wong et al., 2014) A number of these compounds had gone through series of *in vitro* high throughput screenings for the selection of suitable candidates in reversing P-gp mediated MDR.

In early generations, such as 9d (Chan et al., 2006), 61, 62 and 69 (Chan et al., 2009), lead compounds were having good *in vitro* P-gp modulation activities. However, due to high hydrophobicities thus difficulties of solubilizing in aqueous formulation, they could not be proceeded further for *in vivo* characterizations. A major breakthrough has been achieved after the modification of 61 at the PEG linker position by the introduction of an amine group. The resulting compound, FD18, has great improvement in aqueous solubility and an increased biological activity ( $EC_{50} = 148\text{nM}$  towards PTX). Apart from

these, the safety of FD18 has been revealed by *in vitro* cytotoxicity that FD18 did not cause toxicity in murine fibroblasts ( $IC_{50} > 85 \mu M$ ), leading to a selective index of 574. (Chan et al., 2012) Further pharmacokinetic study also showed that FD18 can achieve a plasma concentration higher than  $EC_{50}$  for nearly 10 hours. (Kan, PhD thesis, 2015; Yan et al., 2016)

To characterize FD18 *in vivo*, two human cancer xenografts of LCC6 and LCC6/MDR have been established as assay platforms. Validation of these xenografts has been done through the examination of P-gp expression in tumors and the treatment of PTX at 12 mg/kg (q.o.d. x4 for 2-cycle). LCC6 xenograft P-gp negative and therefore PTX-sensitive. On the other hand, LCC6/MDR tumor are positive and resistant PTX treatment, such model can be used as a P-gp-mediate MDR animal model.

Hereafter, a series of derivatives were synthesized based on FD18 and were tested for *in vivo* toxicity and efficacies. Some of these derivatives were excluded due to the induction of toxicities in healthy Balb/c mice, including severe weight loss of >15% (diF, 2F, 4Ph) and auricular chodritis in some cases (2F, 4Ph). The remaining derivatives (4MeO, 4Cl and N-Pip), together with FD18, were investigated further for their *in vivo* efficacies. Results obtained from efficacy suggested that FD18, at a dosage of 45 mg/kg in combination with PTX at 12 mg/kg (q.o.d. x 12), was the most potent candidate (% T-C = 54%) among all lead compounds and did not cause toxicities in tumor bearing mice. Doubling the dose of FD18 to 90 mg/kg, however, proved to be too toxic.

FM04 is an active metabolite of FD18. *In vitro* characterization of FM04 demonstrated a 50% increase in potency with  $EC_{50}$  towards PTX at 70 nM. Moreover, FM04 behaves

similarly to FD18 in LCC6/MDR cell line which displayed reversing abilities to a panel of anticancer drugs and inhibition to DOX transport. FM04 was also a P-gp substrate although it cannot be pumped by P-gp, making it an even better modulator. Not to mention that FM04 is smaller and more water soluble.

FM04 at 28 mg/kg, when used together with 12 mg/kg PTX, demonstrated slightly better tumor growth inhibition (56%) than FD18 at 45 mg/kg (53%), comparable to that of treatment with PTX at 24 mg/kg, but without causing any observable treatment related toxicity. Apart from this, the degree of druglikeness from FM04 suggests that it is a better drug candidate than FD18.

In summary, lead optimizations of flavonoid compounds have resulted in the production of FD18 which exhibits promising *in vivo* P-gp modulation in a safe manner. The possible working mechanism of FD18 is through direct binding to the substrate binding site of P-gp, therefore inhibited the transport of accumulated intracellular drug back into cytoplasmic region and eventually sensitized resistant cells and tumors. (Chan et al., 2012) DMPK studies revealed FD18 was able to be maintained within the systemic circulation at EC<sub>50</sub> level for more than 10 hours. One of its metabolites, FM04, was found to be a P-gp modulator concomitant with significant improvements of P-gp reversing ability compared to FD18. The current study was completed with an *in vivo* efficacy comparison between FM04 and FD18, showing FM04 was able to resensitize LCC6/MDR tumors towards PTX and resulted in better efficacy than FD18 at the same molar concentration.

## 5.2 Importance of current study

P-gp inhibitors have failed in clinical trials, new P-gp inhibitors are needed. Up to date, the use of flavonoid dimers as P-gp modulators is a feasible approach. The discovery of novel flavonoid dimer FD18 has opened up a new gateway in the field of P-gp inhibitor research. With subsequent discovery of FM04, an even more potent P-gp inhibitor with improved aqueous solubility. It offered a two-way usage in P-gp inhibition by reversing cancer MDR and facilitating oral absorption of non-bioavailable drugs.

## 5.3 Future work

Current mechanistic study of FM04 is still far from completed, further studies are needed; including kinetics study to provide further information to understand the mode of action and to identify the exact binding site of FM04 on P-gp.

Only one xenograft model of LCC6/MDR was used to evaluate the *in vivo* potency of FM04 in this project. To uncover the potential usage of FM04 in treating other resistant cancer types conferred by P-gp, additional xenograft models can be setup. Combination of FM04 with other first line chemotherapeutic agents such as docetaxel for non-small cell lung cancer and DOX for breast cancer treatment may help in expanding the application spectrum of FM04.

## 5.4 Conclusion

Current work demonstrated that FD18, as a dimeric flavonoid P-gp modulator, can reverse P-gp mediated PTX resistance *in vitro* and *in vivo* with the use of a human breast cancer xenograft model. It may become a new class of safe and potent P-gp modulator to be used

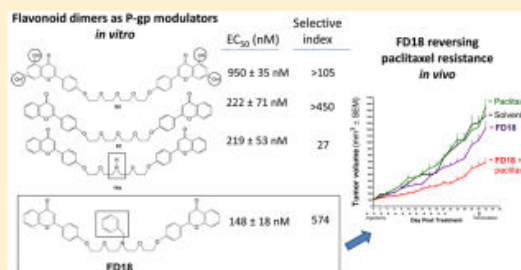
clinically for reversing MDR in cancer. The metabolite FM04 was a druggable metabolite of FD18. It maintains treatment efficacy as FD18, it can also be used orally to inhibit GI tract P-gp in order to facilitate the absorption of chemotherapeutic agents that could not be orally absorbed.

## Appendix 1 Publication

A New Class of Safe, Potent, and Specific P-gp Modulator: Flavonoid Dimer FD18 Reverses P-gp-Mediated Multidrug Resistance in Human Breast Xenograft *in Vivo*Clare S. W. Yan,<sup>†,§</sup> Iris L. K. Wong,<sup>†,§</sup> Kin-Fai Chan,<sup>†</sup> Jason W. Y. Kan,<sup>†</sup> Tsz Cheung Chong,<sup>†</sup> Man Chun Law,<sup>†</sup> Yunzhe Zhao,<sup>†</sup> Shun Wan Chan,<sup>†</sup> Tak Hang Chan,<sup>\*,†,‡</sup> and Larry M. C. Chow<sup>\*,†,‡</sup><sup>†</sup>Department of Applied Biology and Chemical Technology and State Key Laboratory of Chirosciences, Hong Kong Polytechnic University, Hong Kong SAR, China<sup>‡</sup>Department of Chemistry, McGill University, Montreal, Quebec H3A 2K6, Canada

**ABSTRACT:** Flavonoid dimer FD18 is a new class of dimeric P-gp modulator that can reverse cancer drug resistance. FD18 is a potent ( $EC_{50} = 148$  nM for paclitaxel), safe (selective index = 574), and selective P-glycoprotein (P-gp) modulator. FD18 can modulate multidrug resistance toward paclitaxel, vinblastine, vincristine, doxorubicin, daunorubicin, and mitoxantrone in human breast cancer LCC6MDR *in vitro*. FD18 ( $1 \mu\text{M}$ ) can revert chemosensitivity of LCC6MDR back to parental LCC6 level. FD18 was 11- to 46-fold more potent than verapamil. FD18 ( $1 \mu\text{M}$ ) can increase accumulation of doxorubicin by 2.7-fold, daunorubicin (2.1-fold), and rhodamine 123 (5.2-fold) in LCC6MDR. FD18 inhibited P-gp-mediated doxorubicin efflux and has no effect on influx. FD18 at  $1 \mu\text{M}$  did not affect the protein expression level of P-gp. Pharmacokinetics studies indicated that intraperitoneal administration of 45 mg/kg FD18 was enough to maintain a plasma level above  $EC_{50}$  (148 nM) for more than 600 min. Toxicity studies with FD18 (90 mg/kg, i.p. for 12 times in 22 days) with paclitaxel (12 mg/kg, i.v. for 12 times in 22 days) revealed no obvious toxicity or death in mice. *In vivo* efficacy studies indicated that FD18 (45 mg/kg, i.p. for 12 times in 22 days) together with paclitaxel (12 mg/kg, i.v. for 12 times in 22 days) resulted in a 46% reduction in LCC6MDR xenograft volume ( $n = 11$ ;  $648 \pm 84$  mm<sup>3</sup>) compared to paclitaxel control ( $n = 8$ ;  $1201 \pm 118$  mm<sup>3</sup>). There were no animal deaths or significant drop in body weight and vital organ wet weight. FD18 can increase paclitaxel accumulation in LCC6MDR xenograft by 1.8- to 2.2-fold. The present study suggests that FD18 represents a new class of safe and potent P-gp modulator *in vivo*.

**KEYWORDS:** multidrug resistance, P-glycoprotein, flavonoid, dimers



## INTRODUCTION

The phenomenon of multidrug resistance (MDR) was first described by Biedler et al. in an *in vitro*-selected actinomycin D-resistant CHO cell line<sup>1</sup> followed by Ling and co-workers in 1976 with the discovery of the cause of MDR due to overexpression of a membrane permeability glycoprotein (P-glycoprotein, P-gp).<sup>2,3</sup> P-gp, encoded by *ABCBI*, belongs to the ATP binding cassette (ABC) transporter family.<sup>4</sup> It is expressed in liver, kidney, small intestine, and blood–brain barrier. Such localization allows P-gp to function as transporter for nutrients, biologically important molecules, and some harmful xenobiotics in and out of the cell.<sup>5</sup>

More than 40% of the breast tumor has overexpression of P-gp. Hormone treatment or chemotherapy further increases the propensity of P-gp overexpression. These patients are three times more likely to fail in chemotherapy than those who do not.<sup>6</sup> There was a positive relationship between P-gp overexpression and MDR in clinical samples.<sup>7</sup> In order to reverse MDR in clinical cases, many groups have developed P-

gp modulators since 1980s. PSC833 was one of the most potent P-gp modulators *in vitro* and *in vivo*.<sup>8,9</sup> Although PSC833 was a highly potent and specific P-gp modulator and has no immunosuppression activity like cyclosporine A did, clinical trials revealed no significant advantage of PSC833 in prolonging overall survival of patients.<sup>10</sup>

Flavonoid is a large group of polyphenolic chemicals, which can be found in plants, vegetables, and fruits. Our group has been interested in developing synthetic flavonoid dimers<sup>11–17</sup> and derivatives as a new class of potent, safe and specific P-gp modulator. The idea of developing flavonoid dimer as P-gp modulators was inspired by the polyvalency effect observed in numerous biological systems where polyvalent ligands were found to have increased affinities and specificities toward their

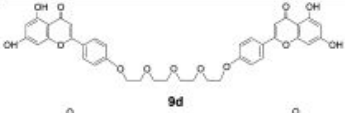
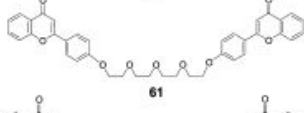
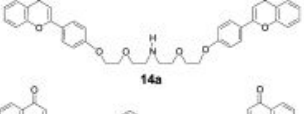
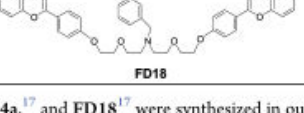
Received: November 18, 2014

Revised: August 11, 2015

Accepted: August 20, 2015

Published: August 20, 2015

Table 1. Flavonoid Dimers Modulate P-gp Mediated PTX Resistance in LCC6MDR Cells<sup>a</sup>

Flavonoid dimers	EC <sub>50</sub> towards PTX (nM)	Cytotoxicity towards L929 (μM)	Selective index	Reference
 9d	950 ± 35	>100	>105	11
 61	222 ± 71	>100	>450	13
 14a	219 ± 53	6 ± 1	27	17
 FD18	148 ± 18	85 ± 5	574	17 and here

<sup>a</sup>Flavonoid dimers **9d**,<sup>11</sup> **61**,<sup>13</sup> **14a**,<sup>17</sup> and **FD18**<sup>17</sup> were synthesized in our research group and characterized for their P-gp modulating activity. IC<sub>50</sub> of LCC6MDR cells toward PTX was measured in the presence of serial dilutions of flavonoid dimers. EC<sub>50</sub> is defined as the concentration of flavonoid dimers needed to reduce the IC<sub>50</sub> of PTX of LCC6MDR by 50%. Toxicity of flavonoid dimers toward normal mouse fibroblasts L929 was also measured. The ratio of IC<sub>50</sub> of the flavonoid dimer toward L929 fibroblasts to EC<sub>50</sub> for reversing PTX resistance is defined as selective index.

receptor compared to monovalent ligands.<sup>18–20</sup> First generation synthetic flavonoid dimers with polyethylene glycol (PEG) as linker were shown to have a higher P-gp modulating activity, compared to monomers, in human breast cancer cell line (LCC6MDR).<sup>11</sup> This proved that the bivalency approach was effective in increasing the potency of flavonoids. Subsequently, we have extended the same bivalency approach to the modulation of another ABC transporter, MRP1.<sup>21</sup> Furthermore, lead optimization has progressively improved the efficacy and selective index of flavonoid dimers in modulating paclitaxel (PTX) resistance in LCC6MDR cells *in vitro*. EC<sub>50</sub> (defined as the concentration of modulator used that can reduce IC<sub>50</sub> of the anticancer drug of LCC6MDR cells by 50%) has improved from 950 nM in the first generation apigenin dimer **9d**,<sup>11</sup> to 222 nM in the dehydroxylated flavonoid dimer **61**<sup>13</sup> (Table 1). However, compound **61** was sparingly soluble in water. Introduction of an amine group into the PEG linker improved both the aqueous solubility as well as the modulating activity. An EC<sub>50</sub> of 219 nM was observed for the flavonoid dimer **14a**<sup>17</sup> (Table 1). Selective index of **14a** can be further increased from 27 to 574 when a benzyl group was added to the amine linker to yield compound **FD18**<sup>17</sup> (Table 1). Among different amine-linked flavonoid dimers, **FD18** appears to offer the best biological and physicochemical profile for further investigations.<sup>17</sup> Here, we have tested the *in vitro* and *in vivo* efficacy of the flavonoid dimer, **FD18**, in reversing PTX resistance in a xenograft model of breast cancer.

## MATERIALS AND METHODS

**Reagents and Drugs.** All drugs and common reagents were purchased from Sigma-Aldrich. PSC833 is a generous gift of Novartis. Paclitaxel (semisynthetic, >98%) was purchased from Wuhan Hezhong Biochemical Manufacture Co, Ltd., Wuhan, China.

**Cell Culture.** The human breast cancer cell lines LCC6 and LCC6MDR were kindly provided by Dr. Robert Clarke

(Georgetown University, United States). LCC6 and LCC6MDR cell lines were cultured in supplemented DMEM media with 10% heat inactivated FBS, 100 U/mL penicillin, and 100 μg/mL of streptomycin. They were maintained at 37 °C in a humidified atmosphere with 5% CO<sub>2</sub>. The cells were split when a confluent monolayer was formed. To split cells, the plate was washed briefly with phosphate-buffered saline (PBS), treated with 0.05% trypsin-EDTA, and harvested by centrifugation.<sup>13</sup>

**Cell Proliferation Assay.** Cells (6500) of LCC6MDR were seeded in each well of 96-well plate and incubated with or without 1 μM of modulator and a series concentration of anticancer drugs (including PTX, vinblastine, vincristine, DOX, DNR, and mitoxantrone) at 37 °C for 5 days. After 5 days incubation, the % of survival was determined by MTS method as reported previously.<sup>17</sup>

**Drug Accumulation Assay.** Drug accumulation assay was carried out according to the reported procedures.<sup>13</sup> Briefly, 1 × 10<sup>6</sup> cells of LCC6 and LCC6MDR cells were incubated with the modulator (either 1 μM of **FD18** or verapamil) and drug [either 20 μM doxorubicin (DOX), 5 μg/mL rhodamine 123 (R123), or 3.6 μM daunorubicin (DNR)] for 150 min at 37 °C. DMSO (0.5%) was used as a negative control. After incubation, cells were washed, lysed with lysis buffer (0.75 M HCl, 0.2% Triton-X100 in isopropanol), and fluorescence level of DOX determined by fluorescence spectrophotometer (excites at 460 nm and emits at 610 nm). The fluorescence level of R123 and DNR in the lysate was determined using an excitation and an emission wavelength pair of 485 and 520 nm.

**DOX Influx and Efflux Studies.** To measure the DOX influx, LCC6 and LCC6MDR cells were coincubated with DOX (8 μM) and **FD18** (1 or 3 μM) in the supplemented DMEM media at 37 °C. DMSO (0.15%) was used as negative control. Cells were harvested after 0, 15, 30, 45, 60, and 75 min for intracellular DOX level determination as described above. To measure DOX efflux, LCC6 and LCC6MDR cells were

incubated in supplemented DMEM containing 20  $\mu\text{M}$  DOX for 2 h at 37 °C. Cells were then washed and further incubated with or without FD18 (1 or 3  $\mu\text{M}$ ). At 0, 15, 30, 60, 90, 120, 150, and 180 min, cells were harvested for measuring the intracellular DOX concentration.

**Western Blot Analysis.** LCC6 and LCC6MDR cells were incubated with 1  $\mu\text{M}$  FD18 for 0 h, 2 h, and 5 days, respectively. After incubation,  $1 \times 10^6$  cells were washed with PBS and harvested by trypsinization. The cell pellet was lysed with 100  $\mu\text{L}$  of lysis buffer (50 mM Tris-HCl pH8.0, 150 mM NaCl, 1.0% NP-40, 0.5% sodium deoxycholate, 0.1% SDS, and 0.2 mM PMSF) for 30 min at 4 °C. After 30 min, the cell suspension was centrifuged at 14 000 rpm for 10 min at 4 °C. The protein concentration of supernatant was determined by Bio-Rad Bradford reagent.

Twenty micrograms of cell lysate was incubated at room temperature for 10 min in Laemmli's sample buffer prior to SDS-PAGE and electroblotting onto Immobilon-P transfer membrane (Millipore). The membrane was cut into half at the size of 75 kDa and blocked with 5% nonfat dry milk (in 0.05% Tween-20, 10 mM Tris, and 150 mM NaCl, pH 7.5) for 1 h at room temperature. The membrane with protein greater than 75 kDa was probed with polyclonal rabbit P-gp antibody (1:500, AB-1, Oncogene Science) at room temperature for 1 h. Another membrane with protein smaller than 75 kDa was probed with monoclonal mouse beta-actin antibody (1:1000, Santa Cruz Technology) at room temperature for 1 h. After incubation, the membranes were washed thrice with washing buffer (0.05% Tween 20, 10 mM Tris, and 150 mM NaCl, pH 7.5). Afterward, the membranes were incubated with 1:3000 dilution of antimouse or antirabbit horseradish peroxidase-conjugated secondary antibody (Santa Cruz Technology) at room temperature for 1 h. After incubation, the membranes were washed thrice with washing buffer and detected with enhanced chemiluminescence Western blotting reagent (Pierce) according to the manufacturer's protocol. Chemiluminescence signal was quantified by ImageJ software.

**Preparation of FD18, PTX, and PSC833 Stocks for *In Vivo* Studies.** A stock solution of 4 mg/mL FD18 was prepared as follows. Four milligrams of FD18 powder was added to 140  $\mu\text{L}$  of normal saline (0.9%) and heated at 80 °C for 5 min with rapid mixing until a milky suspension was formed. The suspension was brought to room temperature. One hundred and forty microliters of ethanol and 140  $\mu\text{L}$  of Cremophor EL were added with continuous mixing until a clear solution was formed. Finally, 580  $\mu\text{L}$  of saline was added. This stock of FD18 has a concentration of 4 mg/mL in 14% ethanol, 14% Cremophor EL, and 72% normal saline. The solution was prepared on the day of use and was stable for 7 days in ambient condition. A stock of 40 mg/mL PTX was prepared as follows. Forty milligrams of PTX was dissolved in 500  $\mu\text{L}$  of ethanol and 500  $\mu\text{L}$  of Cremophor EL to give a stock solution of 40 mg/mL in 50% ethanol and 50% Cremophor EL. Freshly before injection into animals, this stock was diluted 10-fold with saline to give 4 mg/mL in 5% ethanol, 5% Cremophor EL, and 90% normal saline. Such solution was used within 30 min from its dilution to avoid precipitation. PSC833 stock was prepared by dissolving 10 mg of PSC833 in 650  $\mu\text{L}$  of Cremophor EL and 350  $\mu\text{L}$  of ethanol to give a final stock concentration of 10 mg/mL PSC 833 in 65% Cremophor EL and 35% ethanol.

**Pharmacokinetic Studies.** Forty-five milligrams per kilogram FD18 was administered to female Balb/c mice through intraperitoneal (i.p.) injection. FD18 solution was prepared as

described above. i.p. injection of FD18 was done by a 25 G needle. Blood samples were collected in heparinized tubes by cardiac puncture after deep anesthesia by ethyl ether at 0.17, 0.5, 1, 2, 4, 7, 10, 12, and 16 h post-administration of FD18. Blood samples were centrifuged at  $16,100 \times g$  for 10 min immediately after collection to obtain blood plasma. Blood plasma was stored at  $-20$  °C until analysis. Plasma concentration data were analyzed by noncompartmental model. Area under the plasma concentration–time curve (AUC), elimination half-life ( $t_{1/2\beta}$ ), absorption half-life ( $t_{1/2\alpha}$ ), clearance (CL), maximum plasma concentration ( $C_{\text{max}}$ ), and time to maximum plasma concentration ( $T_{\text{max}}$ ) were calculated by PK Solutions 2.0 (Summit Research Service, Ashland, USA).

**High Performance Liquid Chromatography.** Separation and monitoring of FD18 in blood samples was done by HPLC-DAD. The HPLC system consisted of an Agilent 1100 pump, UV–VIS detector, and an automated sample injector with a 100  $\mu\text{L}$  loop. Chromatographic separation of FD18 was carried out by Agilent Prep-sil column (440905–901, 4.6 mm ID  $\times$  250 mm, 5  $\mu\text{M}$ ). Mobile phase consisted of hexane–methanol–ethyl acetate (45:15:40, v/v/v) with a flow rate of 1.0 mL/min. Eluent was recorded at 315 nm with reference to 450 nm.

**Balb/c nu nu Athymic Mice.** Four- to six-week-old athymic nude mice (Balb/c nu/nu), weighting between 15 and 23 g, were purchased from Laboratory Animal Unit, The University of Hong Kong and Animal and Plant Care Facilities, University of Science and Technology, Hong Kong. All mice were quarantined for 7 days before housing in a germ-free environment with a 12 h of light and 12 h of dark cycle. They were fed with sterilized food and water. All investigations were performed following the Cap 340 Animal License from Department of Health (HKSAR Government) and ethical approval from Animals Ethics Subcommittee of the Hong Kong Polytechnic University.

***In Vivo* Toxicity Evaluation Studies.** Healthy 5–7-week old female Balb/c mice were randomized into 9 groups ( $n = 5, 3, \text{ and } 2$  mice per group for groups 1–4, 5, and 6–9, respectively) according to Figure 3C. Groups 1 to 4 were (1) PTX solvent + FD18 solvent, (2) PTX solvent + FD18 (90 mg/kg, 2 injections of 45 mg/kg), (3) PTX (12 mg/kg) + FD18 solvent, and (4) PTX (12 mg/kg) + FD18 (90 mg/kg, 2 injections of 45 mg/kg). PTX was injected intravenously (i.v.) through lateral tail vein. FD18 was administered intraperitoneally (i.p.) at 1 h before and 8 h after PTX administration. Injections were made on every other day, 12 times from day 0 to day 22. For group 5: (5) PSC833 (5 mg/kg) was administered i.p. every other day from day 0 to day 8 for a total of 4 times. For groups 6 to 9: (6) PTX (4 mg/kg) + PSC833 (2.5 mg/kg), (7) PTX (4 mg/kg) + PSC833 (5 mg/kg), (8) PTX (8 mg/kg) + PSC833 (2.5 mg/kg), and (9) PTX (8 mg/kg) + PSC833 (5 mg/kg). PSC833 was administered i.p. at two different doses of 2.5 mg/kg or 5 mg/kg 1 h before PTX. PTX was administered i.v. at 4 or 8 mg/kg. Eight injections were made on days 0, 2, 4, 6, 11, 13, 15, and 17 for a total of 17 days. During and after treatment, mice were monitored for toxicity symptoms such as reduced activity level, loss of appetite, or treatment-related mortality. Weight loss of greater than 10% for three consecutive days during treatment is being considered as treatment-related toxicity; such animal will be euthanized. The remaining mice were sacrificed by cervical dislocation after anesthetization 1 week after completion of treatment to observe whether there was any delayed toxicity.

Table 2. Effects of FD18 in Modulating P-gp Mediated Resistance in LCC6MDR *in Vitro*

Anticancer drugs	IC <sub>50</sub> towards different anticancer drugs <sup>a</sup>							
	LCC6MDR	(RF) <sup>b</sup>	LCC6	(RF) <sup>b</sup>	LCC6MDR + 1.0 μM FD18	(RF) <sup>b</sup>	LCC6MDR + 1.0 μM Verapamil	(RF) <sup>b</sup>
PTX	153.1 ± 2.9	(1.0)	1.6 ± 0.3	(95.7)	1.1 ± 0.1	(139.2)	43.9 ± 2.9	(3.5)
Vinblastine	9.2 ± 1.1	(1.0)	0.21 ± 0.05	(43.0)	0.28 ± 0.04	(32.9)	2.7 ± 0.5	(3.4)
Vincristine	27.9 ± 2.7	(1.0)	0.26 ± 0.02	(108.8)	0.23 ± 0.01	(121.3)	9.5 ± 3.5	(3.0)
DOX	1040 ± 124	(1.0)	27.0 ± 4.6	(38.6)	26.7 ± 5.3	(39.0)	81.5 ± 9.7	(12.7)
Mitoxantrone	1050 ± 147	(1.0)	37.4 ± 11.7	(28.1)	18.5 ± 2.5	(56.9)	194.0 ± 48.7	(5.4)
DNR	1340 ± 227	(1.0)	22.1 ± 2.2	(60.5)	22.2 ± 1.0	(60.2)	239.0 ± 88.1	(5.6)
Cisplatin	25.9 ± 3.4	(1.0)	13.1 ± 3.3	(2.0)	20.4 ± 3.8	(1.2)	22.9	(1.1)

<sup>a</sup>IC<sub>50</sub> of PTX, vinblastine, vincristine, DOX, mitoxantrone, and DNR toward LCC6 and LCC6MDR cells were determined with or without 1.0 μM of FD18 or verapamil. IC<sub>50</sub> unit used is nM. <sup>b</sup>RF (relative fold) is defined as the ratio of IC<sub>50</sub> of LCC6MDR cells without modulator to LCC6MDR cells with modulator. Higher RF values mean higher sensitivity to that drug.

**Balb/c nu nu Mice Xenografted with LCC6MDR and Passages.** Cells ( $1-5 \times 10^7$ ) of LCC6 or LCC6MDR cells were resuspended in 200 μL of PBS and injected i.p. into each female Balb/c nu nu mouse. Cells were grown for at least two and no more than ten peritoneal passages before being inoculated subcutaneously (s.c.) onto the rear flank (either left or right) of female Balb/c nu nu mice. When a solid tumor of 200–250 mm<sup>3</sup> was formed, mice were sacrificed and tumor was excised and cut into cubes of 1 mm<sup>3</sup> and then xenografted s.c. onto the rear flank (left or right) of another female Balb/c nu nu mouse.

**In Vivo Efficacy of PTX on LCC6 and LCC6MDR Xenografted in Balb/c nu nu Mice without Modulator.** Five- to seven-week-old female Balb/c nu nu mice ( $n = 6$ ) were treated when LCC6MDR or LCC6 tumor size reached 150–200 mm<sup>3</sup>. There were two treatment groups: (1) DMSO (3.75 mL/kg, i.p.) and (2) DMSO (3.75 mL/kg, i.p., 1 h before PTX) + PTX (12 mg/kg, i.v.). Injections were made on day 0, 2, 4, 6, 11, 13, 15, and 17. Tumor growth was measured by electronic caliper on injection day, and the estimated tumor volume was calculated using the following formula:

$$\text{estimated tumor volume (mm}^3\text{)} = \frac{lw^2}{2}$$

where  $l$  stands for the longest diameter of the tumor and  $w$  is the diameter perpendicular to the longest diameter, assuming all mice carry spherically shaped tumor. Mice that show symptoms of toxicity or having tumor ulceration were terminated and were not included in the calculation of tumor volumes.

Tumor doubling time was determined using the following formula:

$$\text{tumor doubling time} = \frac{T_i \log 2}{3 \log \left( \frac{D_f}{D_i} \right)}$$

where  $T_i$  stands for interval time,  $D_f$  stands for final diameter, and  $D_i$  stands for initial diameter.

**In Vivo Efficacy of FD18 and PSC833 on Modulating PTX Resistance in LCC6MDR Xenograft.** Treatment of LCC6MDR-xenografted Balb/c female nu nu mice started when tumor volume reached about 100–150 mm<sup>3</sup>. Animals were randomized into five groups ( $n = 8$  to 11 mice per group). Treatment dosage and schedule were selected or adjusted from

the toxicity study. FD18 was adjusted to 45 mg/kg with PTX concentration remain unchanged. Concentration of PSC833 and PTX were selected at 2.5 mg/kg and 8 mg/kg, respectively. Survival and vital organ weights were recorded during treatment and after termination accordingly. Animals that experienced treatment-related mortality or have weight loss greater or equal to 10% for three or more consecutive days were euthanized. Statistical analysis on tumor volumes between control groups and treatment group was done by using one-way ANOVA with Dunnett's multiple comparison test after treatment period.

**In Vivo PTX Accumulation in Tumor.** LCC6MDR xenograft models in 5–7 weeks female Balb/c nu nu mice were setup as described above. Treatment started when the tumor reached the size of about 100 mm<sup>3</sup>. FD18 (45 mg/kg, i.p.) was being administered 1 h before PTX (40 mg/kg, i.v.), and tumor samples were collected 7 h post-PTX administration. Each excised tumor was homogenized with 1 mL of water in the presence of 50 μL docetaxel at 60 μg/mL as internal standard. The homogenate was extracted thrice for PTX using 3 mL of diethyl ether, vortexed, and centrifuged at 2700 ×  $g$  for 5 min. Supernatant was collected and dried at 80 °C. Extracted PTX samples were stored at –20 °C until HPLC analysis. Reconstitution of extracted PTX samples was performed by adding 50 μL of HPLC grade acetonitrile (ACN), followed by filtering through 0.2 μm nylon filter before HPLC analysis (C18 reverse phase column). Mobile phase of HPLC was composed of 50% ACN and 50% H<sub>2</sub>O with a flow rate of 1.0 mL/min. Eluent was monitored at 230 nm.

## RESULTS

### FD18 Modulates P-gp Mediated MDR *in Vitro*.

Compared to parental LCC6, P-gp-overexpressing LCC6MDR cells were resistant to a panel of anticancer drugs including paclitaxel (PTX), vinblastine, vincristine, doxorubicin (DOX), mitoxantrone, and daunorubicin (DNR) by 28- to 110-fold (Table 2). Treatment of LCC6MDR cells with 1 μM of FD18 lowered the IC<sub>50</sub> of LCC6MDR toward these drugs by 33- to 140-fold (Table 2). IC<sub>50</sub> was restored to a level comparable to or even lower than that of parental LCC6 cells. In comparison, verapamil at 1 μM only exhibited about 3- to 13-fold sensitization effect (Table 2). Therefore, FD18 can reverse P-gp mediated MDR and is about 11- to 46-fold more potent than verapamil.

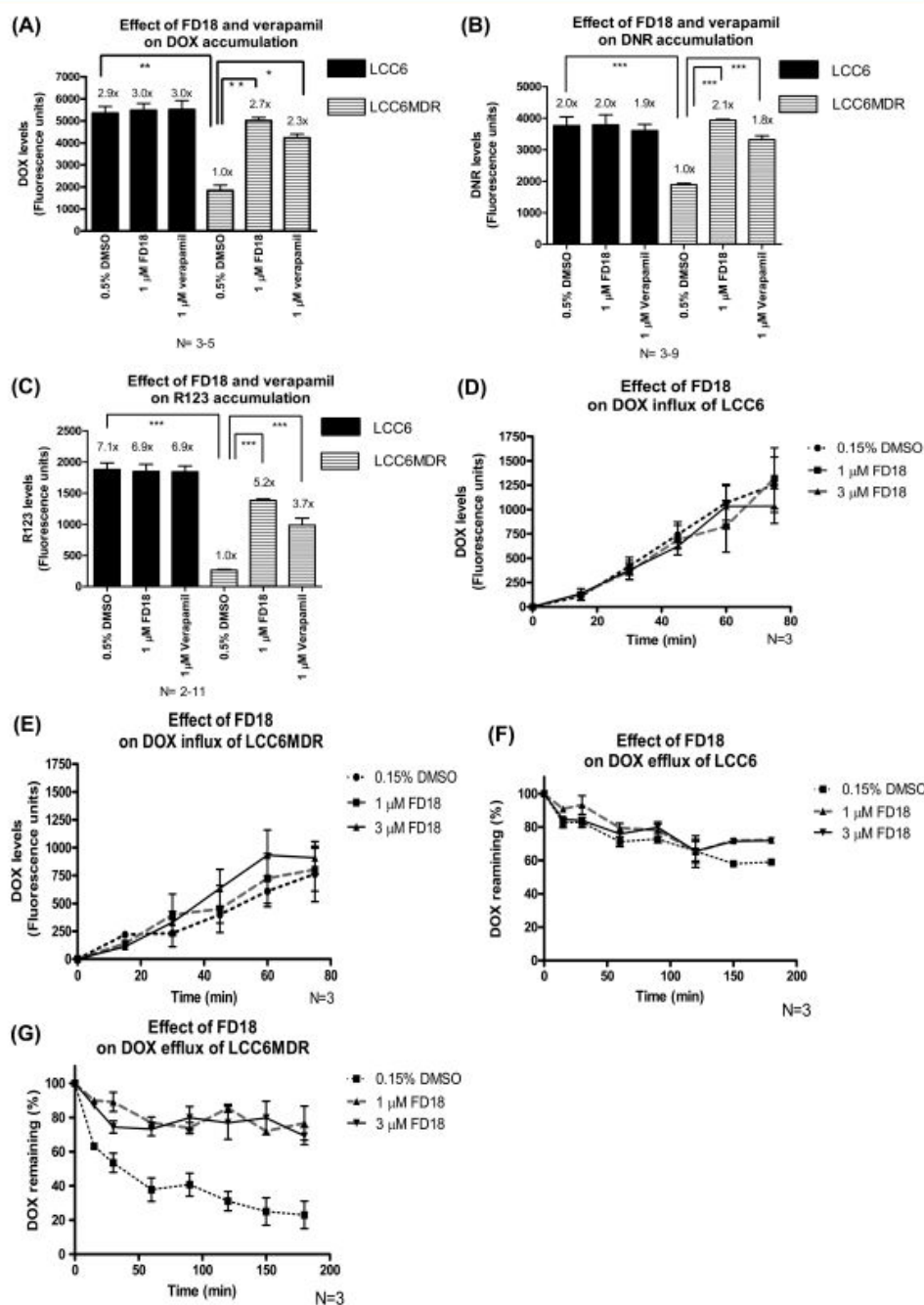


**Figure 1.** Effect of P-gp modulators on intracellular accumulation of P-gp substrates in LCC6 and LCC6MDR cells. Cells (black bars = LCC6; striped bars = LCC6MDR) were treated with 0.5% DMSO (negative control), verapamil, or FD18, followed by different P-gp substrates including DOX (A), DNR (B), or R123 (C). Intracellular accumulation was measured by spectrofluorometry.  $N = 2-11$  independent experiments. The results are presented as mean  $\pm$  standard error of mean. \* signifies  $P < 0.005$ , \*\*  $P < 0.001$ , and \*\*\*  $P < 0.0005$  relative to the negative control of LCC6MDR. Influx of DOX was measured in LCC6 (D) or LCC6MDR (E) cells in the presence of FD18 (1 or 3  $\mu$ M) or 0.15% of DMSO (negative control). Efflux of DOX was measured in LCC6 (F) or LCC6MDR (G) cells in the presence of FD18 (1 or 3  $\mu$ M) or 0.15% of DMSO (negative control). The results are presented as mean  $\pm$  standard error of mean.

**Effects of FD18 on Intracellular DOX, DNR, and R123 Accumulation in LCC6MDR Cells.** We determined whether the modulation of P-gp-mediated drug resistance by FD18 was associated with a concomitant increase in drug accumulation. Accumulation level of DOX, DNR, and rhodamine 123 (R123) in LCC6 cells were 2.9-, 2.0-, and 7.1-fold higher than that in LCC6MDR cells, respectively (Figure 1A–C). Treatment of LCC6 cells with 1  $\mu$ M of FD18 or verapamil did not change intracellular DOX, DNR, and R123 accumulation (Figure 1A–C). In contrast, treatment of LCC6MDR cells with 1  $\mu$ M of FD18 or verapamil resulted in an increase in accumulation of DOX by 2.7- and 2.3-fold, respectively (Figure 1A), DNR by 2.1- and 1.8-fold, respectively (Figure 1B), and R123 by 5.2- and 3.7-fold, respectively (Figure 1C). This result suggests that the modulation of P-gp activity by FD18 is due to the inhibition of P-gp's transport activity.

**Effect of FD18 on DOX Influx and Efflux in LCC6MDR Cells.** We investigated whether the increased accumulation of DOX in LCC6MDR cells induced by FD18 treatment was due to increased DOX influx or reduced DOX efflux. FD18 (1 or 3  $\mu$ M) did not have any significant effect on DOX influx in either LCC6 (Figure 1D) or LCC6MDR cells (Figure 1E). FD18 (1 or 3  $\mu$ M) did not have any effect on DOX efflux in LCC6 cells either (Figure 1F). In contrast, FD18 (1 or 3  $\mu$ M) significantly reduced DOX efflux in LCC6MDR cells. Without FD18, 77% of DOX was effluxed out of LCC6MDR cells in 3 h (Figure 1G). In the presence of 1 or 3  $\mu$ M of FD18, only 23% and 31% of DOX was effluxed out of LCC6MDR cells, respectively (Figure 1G). These results suggest that reversal of P-gp-mediated resistance by FD18 is due to an inhibition of P-gp-mediated drug efflux, leading to an increased drug accumulation and thus restoring the drug sensitivity.

**Effect of FD18 on P-Glycoprotein Protein Expression Level in LCC6 and LCC6MDR Cells.** The above data demonstrates that FD18 can increase DOX accumulation by inhibiting the P-gp mediated DOX efflux. To ascertain that P-gp level did not change upon FD18 treatment, we have measured P-gp level in LCC6 and LCC6MDR cells after treatment with FD18. We treated the LCC6 and LCC6MDR cells with 1  $\mu$ M FD18 for 0 h, 2 h (period used for studying DOX accumulation assay), and 5 days (period used for studying proliferation assay). No P-gp was detected in LCC6 parental cells with or without FD18 treatment (Figure 2A). In contrast, P-gp expression level was significantly higher in LCC6MDR cells (Figure 2A). Treatment with FD18 for 5 days or 2 h did not affect P-gp expression significantly compared to no treatment control (Figure 2B). This data suggests that FD18 only affects DOX efflux by inhibiting P-gp's function and not the expression level.

**Pharmacokinetics of FD18 in Mice after Intraperitoneal Administration.** Prior to testing the efficacy of FD18 in reversing P-gp mediated resistance *in vivo*, we have investigated the pharmacokinetics of FD18 in female Balb/c mice. Forty-five milligrams per kilogram of FD18 was administered intraperitoneally (i.p.) to Balb/c mice, and its plasma concentration was monitored from 0 to 960 min (Figure 3A). FD18 exhibited a rapid rate of absorption with plasma concentration reaching approximately 1000 ng/mL 10 min post i.p. administration with rapid distribution into extravascular tissues. The first-order elimination with  $C_{max}$  of plasma FD18 concentration was observed at 120 min post i.p. administration. Detailed pharmacokinetics parameters are shown in Figure 3B. Administration of 45 mg/kg of FD18 was enough to maintain a

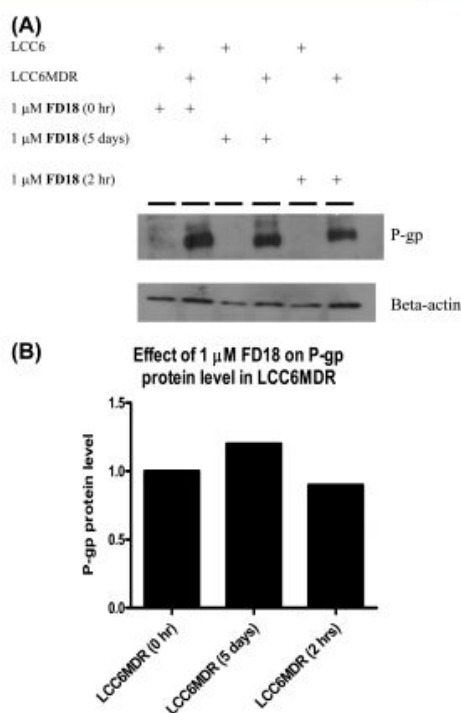


**Figure 2.** Effect of FD18 on P-gp level in LCC6 and LCC6MDR cells. LCC6 and LCC6MDR cells were treated with 1  $\mu$ M FD18 for 0 h, 2 h, and 5 days. Cells ( $1 \times 10^6$ ) were harvested and lysed. Twenty micrograms of cell lysate was subjected to SDS-PAGE and Western blot analysis. The protein loading was normalized to beta actin. (A) Western blot analysis using P-gp antibody (AB-1) or beta-actin antibody. (B) Western blot signal, after normalization to beta actin signal, was quantified by ImageJ software.

plasma level of FD18 above its *in vitro*  $EC_{50}$  (148 nM for PTX)<sup>17</sup> for more than 600 min.

In a separate study, FD18 was administered to SD rat via oral administration at 50 mg/kg (data not shown). The  $C_{max}$  for FD18 (oral, 50 mg/kg) was 55 ng/mL. Oral bioavailability of FD18 was estimated by dose normalized  $AUC_{(0-\infty)}$  (oral 50 mg/kg) to  $AUC_{(0-\infty)}$  (IV 15 mg/kg). The oral bioavailability of FD18 was 2.4%. Such a low oral bioavailability precludes FD18 from being administered orally for subsequent *in vivo* efficacy study.

**Evaluation of *in Vivo* Toxicity of FD18.** Toxicity of FD18 in Balb/c mice, with or without PTX, was evaluated. Controls with solvent alone (Figure 3C, Group 1), PTX solvent with FD18 (Figure 3C, Group 2), or PTX with FD18 solvent (Figure 3C, Group 3) induced no animal deaths and a gain of body weight from 7.7 to 16.3%. FD18 (90 mg/kg; i.p.), when used together with PTX (12 mg/kg, i.v.), induced no animal deaths but caused a minor body weight loss of 4.2% after a total treatment of 12 times in a period of 22 days (Figure 3C, Group 4). All four groups of animals did not show any obvious toxicity symptoms like reduced activity, hypothermia, or body shivering. Maximum tolerated dose (MTD), defined as the highest dose causing less than 10% body weight loss with no animal deaths for FD18 was greater than 90 mg/kg when used together with PTX at 12 mg/kg. These results suggested that FD18 at that

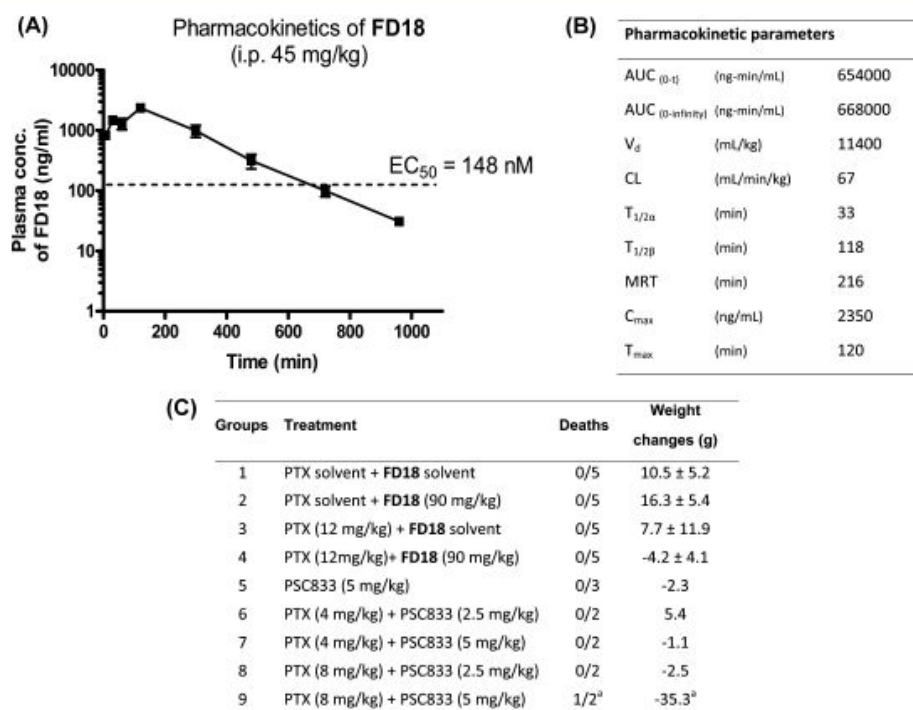


**Figure 3.** Pharmacokinetics and toxicity studies of FD18. Plasma concentration profile of FD18 in female Balb/c mice after i.p. injection of 45 mg/kg of FD18 ( $n = 4-5$  for each data point, except for the 960 min data point where only one sample was obtained). (A) The dash line indicates the corresponding EC<sub>50</sub> concentration of FD18 obtained *in vitro* for reversing PTX resistance (148 nM).<sup>17</sup> Pharmacokinetic parameters are presented. (B) AUC<sub>(0-1)</sub>, area under the curve (AUC) from 0 to 960 min calculated by trapezoid rule; AUC<sub>(0-infinity)</sub>, AUC from 0 min to infinity calculated by trapezoid rule; V<sub>d</sub>, volume of distribution; CL, Clearance; T<sub>1/2α</sub>, elimination half-life; T<sub>1/2β</sub>, distribution half-life; MRT, median resistance time; C<sub>max</sub>, maximum plasma concentration (observed); T<sub>max</sub>, time to reach maximum plasma concentration (observed). Toxicity studies of FD18 were performed as described in the text. (C) Balb/c mice were divided into 9 groups and treated accordingly. Toxicity symptoms, body weight, and death, if any, were monitored during and after treatment. Weight changes are presented in mean ± SEM. PTX was dissolved in a mixture of 5% absolute ethanol, 5% Cremophor EL, and 90% of 0.9% saline. FD18 was dissolved in a mixture of 14% absolute ethanol, 14% Cremophor EL, and 72% of 0.9% saline. PSC833 was dissolved in 65% Cremophor EL and 35% ethanol. <sup>a</sup>Both animals showed reduced activity and one animal died on day 16. Weight change of the remaining animal was reported here.

dose did not induce significant acute toxicity in Balb/c mice even in the presence of PTX.

In contrast, another potent P-gp modulator PSC833 (5 mg/kg, i.p.), when used together with PTX (8 mg/kg, i.v.), resulted in severe toxicity with 50% animal death (1 out of 2) with a total treatment of 8 times in a period of 17 days (Figure 3C, Group 9). The remaining animal has a 35% drop in body weight at the end of 22 days of treatment with toxicity symptoms like reduced activity levels, hypothermia, and body shivering. Therefore, MTD for PSC833 was below 5.0 mg/kg when used together with PTX at 8 mg/kg. These results suggested that, when combined with PTX, i.p. injection of FD18 was more tolerated than PSC833 in Balb/c mice.

**In Vivo Efficacy of FD18 and PSC833 on Modulating PTX Resistance in LCC6MDR Xenograft.** Here, we established an *in vivo* PTX-resistant human breast cancer xenograft model in female Balb/c nu nu mice. Without any PTX treatment, parental LCC6 xenograft can grow to 611 ± 8 mm<sup>3</sup> in 27 days (Figure 4A). Upon PTX treatment (12 mg/kg; i.v. for 8 times in 17 days), LCC6 xenograft volume was reduced to 248 ± 78 mm<sup>3</sup> on the 27th day (Figure 4A). This result suggested that LCC6 xenograft was sensitive to PTX

treatment. In contrast, LCC6MDR xenograft did not respond to PTX treatment. It can grow to 1029 ± 82 and 879 ± 127 mm<sup>3</sup> on the 27th day for solvent control or upon PTX treatment (12 mg/kg; i.v. for 8 times in 17 days), respectively (Figure 4A). These results suggested that LCC6MDR xenograft can be used as a P-gp-mediated PTX-resistant human breast cancer model.

We tested if FD18 can modulate P-gp-mediated PTX resistance using the above animal model. FD18 (solvent or 45 mg/kg; i.p.) was administered 1 h before PTX (solvent or 12 mg/kg; i.v.). Treatment protocol included a total of 12 times in a period of 22 days (arrows in Figure 4B). There was no significant difference in LCC6MDR xenograft volume on the 32nd day for controls including [PTX solvent + FD18 solvent] (1422 ± 174 mm<sup>3</sup>), [PTX solvent + FD18 (45 mg/kg)] (1225 ± 84 mm<sup>3</sup>), and [PTX (12 mg/kg) + FD18 solvent] (1201 ± 118 mm<sup>3</sup>) (Figure 4B and 4C). Tumor doubling time was almost identical (9 days) for these 3 controls (Figure 4C). In contrast, treatment with [PTX (12 mg/kg) + FD18 (45 mg/kg)] effectively reduced LCC6MDR tumor volume to 648 ± 83 mm<sup>3</sup> ( $P < 0.01$ ) after 30 days of treatment (Figure 4B,C). Tumor doubling time was increased to 13.0 ± 0.7 days (Figure

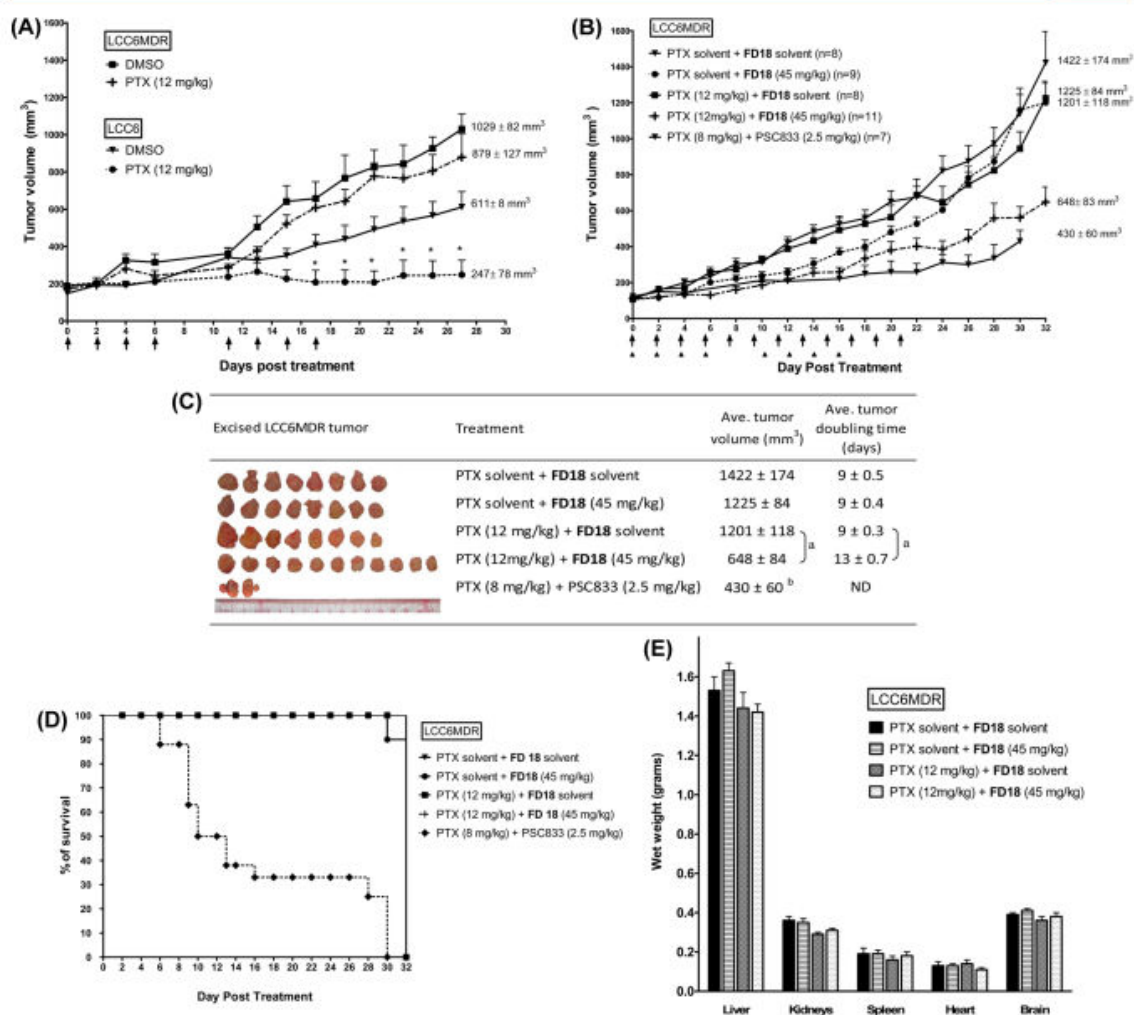


**Figure 4.** *In vivo* efficacy of FD18 on modulating P-gp-mediated PTX resistance. Balb/c nu nu mice were xenografted with either LCC6 or LCC6MDR cells and used as an *in vivo* PTX-sensitive or PTX-resistant human breast cancer model, respectively. Xenografted mice were treated with PTX with or without P-gp modulators FD18 or PSC833, and the tumor volume was measured. (A) LCC6 and LCC6MDR xenografted Balb/c nu nu mice were treated with PTX (12 mg/kg; i.v. eight times in 17 days) or DMSO control. Arrows indicate treatment was made on that day. Asterisks indicate significant tumor volume reduction in PTX-treatment group of LCC6 xenograft compared to DMSO group ( $P < 0.01$ ). (B) Four groups of LCC6MDR xenografted Balb/c nu nu mice were treated with PTX (solvent or 12 mg/kg; i.v.) 1 h after FD18 (solvent control or 45 mg/kg; i.p.) for 12 times in 22 days (indicated by arrows). In parallel, another group of LCC6MDR xenografted Balb/c nu nu mice was treated with PTX (8 mg/kg; i.v.) 1 h after PSC833 (2.5 mg/kg; i.p.) for 8 times in 17 days (indicated by arrow heads). The number of animals used ( $n$ ) ranges from 7 to 11. Tumor volume was measured on the day when animals were sacrificed, and the average tumor volume is shown. (C) LCC6MDR xenograft volume from (B) was monitored throughout the treatment period and used to calculate average doubling time (days). <sup>a</sup>One-way ANOVA with Dunnett's multiple comparison test with  $P < 0.01$ . <sup>b</sup>Average tumor volume calculated from only two remaining animals on the last day of experiment. ND = not determined. (D) The number of mice death was recorded during the treatment in a form of survival curve. No animal deaths occurred in any of the FD18 treatment groups except one animal in the [PTX solvent + FD18 (45 mg/kg)] control group died on 31st day due to reasons unrelated to treatment. Progressive animal deaths were observed on sixth day in the [PTX (8 mg/kg; i.v.) + PSC833 (2.5 mg/kg; i.p.)] positive control group, remaining animals ( $n = 2$  out of 7) were terminated on 30th day due to severe drug induced toxicities. (E) At the end of the experiment, animals were sacrificed and the weight of vital organs including liver, kidney, spleen, heart and brain was measured. (D) Animals were sacrificed on day 32, except for PSC833 group where animals were sacrificed on day 30. Excised LCC6MDR tumors were pictured, and the average xenograft volume calculated. (E) Statistical analysis was done by using one-way ANOVA with Dunnett's multiple comparison test on day 32 between treatment group [PTX (12 mg/kg) + FD18 (45 mg/kg)] and its solvent controls.

4C). No animal deaths occurred in any of the four groups except one animal in the [PTX solvent + FD18 (45 mg/kg)] control group died on the 31st day due to reasons unrelated to

treatment (Figure 4D). There was no significant difference in wet weight of vital organs (liver, kidneys, spleen, heart, and brain) in all three solvent controls and [PTX (12 mg/kg) +

**FD18** (45 mg/kg)] group (Figure 4E). These results suggested that i.p. administration of **FD18** (45 mg/kg) was effective in modulating P-gp-mediated PTX resistance in *in vivo* LCC6MDR xenografted Balb/c nu nu mice model. Such P-gp modulation did not induce any significant toxicity.

In parallel, we measured the ability of PSC833 in modulating P-gp-mediated PTX resistance in the same animal model. PSC833 (2.5 mg/kg; i.p.) was administered 1 h before PTX. Treatment protocol included a total of eight times in a period of 17 days (arrow heads in Figure 4B). Treatment with [PTX (8 mg/kg; i.v.) + PSC833 (2.5 mg/kg; i.p.)] resulted in a reduction of LCC6MDR tumor volume to  $430 \pm 60 \text{ mm}^3$  after 30 days of treatment (Figure 4B,C). However, we observed significant toxicity (five deaths out of seven animals) starting from day 6 of treatment (Figure 4D). The two remaining animals also have a significant weight loss higher than 20% (data not shown). These results suggested that i.p. administration of PSC833 (2.5 mg/kg), although effective in modulating P-gp-mediated PTX resistance in LCC6MDR xenograft model, can induce severe *in vivo* toxicity and animal deaths.

**Effect of FD18 on PTX Accumulation in LCC6MDR Tumors.** Here, we investigated the mechanism by which **FD18** sensitized LCC6MDR xenograft to PTX *in vivo*. Balb/c nu nu mice carrying LCC6MDR xenograft were administered with PTX with or without **FD18**. The xenograft was removed 7 h later. PTX level in the xenograft was determined. We found that there was no significant difference between the two controls of [PTX (40 mg/kg; i.v.)] ( $4347 \pm 397 \text{ ng/g tissue}$ ) and [PTX (40 mg/kg; i.v.) + **FD18** solvent] ( $3501 \pm 720 \text{ ng/g tissue}$ ) (Figure 5). In contrast, PTX level in the xenograft of [PTX (40

mg/kg; i.v.) + **FD18** (45 mg/kg; i.p.)] group was significantly ( $P < 0.01$ ) increased to  $7829 \pm 701 \text{ ng/g tissue}$  (Figure 5). This represented an increase by 2.2- and 1.8-fold over the two controls, respectively. This result suggested that **FD18** can sensitize LCC6MDR to PTX by inhibiting P-gp-mediated PTX efflux in the xenograft.

## DISCUSSION

Since P-gp and the other multidrug resistant proteins possess a pseudodimeric structure, new P-gp modulators with dimeric structure have recently been developed to target them, reviewed in refs 15 and 16. This new class of P-gp modulator has a chemical structure of two monomers linked together by a linker with variable length. Not only do dimeric modulators show an increase in potency over their corresponding monomers, but also their potency can be further increased by varying the linker length between the monomers to make a better fit to the putative binding sites on P-gp. Specificity (e.g., preference for P-gp over MRP1 or vice versa) can also be increased by manipulating the structure of linker and monomer as well as length of linker. Some of these dimeric modulators, including stipiamide dimer,<sup>20</sup> flavonoid dimers,<sup>13,17,21</sup> emetine dimers,<sup>22</sup> quinine dimers,<sup>23,24</sup> and cage dimeric 1,4-dihydropyridines<sup>25</sup> can reverse P-gp-mediated cancer drug resistance *in vitro*. Others can reverse P-gp mediated stibogluconate and pentamidine resistance in parasitic protozoan *Leishmania*.<sup>12,14</sup> However, despite the extensive *in vitro* activities reported for these new dimeric P-gp modulators, there is a paucity of data on the *in vivo* activities of these compounds. Because of their dimeric structures, these modulators in general have higher molecular weight and may not have ideal drug-like properties. The present study of **FD18** represents the first *in vivo* examination on the pharmacokinetics, toxicity, and efficacy of the dimeric modulator approach to overcome multidrug resistance.

**FD18** has several advantages over other P-gp modulators. First, it can reverse P-gp mediated resistance to a panel of anticancer drugs including PTX, vinblastine, vincristine, DOX, DNR, and mitoxantrone in LCC6MDR cells *in vitro*. **FD18** at  $1 \mu\text{M}$  can completely revert the chemosensitivity level back to that of parental LCC6 cells (Table 2). **FD18** was about 11- to 46-fold more potent than the first generation MDR modulator, verapamil. The high potency of **FD18** ( $\text{EC}_{50} = 148 \text{ nM}$  for PTX) was a result of a series of lead optimization efforts reported previously.<sup>11,13,17</sup> **FD18** was also previously demonstrated to be more selective toward P-gp (RF = 59 for reversing P-gp mediated resistance) over MRP1 (RF = 2 for reversing MRP1-mediated resistance) and BCRP (RF = 4 for reversing BCRP-mediated resistance) transporters.<sup>17</sup> Second, **FD18** was relatively nontoxic to L929 fibroblast *in vitro* ( $\text{IC}_{50} = 85 \mu\text{M}$ ) with a high selective index of 574 for PTX. This appears to be supported by *in vivo* toxicity experiment. When used together with PTX in Balb/c mice *in vivo*, **FD18** was relatively safe (no significant body weight reduction or animal deaths) at 90 mg/kg i.p. Third, **FD18** exhibited promising plasma bioavailability after i.p. injection. Administration of 45 mg/kg of **FD18** was enough to maintain a plasma level of **FD18** above its *in vitro*  $\text{EC}_{50}$  (148 nM for PTX)<sup>17</sup> for more than 600 min. Finally, **FD18** (45 mg/kg) exhibited potent P-gp modulating activity and restored the antitumor activity of PTX (12 mg/kg) in LCC6MDR xenograft without inducing any observable toxicity or animal deaths.

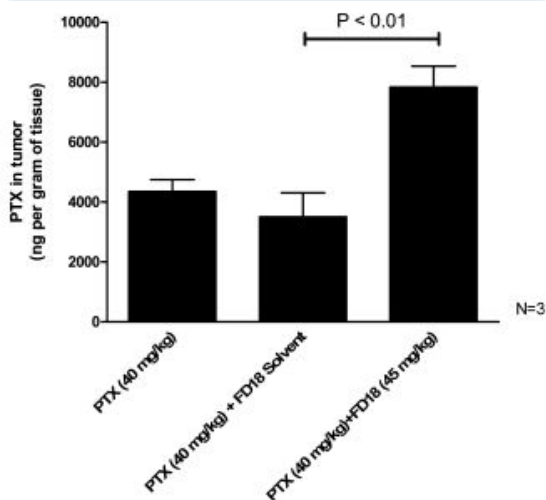


**Figure 5.** *In vivo* PTX accumulation in tumor after treatment with **FD18**. **FD18** (45 mg/kg) was administered (i.p.) to female Balb/c nu nu mice bearing LCC6MDR xenograft. One hour after the **FD18** injection, 40 mg/kg of PTX was administered through i.v. injection. The tumor was collected after 7 h of PTX administration. PTX level in the tumor was determined by HPLC after extraction (see Materials and Methods).  $N = 3$  independent experiments. The value was presented as mean  $\pm$  standard error of mean. Student *t* test performed between [PTX (40 mg/kg) + **FD18** solvent] and [PTX (40 mg/kg) + **FD18** (45 mg/kg)] gave a  $P$  value  $< 0.01$ .

We proposed that **FD18** inhibited P-gp by binding to the substrate-binding pocket of P-gp. Like other P-gp substrates (e.g., verapamil), **FD18** can stimulate P-gp ATPase over basal level by 3.3-fold.<sup>17</sup> This was different from the flavonoid monomers that were shown to bind and inhibit the ATPase domain of P-gp.<sup>11</sup> Biochemical studies suggested that **FD18** was a competitive inhibitor of DOX toward P-gp with a  $K_i$  of 0.28–0.34  $\mu\text{M}$  and a Hill coefficient of 1.17.<sup>17</sup> By binding to the substrate binding pocket on P-gp, **FD18** would inhibit the efflux of other P-gp substrates like PTX or DOX. This would explain the increase in PTX accumulation in LCC6MDR xenograft in Balb/c nu nu mice after **FD18** treatment. **FD18** itself could also be a substrate of P-gp and be transported out of the cells. Indeed, LCC6MDR cells accumulated less **FD18** than LCC6 cell line by 1.7- to 2.1-fold.<sup>17</sup>

It is perhaps instructive to compare the **FD18** results with similar *in vivo* study using PSC833. PSC833 is a potent P-gp modulator with  $\text{EC}_{50}$  of 2.3 nM for PTX in the LCC6MDR cells. Its *in vitro* therapeutic index is also high (>44 000) as it is essentially nontoxic to L929 fibroblasts ( $\text{IC}_{50} > 100 \mu\text{M}$ ). However, in our hand, PSC833 induced severe *in vivo* toxicity when used together with PTX. At a dosage that was nontoxic to healthy Bulb/c mice, similar (lower) dosage on tumor-bearing mice led to high mortality (Figures 3C and 4D). So, even though PSC833 was more effective than **FD18** in reducing tumor volume for the surviving animals (Figure 4B,C), **FD18** would have been a better therapeutic agent than PSC833 in this cancer model. The mechanism by which PSC833 induced *in vivo* toxicity for tumor-bearing mice was unknown although drug–drug interaction between PSC833 and PTX could not be excluded. As we did not explore a different administration route of PSC833 or **FD18** other than *i.p.*, we do not know whether the different toxicity of the two agents, when used together with PTX, can be changed by using other administrative routes.

In summary, this work demonstrated that **FD18**, as a new class of dimeric P-gp modulator, was effective in reversing P-gp-mediated PTX resistance in *in vivo* human breast xenograft tumor model. **FD18** can potentially represent a new class of safe and potent P-gp modulator for treatment of P-gp mediated MDR cancers in clinic.

## AUTHOR INFORMATION

### Corresponding Authors

\*Phone: (852)-34008662. Fax: (852)-23649932. E-mail: bclchow@polyu.edu.hk.

\*Phone: (852)-34008670. Fax: (852)-23649932. E-mail: bcchanth@polyu.edu.hk.

### Author Contributions

<sup>§</sup>C.S.W.Y. and I.L.K.W. contributed equally to this work.

### Notes

The authors declare the following competing financial interest(s): Compound described in this publication has been filed for patent protection and could lead to potential commercialization in the future.

## ACKNOWLEDGMENTS

We are grateful for funding support from the Hong Kong Research Grants Council (PolyU 5602/09M and PolyU 5606/11M). The authors acknowledge the support of the Research Projects of Strategic Importance (1-ZE22) by The Hong Kong Polytechnic University.

## REFERENCES

- (1) Biedler, J. L.; Riehm, H. Cellular resistance to actinomycin D in Chinese hamster cells *in vitro*: cross-resistance, radioautographic, and cytogenetic studies. *Cancer Res.* **1970**, *30* (4), 1174–84.
- (2) Juliano, R. L.; Ling, V. A surface glycoprotein modulating drug permeability in Chinese hamster ovary cell mutants. *Biochim. Biophys. Acta, Biomembr.* **1976**, *455* (1), 152–62.
- (3) Van der Bliek, A. M.; Van der Velde-Koerts, T.; Ling, V.; Borst, P. Overexpression and amplification of five genes in a multidrug-resistant Chinese hamster ovary cell line. *Mol. Cell. Biol.* **1986**, *6* (5), 1671–8.
- (4) Ueda, K.; Cornwell, M. M.; Gottesman, M. M.; Pastan, I.; Roninson, I. B.; Ling, V.; Riordan, J. R. The *mdr1* gene, responsible for multidrug-resistance, codes for P-glycoprotein. *Biochem. Biophys. Res. Commun.* **1986**, *141* (3), 956–62.
- (5) Ling, V. Multidrug resistance: molecular mechanisms and clinical relevance. *Cancer Chemother. Pharmacol.* **1997**, *40* (Suppl), S3–8.
- (6) Trock, B. J.; Leonessa, F.; Clarke, R. Multidrug resistance in breast cancer: a meta-analysis of MDR1/gp170 expression and its possible functional significance. *J. Natl. Cancer Inst.* **1997**, *89* (13), 917–31.
- (7) Faneyte, I. F.; Kristel, P. M.; van de Vijver, M. J. Determining MDR1/P-glycoprotein expression in breast cancer. *Int. J. Cancer* **2001**, *93* (1), 114–22.
- (8) Advani, R.; Fisher, G. A.; Lum, B. L.; Hausdorff, J.; Halsey, J.; Litchman, M.; Sikic, B. I. A phase I trial of doxorubicin, paclitaxel, and valspodar (PSC 833), a modulator of multidrug resistance. *Clin. Cancer Res.* **2001**, *7* (5), 1221–9.
- (9) Krishna, R.; Mayer, L. D. Multidrug resistance (MDR) in cancer. Mechanisms, reversal using modulators of MDR and the role of MDR modulators in influencing the pharmacokinetics of anticancer drugs. *Eur. J. Pharm. Sci.* **2000**, *11* (4), 265–83.
- (10) Friedenberg, W. R.; Rue, M.; Blood, E. A.; Dalton, W. S.; Shustik, C.; Larson, R. A.; Sonneveld, P.; Greipp, P. R. Phase III study of PSC-833 (valspodar) in combination with vincristine, doxorubicin, and dexamethasone (valspodar/VAD) versus VAD alone in patients with recurring or refractory multiple myeloma (E1A95). *Cancer* **2006**, *106* (4), 830–838.
- (11) Chan, K. F.; Zhao, Y.; Burkett, B. A.; Wong, I. L.; Chow, L. M.; Chan, T. H. Flavonoid dimers as bivalent modulators for P-glycoprotein-based multidrug resistance: synthetic apigenin homodimers linked with defined-length poly(ethylene glycol) spacers increase drug retention and enhance chemosensitivity in resistant cancer cells. *J. Med. Chem.* **2006**, *49* (23), 6742–59.
- (12) Wong, I. L.; Chan, K. F.; Burkett, B. A.; Zhao, Y.; Chai, Y.; Sun, H.; Chan, T. H.; Chow, L. M. Flavonoid dimers as bivalent modulators for pentamidine and sodium stibogluconate resistance in leishmania. *Antimicrob. Agents Chemother.* **2007**, *51* (3), 930–40.
- (13) Chan, K. F.; Zhao, Y.; Chow, T. W.; Yan, C. S.; Ma, D. L.; Burkett, B. A.; Wong, I. L.; Chow, L. M.; Chan, T. H. Flavonoid dimers as bivalent modulators for p-glycoprotein-based multidrug resistance: structure-activity relationships. *ChemMedChem* **2009**, *4* (4), 594–614.
- (14) Wong, I. L.; Chan, K. F.; Zhao, Y.; Chan, T. H.; Chow, L. M. Quinacrine and a novel apigenin dimer can synergistically increase the pentamidine susceptibility of the protozoan parasite *Leishmania*. *J. Antimicrob. Chemother.* **2009**, *63* (6), 1179–90.
- (15) Chow, L. M.; Chan, T. H. Novel classes of dimer antitumor drug candidates. *Curr. Pharm. Des.* **2009**, *15* (6), 659–74.
- (16) Chan, K. F.; Wong, I. L. K.; Burkett, B. A.; Zhao, Y.; Yan, C. S. W.; Kan, J. W. Y.; Tsang, K. H.; Lam, C. Y.; Chan, T. H.; Chow, L. M. C. Flavonoid dimer as modulator of drug resistance in cancer. *Progress in Nutrition* **2010**, *12*, 51–57.
- (17) Chan, K. F.; Wong, I. L.; Kan, J. W.; Yan, C. S.; Chow, L. M.; Chan, T. H. Amine linked flavonoid dimers as modulators for p-glycoprotein-based multidrug resistance: structure-activity relationship and mechanism of modulation. *J. Med. Chem.* **2012**, *55* (5), 1999–2014.
- (18) Ambudkar, S. V.; Dey, S.; Hrycyna, C. A.; Ramachandra, M.; Pastan, I.; Gottesman, M. M. Biochemical, cellular, and pharmaco-

logical aspects of the multidrug transporter. *Annu. Rev. Pharmacol. Toxicol.* **1999**, *39*, 361–98.

(19) Rao, J.; Lahiri, J.; Isaacs, L.; Weis, R. M.; Whitesides, G. M. A trivalent system from vancomycin-D-ala-D-Ala with higher affinity than avidin-biotin. *Science* **1998**, *280* (5364), 708–11.

(20) Sauna, Z. E.; Andrus, M. B.; Turner, T. M.; Ambudkar, S. V. Biochemical basis of polyvalency as a strategy for enhancing the efficacy of P-glycoprotein (ABCB1) modulators: stipiamide homodimers separated with defined-length spacers reverse drug efflux with greater efficacy. *Biochemistry* **2004**, *43* (8), 2262–71.

(21) Wong, I. L.; Chan, K. F.; Tsang, K. H.; Lam, C. Y.; Zhao, Y.; Chan, T. H.; Chow, L. M. Modulation of multidrug resistance protein 1 (MRP1/ABCC1)-mediated multidrug resistance by bivalent apigenin homodimers and their derivatives. *J. Med. Chem.* **2009**, *52* (17), 5311–22.

(22) Pires, M. M.; Hrycyna, C. A.; Chmielewski, J. Bivalent probes of the human multidrug transporter P-glycoprotein. *Biochemistry* **2006**, *45* (38), 11695–11702.

(23) Kuriakose, J.; Hrycyna, C. A.; Chmielewski, J. Click chemistry-derived bivalent quinine inhibitors of P-glycoprotein-mediated cellular efflux. *Bioorg. Med. Chem. Lett.* **2012**, *22* (13), 4410–4412.

(24) Pires, M. M.; Emmert, D.; Hrycyna, C. A.; Chmielewski, J. Inhibition of P-glycoprotein-mediated paclitaxel resistance by reversibly linked quinine homodimers. *Mol. Pharmacol.* **2009**, *75* (1), 92–100.

(25) Coburger, C.; Wollmann, J.; Krug, M.; Baumert, C.; Seifert, M.; Molnár, J.; Lage, H.; Hilgeroth, A. Novel structure–activity relationships and selectivity profiling of cage dimeric 1,4-dihydropyridines as multidrug resistance (MDR) modulators. *Bioorg. Med. Chem.* **2010**, *18* (14), 4983–4990.

## References

- Advani R, Fisher GA, Lum BL et al. A phase I trial of Doxorubicin, Paclitaxel, and valspodar (PSC 833), a modulator of multidrug resistance. *Clinical Cancer Research* 2001; 7 (5):1221-9.
- Aller SG, Yu J, Ward A et al. Structure of P-glycoprotein reveals a molecular basis for poly-specific drug binding. *Science* 2009; 323 (5922):1718-22.
- Ambudkar SV, Dey S, Hrycyna CA et al. Biochemical, cellular, and pharmacological aspects of the multidrug transporter. *Annual review of pharmacology and toxicology* 1999; 39:361-98.
- Atadja P, Watanabe T, Xu H et al. PSC-833, a frontier in modulation of P-glycoprotein mediated multidrug resistance. *Cancer Metastasis Review* 1998; 17 (2):163-8.
- Baekelandt M, Lehne G, Trope CG et al. Phase I/II trial of the multidrug-resistance modulator valspodar combined with cisplatin and Doxorubicin in refractory ovarian cancer. *Journal of clinical oncology : official journal of the American Society of Clinical Oncology* 2001; 19 (12):2983-93.
- Bao L, Matsumura Y, Baban D et al. Effects of inoculation site and Matrigel on growth and metastasis of human breast cancer cells. *British journal of cancer* 1994; 70 (2):228-32.
- Baranczewski P, Stanczak A, Sundberg K et al. Introduction to in vitro estimation of metabolic stability and drug interactions of new chemical entities in drug discovery and development. *Pharmacological reports : PR* 2006; 58 (4):453-72.
- Biedler JL, Riehm H. Cellular resistance to actinomycin D in Chinese hamster cells in vitro: cross-resistance, radioautographic, and cytogenetic studies. *Cancer research* 1970; 30 (4):1174-84.
- Bisogno G, Cowie F, Boddy A et al. High-dose Cyclosporin with etoposide--toxicity and pharmacokinetic interaction in children with solid tumors. *British journal of cancer* 1998; 77 (12):2304-9.
- Bissery MC, Guenard D, Gueritte-Voegelein F et al. Experimental antitumor activity of taxotere (RP 56976, NSC 628503), a taxol analogue. *Cancer research* 1991; 51 (18):4845-52.
- Boesch D, Gaveriaux C, Jachez B et al. In vivo circumvention of P-glycoprotein-mediated multidrug resistance of tumor cells with SDZ PSC 833. *Cancer research* 1991; 51 (16):4226-33.
- Boumendjel A, Di Pietro A, Dumontet C et al. Recent advances in the discovery of flavonoids and analogs with high-affinity binding to P-glycoprotein responsible for cancer cell multidrug resistance. *Medicinal Research Reviews* 2002; 22 (5):512-29.
- Brakebusch C. PT. *Mouse as a Model Organism: From Animals to Cells*. Springer Press 2011.

- Cairo MS, Siegel S, Anas N et al. Clinical trial of continuous infusion Verapamil, bolus vinblastine, and continuous infusion VP-16 in drug-resistant pediatric tumors. *Cancer research* 1989; 49 (4):1063-6.
- Campos FC, Victorino VJ, Martins-Pinge MC et al. Systemic toxicity induced by Paclitaxel in vivo is associated with the solvent cremophor EL through oxidative stress-driven mechanisms. *Food and chemical toxicology : an international journal published for the British Industrial Biological Research Association* 2014; 68:78-86.
- Chambers SK, Davis CA, Chambers JT et al. Phase I trial of intravenous carboplatin and Cyclosporin A in refractory gynecologic cancer patients. *Clinical cancer research : an official journal of the American Association for Cancer Research* 1996; 2 (10):1699-704.
- Chan KF, Wong IL, Kan JW et al. Amine linked flavonoid dimers as modulators for P-glycoprotein-based multidrug resistance: structure-activity relationship and mechanism of modulation. *Journal of medicinal chemistry* 2012; 55 (5):1999-2014.
- Chan KF, Zhao Y, Burkett BA et al. Flavonoid dimers as bivalent modulators for P-glycoprotein-based multidrug resistance: synthetic apigenin homodimers linked with defined-length poly(ethylene glycol) spacers increase drug retention and enhance chemosensitivity in resistant cancer cells; *Journal of Medicinal Chemistry* 2006; 49(23): p.6742-6759.
- Chan KF, Zhao Y, Chow TW et al. Flavonoid dimers as bivalent modulators for p-glycoprotein-based multidrug resistance: structure-activity relationships. *ChemMedChem* 2009; 4 (4):594-614.
- Chauncey TR, Rankin C, Anderson JE et al. A phase I study of induction chemotherapy for older patients with newly diagnosed acute myeloid leukemia (AML) using mitoxantrone, etoposide, and the MDR modulator PSC 833: a southwest oncology group study 9617. *Leukemia research* 2000; 24 (7):567-74.
- Chen CJ, Chin JE, Ueda K et al. Internal duplication and homology with bacterial transport proteins in the *mdr1* (P-glycoprotein) gene from multidrug-resistant human cells. *Cell* 1986; 47 (3):381-9.
- Chico I, Kang MH, Bergan R et al. Phase I study of infusional Paclitaxel in combination with the P-glycoprotein antagonist PSC 833. *Journal of clinical oncology : official journal of the American Society of Clinical Oncology* 2001; 19 (3):832-42.
- Clarke R. Issues in experimental design and endpoint analysis in the study of experimental cytotoxic agents in vivo in breast cancer and other models. *Breast cancer research and treatment* 1997; 46 (2-3):255-78.
- Colombo T, Gonzalez Paz O, D'Incalci M. Distribution and activity of Doxorubicin combined with SDZ PSC 833 in mice with P388 and P388/DOX leukaemia. *British journal of cancer* 1996; 73 (7):866-71.

- Covelli A. [SDZ PSC 833: a novel modulator of MDR]. *Tumori* 1997; 83 (5 Supplementary):S21-4.
- Cremer MA, Pitcock JA, Stuart JM et al. Auricular chondritis in rats. An experimental model of relapsing polychondritis induced with type II collagen. *The Journal of experimental medicine* 1981; 154 (2):535-40.
- Cripe LD, Uno H, Paietta EM et al. Zosuquidar, a novel modulator of P-glycoprotein, does not improve the outcome of older patients with newly diagnosed acute myeloid leukemia: a randomized, placebo-controlled trial of the Eastern Cooperative Oncology Group 3999. *Blood* 2010; 116 (20):4077-85.
- Dantzig AH, Law KL, Cao J et al. Reversal of multidrug resistance by the P-glycoprotein modulator, LY335979, from the bench to the clinic. *Current medicinal chemistry* 2001; 8 (1):39-50.
- Dantzig AH, Shepard RL, Cao J et al. Reversal of P-glycoprotein-mediated multidrug resistance by a potent cyclopropyldibenzosuberane modulator, LY335979. *Cancer research* 1996; 56 (18):4171-9.
- Dantzig AH, Shepard RL, Law KL et al. Selectivity of the multidrug resistance modulator, LY335979, for P-glycoprotein and effect on cytochrome P-450 activities. *The Journal of pharmacology and experimental therapeutics* 1999; 290 (2):854-62.
- Davidson A, Dick G, Pritchard-Jones K et al. EVE/Cyclosporin (etoposide, Vincristine, epirubicin with high-dose Cyclosporin)-chemotherapy selected for multidrug resistance modulation. *European journal of cancer* 2002; 38 (18):2422-7.
- Dawson RJ, Locher KP. Structure of a bacterial multidrug ABC transporter. *Nature* 2006; 443 (7108):180-5.
- de Bruijn MH, Van der Blik AM, Biedler JL et al. Differential amplification and disproportionate expression of five genes in three multidrug-resistant Chinese hamster lung cell lines. *Molecular and cellular biology* 1986; 6 (12):4717-22.
- Desai N, Trieu V, Yao Z et al. Increased antitumor activity, intratumor Paclitaxel concentrations, and endothelial cell transport of cremophor-free, albumin-bound Paclitaxel, ABI-007, compared with cremophor-based Paclitaxel. *Clinical Cancer Research* 2006; 12 (4):1317-24.
- Di Pietro A, Conseil G, Perez-Victoria JM et al. Modulation by flavonoids of cell multidrug resistance mediated by P-glycoprotein and related ABC transporters. *Cellular and Molecular Life Sciences* 2002; 59 (2):307-22.
- Easty GC, Ambrose EJ. The antigenic composition of mouse ascites tumor cells using in vitro and gel-diffusion techniques. *British journal of cancer* 1957; 11 (2):287-95.

- Erlichman C, Moore M, Thiessen JJ et al. Phase I pharmacokinetic study of Cyclosporin A combined with Doxorubicin. *Cancer research* 1993; 53 (20):4837-42.
- Ermolaeva LA, Dubskaya, T.Y., Fomina, T.I. Toxic effect of an antitumor drug Paclitaxel on morphofunctional characteristics of the liver in rats. *Bulletin of Experimental Biology and Medicine* 2008; 145 (263):225-8.
- Fiebig HH, Maier A, Burger AM. Clonogenic assay with established human tumor xenografts: correlation of in vitro to in vivo activity as a basis for anticancer drug discovery. *European journal of cancer* 2004; 40 (6):802-20.
- Flanagan SP. 'Nude', a new hairless gene with pleiotropic effects in the mouse. *Genetic research* 1966; 8 (3):295-309.
- Fracasso PM, Goldstein LJ, de Alwis DP et al. Phase I study of docetaxel in combination with the P-glycoprotein inhibitor, zosuquidar, in resistant malignancies. *Clinical cancer research : an official journal of the American Association for Cancer Research* 2004; 10 (21):7220-8.
- Friedenberg WR, Rue M, Blood EA et al. Phase III study of PSC-833 (valspodar) in combination with Vincristine, Doxorubicin, and dexamethasone (valspodar/VAD) versus VAD alone in patients with recurring or refractory multiple myeloma (E1A95): a trial of the Eastern Cooperative Oncology Group. *Cancer* 2006; 106 (4):830-8.
- Gelderblom H, Verweij J, Nooter K et al. Cremophor EL: the drawbacks and advantages of vehicle selection for drug formulation. *European journal of cancer* 2001; 37 (13):1590-8.
- Gottesman MM. How cancer cells evade chemotherapy: sixteenth Richard and Hinda Rosenthal Foundation Award Lecture. *Cancer research* 1993; 53 (4):747-54.
- Gottesman MM. Mechanisms of cancer drug resistance. *Annual Review of Medicine* 2002; 53:615-27.
- Gottesman MM. Multidrug resistance during chemical carcinogenesis: a mechanism revealed? *Journal of the National Cancer Institute* 1988; 80 (17):1352-3.
- Gottesman MM, Ambudkar SV, Xia D. Structure of a multidrug transporter. *Nature biotechnology* 2009; 27 (6):546-7.
- Grey M, Borg AG, Wood P et al. Effect on cell kill of addition of multidrug resistance modifiers Cyclosporin A and PSC 833 to cytotoxic agents in acute myeloid leukaemia. *Leukemia research* 1997; 21 (9):867-74.
- Gunaratna C. Drug Metabolism and Pharmacokinetics in Drug Discovery: A Primer For Bioanalytical Chemists, Part I. *Current Separations* 2001; 19 (3):87-92.

- Horio M, Gottesman MM, Pastan I. ATP-dependent transport of vinblastine in vesicles from human multidrug-resistant cells. *Proceedings of the National Academy of Sciences of the United States of America* 1988; 85 (10):3580-4.
- Hyafil F, Vergely C, Du Vignaud P et al. In vitro and in vivo reversal of multidrug resistance by GF120918, an acridonecarboxamide derivative. *Cancer research* 1993; 53 (19):4595-602.
- Jacob D. DJ, Fang B. Xenograftic tumor models in mice for cancer research, a technical review. *Gene Therapy And Molecular Biology* 2004; 8:213-9.
- Jang SH, Wientjes MG, Au JL. Kinetics of P-glycoprotein-mediated efflux of Paclitaxel. *The Journal of pharmacology and experimental therapeutics* 2001; 298 (3):1236-42.
- Jin J, Wang FP, Wei H et al. Reversal of multidrug resistance of cancer through inhibition of P-glycoprotein by 5-bromotetrandrine. *Cancer Chemother Pharmacol* 2005; 55 (2):179-88.
- Jin MS, Oldham ML, Zhang Q et al. Crystal structure of the multidrug transporter P-glycoprotein from *Caenorhabditis elegans*. *Nature* 2012; 490 (7421):566-9.
- Johnson JI, Decker S, Zaharevitz D et al. Relationships between drug activity in NCI preclinical in vitro and in vivo models and early clinical trials. *British journal of cancer* 2001; 84 (10):1424-31.
- Juliano RLaL, V. A surface glycoprotein modulating drug permeability in Chinese hamster ovary cell mutants. *Biochimica et Biophysica Acta* 1976; 455 (1):152-62.
- Kahan BD. The ruby anniversary: forty years of publication of *Transplantation Proceedings* - the first decade: the flowering of immunology and immunogenetics. *Transplantation proceedings* 2009; 41 (1):5-10.
- Kankesan J, Vanama R, Yusuf A et al. Effect of PSC 833, an inhibitor of P-glycoprotein on N-methyl-N-nitrosourea induced mammary carcinogenesis in rats. *Carcinogenesis* 2004; 25 (3):425-30.
- Kelland LR. Of mice and men: values and liabilities of the athymic nude mouse model in anticancer drug development. *European journal of cancer* 2004; 40 (6):827-36.
- Kim JB, O'Hare MJ, Stein R. Models of breast cancer: is merging human and animal models the future? *Breast cancer research : BCR* 2004; 6 (1):22-30.
- Kim SC, Kim DW, Shim YH et al. In vivo evaluation of polymeric micellar Paclitaxel formulation: toxicity and efficacy. *Journal of controlled release : official journal of the Controlled Release Society* 2001; 72 (1-3):191-202.
- Kindred B. Antibody response in genetically thymus-less nude mice injected with normal thymus cells. *Journal of immunology* 1971; 107 (5):1291-5.

- Kirchmair J, Goller AH, Lang D et al. Predicting drug metabolism: experiment and/or computation? *Nature reviews. Drug discovery* 2015; 14 (6):387-404.
- Kitagaki M, Hirota M. Auricular chondritis caused by metal ear tagging in C57BL/6 mice. *Veterinary pathology* 2007; 44 (4):458-66.
- Kodan A, Yamaguchi T, Nakatsu T et al. Structural basis for gating mechanisms of a eukaryotic P-glycoprotein homolog. *Proceedings of the National Academy of Sciences of the United States of America* 2014; 111 (11):4049-54.
- Krishna R, Mayer LD. Multidrug resistance (MDR) in cancer. Mechanisms, reversal using modulators of MDR and the role of MDR modulators in influencing the pharmacokinetics of anticancer drugs. *Eur J Pharm Sci* 2000a; 11 (4):265-83.
- Krishna R, St-Louis M, Mayer LD. Increased intracellular drug accumulation and complete chemosensitization achieved in multidrug-resistant solid tumors by co-administering valsopodar (PSC 833) with sterically stabilized liposomal Doxorubicin. *International Journal of Cancer* 2000b; 85 (1):131-41.
- Kuppens IE, Witteveen EO, Jewell RC et al. A phase I, randomized, open-label, parallel-cohort, dose-finding study of elacridar (GF120918) and oral topotecan in cancer patients. *Clinical cancer research : an official journal of the American Association for Cancer Research* 2007; 13 (11):3276-85.
- Lancet JE, Baer MR, Duran GE et al. A phase I trial of continuous infusion of the multidrug resistance inhibitor zosuquidar with Daunorubicin and cytarabine in acute myeloid leukemia. *Leukemia research* 2009; 33 (8):1055-61.
- Law LW, Dunn TB, et al. Observations on the effect of a folic-acid antagonist on transplantable lymphoid leukemias in mice. *Journal of the National Cancer Institute* 1949; 10 (1):179-92.
- Lee CH. Reversing agents for ATP-binding cassette (ABC) transporters: application in modulating multidrug resistance (MDR). *Curr Med Chem Anticancer Agents* 2004; 4 (1):43-52.
- Leite DF, Echevarria-Lima J, Salgado LT et al. In vivo and in vitro modulation of MDR molecules in murine thymocytes. *International immunopharmacology* 2006; 6 (2):204-15.
- Leonessa F, Green D, Licht T et al. MDA435/LCC6 and MDA435/LCC6MDR1: ascites models of human breast cancer. *British journal of cancer* 1996; 73 (2):154-61.
- Lhomme C, Joly F, Walker JL et al. Phase III study of valsopodar (PSC 833) combined with Paclitaxel and carboplatin compared with Paclitaxel and carboplatin alone in patients with stage IV or suboptimally debulked stage III epithelial ovarian cancer or primary peritoneal cancer. *Journal of clinical oncology : official journal of the American Society of Clinical Oncology* 2008; 26 (16):2674-82.

- Ling V. Multidrug resistance: molecular mechanisms and clinical relevance. *Cancer Chemotherapy and Pharmacology* 1997; 40 Supplementary:S3-8.
- Lipinski CA, Lombardo F, Dominy BW et al. Experimental and computational approaches to estimate solubility and permeability in drug discovery and development settings. *Advanced drug delivery reviews* 1997; 23 (1-3):3-25.
- Loo TW, Bartlett MC, Clarke DM. Permanent Activation of the Human P-glycoprotein by Covalent Modification of a Residue in the Drug-binding Site. *Journal of Biological Chemistry* 2003; 278 (23) 20449-20452
- Loo TW, Clarke DM. Recent progress in understanding the mechanism of P-glycoprotein-mediated drug efflux. *The Journal of Membrane Biology* 2005; 206 (3):173-85.
- Loor F, Tiberghien F, Wenandy T et al. Cyclosporins: structure-activity relationships for the inhibition of the human MDR1 P-glycoprotein ABC transporter. *Journal of medicinal chemistry* 2002; 45 (21):4598-612.
- Lopes de Menezes DE, Hu Y, Mayer LD. Combined treatment of Bcl-2 antisense oligodeoxynucleotides (G3139), p-glycoprotein inhibitor (PSC833), and sterically stabilized liposomal Doxorubicin suppresses growth of drug-resistant growth of drug-resistant breast cancer in severely combined immunodeficient mice. *Journal of experimental therapeutics & oncology* 2003; 3 (2):72-82.
- Lopes EC, Garcia M, Benavides F et al. Multidrug resistance modulators PSC 833 and CsA show differential capacity to induce apoptosis in lymphoid leukemia cell lines independently of their MDR phenotype. *Leukemia research* 2003; 27 (5):413-23.
- Lopes EC, Scolnik M, Alvarez E et al. Modulator activity of PSC 833 and Cyclosporin-A in Vincristine and Doxorubicin-selected multidrug resistant murine leukemic cells. *Leukemia research* 2001; 25 (1):85-93.
- Mammen M, Choi S-K, Whitesides GM. Polyvalent Interactions in Biological Systems: Implications for Design and Use of Multivalent Ligands and Inhibitors. *Angewandte Chemie International Edition* 1998; 37 (20):2754-94.
- Martin C, Berridge G, Mistry P et al. The molecular interaction of the high affinity reversal agent XR9576 with P-glycoprotein. *British journal of pharmacology* 1999; 128 (2):403-11.
- Mecklenburg L, Tobin DJ, Cirlan MV et al. Premature termination of hair follicle morphogenesis and accelerated hair follicle cycling in Iasi congenital atrichia (fzica) mice points to fuzzy as a key element of hair cycle control. *Experimental dermatology* 2005; 14 (8):561-70.
- Meingassner JG. Sympathetic auricular chondritis in rats: a model of autoimmune disease? *Laboratory animals* 1991; 25 (1):68-78.

- Menna P, Salvatorelli E, Minotti G. Cardiotoxicity of antitumor drugs. *Chemical research in toxicology* 2008; 21 (5):978-89.
- Mistry P, Plumb J, Eccles S et al. In vivo efficacy of XR9051, a potent modulator of P-glycoprotein mediated multidrug resistance. *British journal of cancer* 1999; 79 (11-12):1672-8.
- Mistry P, Stewart AJ, Dangerfield W et al. In vitro and in vivo reversal of P-glycoprotein-mediated multidrug resistance by a novel potent modulator, XR9576. *Cancer research* 2001; 61 (2):749-58.
- Morschhauser F, Zinzani PL, Burgess M et al. Phase I/II trial of a P-glycoprotein inhibitor, Zosuquidar.3HCl trihydrochloride (LY335979), given orally in combination with the CHOP regimen in patients with non-Hodgkin's lymphoma. *Leukemia & lymphoma* 2007; 48 (4):708-15.
- Ozols RF, Cunnion RE, Klecker RW, Jr. et al. Verapamil and Adriamycin in the treatment of drug-resistant ovarian cancer patients. *Journal of clinical oncology : official journal of the American Society of Clinical Oncology* 1987; 5 (4):641-7.
- Pal D, Mitra AK. MDR- and CYP3A4-mediated drug-drug interactions. *Journal of Neuroimmune Pharmacology* 2006; 1 (3):323-39.
- Pantelouris EM, Hair J. Thymus dysgenesis in nude (nu nu) mice. *Journal of embryology and experimental morphology* 1970; 24 (3):615-23.
- Patnaik A, Warner E, Michael M et al. Phase I dose-finding and pharmacokinetic study of Paclitaxel and carboplatin with oral valspodar in patients with advanced solid tumors. *Journal of clinical oncology : official journal of the American Society of Clinical Oncology* 2000; 18 (21):3677-89.
- Pérez-Victoria JM, Chiquero MJ, Conseil G et al. Correlation between the Affinity of Flavonoids Binding to the Cytosolic Site of *Leishmania tropica* Multidrug Transporter and Their Efficiency To Revert Parasite Resistance to Daunomycin. *Biochemistry* 1999; 38 (6):1736-43.
- Planting AS, Sonneveld P, van der Gaast A et al. A phase I and pharmacologic study of the MDR converter GF120918 in combination with Doxorubicin in patients with advanced solid tumors. *Cancer chemotherapy and pharmacology* 2005; 55 (1):91-9.
- Prasad VVTS, Gopalan ROG. Continued use of MDA-MB-435, a melanoma cell line, as a model for human breast cancer, even in year, *Nature Partner Journal Breast Cancer*; 2015; 1:15002.
- Price JE, Polyzos A, Zhang RD et al. Tumorigenicity and metastasis of human breast carcinoma cell lines in nude mice. *Cancer research* 1990; 50 (3):717-21.

- Prieur DJ, Young DM, Counts DF. Auricular chondritis in fawn-hooded rats. A spontaneous disorder resembling that induced by immunization with type II collagen. *The American journal of pathology* 1984; 116 (1):69-76.
- Pusztai L, Wagner P, Ibrahim N et al. Phase II study of tariquidar, a selective P-glycoprotein inhibitor, in patients with chemotherapy-resistant, advanced breast carcinoma. *Cancer* 2005; 104 (4):682-91.
- Rabah SO. Acute Taxol nephrotoxicity: Histological and ultrastructural studies of mice kidney parenchyma. *Saudi Journal of Biological Sciences* 2010; 17 (2):105-14.
- Rangarajan A, Weinberg RA. Opinion: Comparative biology of mouse versus human cells: modelling human cancer in mice. *Nature reviews. Cancer* 2003; 3 (12):952-9.
- Rao J, Lahiri J, Isaacs L et al. A trivalent system from vancomycin.D-ala-D-Ala with higher affinity than avidin.biotin. *Science* 1998; 280 (5364):708-11.
- Raviv Y, Pollard HB, Bruggemann EP et al. Photosensitized labeling of a functional multidrug transporter in living drug-resistant tumor cells. *The Journal of biological chemistry* 1990; 265 (7):3975-80.
- Rose WC. Taxol: a review of its preclinical in vivo antitumor activity. *Anti-cancer drugs* 1992; 3 (4):311-21.
- Rowinsky EK, Donehower RC. The clinical pharmacology of Paclitaxel (Taxol). *Seminars in oncology* 1993; 20 (4 Supplementary 3):16-25.
- Ruff P, Vorobiof DA, Jordaan JP et al. A randomized, placebo-controlled, double-blind phase 2 study of docetaxel compared to docetaxel plus zosuquidar (LY335979) in women with metastatic or locally recurrent breast cancer who have received one prior chemotherapy regimen. *Cancer chemotherapy and pharmacology* 2009; 64 (4):763-8.
- Rygaard J, Povlsen CO. Heterotransplantation of a human malignant tumour to "Nude" mice. *Acta pathologica et microbiologica Scandinavica* 1969; 77 (4):758-60.
- Sandler A, Gordon M, De Alwis DP et al. A Phase I trial of a potent P-glycoprotein inhibitor, zosuquidar trihydrochloride (LY335979), administered intravenously in combination with Doxorubicin in patients with advanced malignancy. *Clinical cancer research : an official journal of the American Association for Cancer Research* 2004; 10 (10):3265-72.
- Sharom FJ. Complex Interplay between the P-Glycoprotein Multidrug Efflux Pump and the Membrane: Its Role in Modulating Protein Function. *Frontiers in Oncology* 2014; 4:41.
- Shepard RL, Cao J, Starling JJ et al. Modulation of P-glycoprotein but not MRP1- or BCRP-mediated drug resistance by LY335979. *International journal of cancer* 2003; 103 (1):121-5.

Shultz LD, Ishikawa F, Greiner DL. Humanized mice in translational biomedical research. *Nature reviews. Immunology* 2007; 7 (2):118-30.

Slapak CA, Dahlheimer J, Piwnica-Worms D. Reversal of multidrug resistance with LY335979: functional analysis of P-glycoprotein-mediated transport activity and its modulation in vivo. *Journal of clinical pharmacology* 2001; Supplementary:29S-38S.

Slate DL, Bruno NA, Casey SM et al. RS-33295-198: a novel, potent modulator of P-glycoprotein-mediated multidrug resistance. *Anticancer research* 1995; 15 (3):811-4.

Slater LM, Sweet P, Stupecky M et al. Cyclosporin A reverses Vincristine and Daunorubicin resistance in acute lymphatic leukemia in vitro. *The Journal of clinical investigation* 1986a; 77 (4):1405-8.

Slater LM, Sweet P, Stupecky M et al. Cyclosporin A corrects Daunorubicin resistance in Ehrlich ascites carcinoma. *British journal of cancer* 1986b; 54 (2):235-8.

Society AC. *Cancer Facts & Figures 2016*. Atlanta: American Cancer Society 2016.

Song S, Suzuki H, Terasaki T et al. Modulation of the tumor disposition of vinca alkaloids by PSC 833 in vitro and in vivo. *The Journal of pharmacology and experimental therapeutics* 1998; 287 (3):963-8.

Sonneveld P, Suci S, Weijermans P et al. Cyclosporin A combined with Vincristine, Doxorubicin and dexamethasone (VAD) compared with VAD alone in patients with advanced refractory multiple myeloma: an EORTC-HOVON randomized phase III study (06914). *British journal of haematology* 2001; 115 (4):895-902.

Spang-Thomsen M, Visfeldt J. Homozygous nu/nu mice with transplanted human malignant tumors. *The American journal of pathology* 1976; 84 (1):193-6.

Stewart A, Steiner J, Mellows G et al. Phase I trial of XR9576 in healthy volunteers demonstrates modulation of P-glycoprotein in CD56+ lymphocytes after oral and intravenous administration. *Clinical cancer research : an official journal of the American Association for Cancer Research* 2000; 6 (11):4186-91.

Stiff PJ, Bayer R, Tan S et al. High-dose chemotherapy combined with escalating doses of Cyclosporin A and an autologous bone marrow transplant for the treatment of drug-resistant solid tumors: a phase I clinical trial. *Clinical cancer research : an official journal of the American Association for Cancer Research* 1995; 1 (12):1495-502.

Suggitt M, Bibby MC. 50 years of preclinical anticancer drug screening: empirical to target-driven approaches. *Clinical cancer research : an official journal of the American Association for Cancer Research* 2005; 11 (3):971-81.

Tan B, Piwnica-Worms D, Ratner L. Multidrug resistance transporters and modulation. *Current Opinion in Oncology* 2000; 12 (5):450-8.

- Teicher BA. Tumor models for efficacy determination. *Molecular cancer therapeutics* 2006; 5 (10):2435-43.
- Teicher BA. Tumor models in cancer research. Humana Press 2002:73-97.
- Teicher BA et al. Anticancer drug development guide: preclinical screening, clinical trials, and approval. Humana Press 2004:25-182.
- Toffoli G, Sorio R, Gigante M et al. Cyclosporin A as a multidrug-resistant modulator in patients with renal cell carcinoma treated with teniposide. *British journal of cancer* 1997; 75 (5):715-21.
- Tsuruo T. [Reversal of acquired resistance to vinca alkaloids and anthracycline antibiotics by calcium channel blockers and calmodulin inhibitors]. *Gan to kagaku ryoho. Cancer & chemotherapy* 1984; 11 (3 Pt 2):750-9.
- Tsuruo T, Iida H, Tsukagoshi S et al. Overcoming of Vincristine resistance in P388 leukemia in vivo and in vitro through enhanced cytotoxicity of Vincristine and vinblastine by Verapamil. *Cancer research* 1981; 41 (5):1967-72.
- Tsuruo T, Iida H, Tsukagoshi S et al. Potentiation of Vincristine and Adriamycin effects in human hemopoietic tumor cell lines by calcium antagonists and calmodulin inhibitors. *Cancer research* 1983; 43 (5):2267-72.
- Twentyman PR, Fox NE, White DJ. Cyclosporin A and its analogues as modifiers of Adriamycin and Vincristine resistance in a multi-drug resistant human lung cancer cell line. *British journal of cancer* 1987; 56 (1):55-7.
- Twentyman PR, Reeve JG, Koch G et al. Chemosensitisation by Verapamil and Cyclosporin A in mouse tumor cells expressing different levels of P-glycoprotein and CP22 (sorcin). *British journal of cancer* 1990; 62 (1):89-95.
- Twentyman PR, Wright KA, Wallace HM. Effects of Cyclosporin A and a non-immunosuppressive analogue, O-acetyl Cyclosporin A, upon the growth of parent and multidrug resistant human lung cancer cells in vitro. *British Journal of Cancer* 1992; 65 (3):335-40.
- Ueda K, Cornwell MM, Gottesman MM et al. The *mdr1* gene, responsible for multidrug-resistance, codes for P-glycoprotein. *Biochemical and Biophysical Research Communications* 1986; 141 (3):956-62.
- Ursu O, Rayan A, Goldblum A et al. Understanding drug-likeness. *Wiley Interdisciplinary Reviews: Computational Molecular Science* 2011; 1 (5):760-81.
- Visonneau S, Cesano A, Torosian MH et al. Growth characteristics and metastatic properties of human breast cancer xenografts in immunodeficient mice. *The American journal of pathology* 1998; 152 (5):1299-311.

- Walker J, Martin C, Callaghan R. Inhibition of P-glycoprotein function by XR9576 in a solid tumor model can restore anticancer drug efficacy. *European Journal of Cancer* 2004; 40 (4):594-605.
- Warner E, Tobe SW, Andrulis IL et al. Phase I-II study of vinblastine and oral Cyclosporin A in metastatic renal cell carcinoma. *American journal of clinical oncology* 1995; 18 (3):251-6.
- Watanabe T, Tsuge H, Oh-Hara T et al. Comparative study on reversal efficacy of SDZ PSC 833, Cyclosporin A and Verapamil on multidrug resistance in vitro and in vivo. *Acta Oncologica* 1995; 34 (2):235-41.
- White RE. High-throughput screening in drug metabolism and pharmacokinetic support of drug discovery. *Annual review of pharmacology and toxicology* 2000; 40:133-57.
- White RE. Short- and long-term projections about the use of drug metabolism in drug discovery and development. *Drug metabolism and disposition: the biological fate of chemicals* 1998; 26 (12):1213-6.
- Wong IL, Chan KF, Chan TH et al. Flavonoid dimers as novel, potent antileishmanial agents. *Journal of Medicinal Chemistry* 2012; 55 (20):8891-902.
- Wong IL, Chan KF, Chen YF et al. In vitro and in vivo efficacy of novel flavonoid dimers against cutaneous leishmaniasis. *Antimicrobial agents and chemotherapy* 2014; 58 (6):3379-88.
- Yan CS, Wong IL, Chan KF et al. A New Class of Safe, Potent, and Specific P-gp Modulator: Flavonoid Dimer FD18 Reverses P-gp-Mediated Multidrug Resistance in Human Breast Xenograft in Vivo. *Molecular pharmaceutics* 2015; 12 (10):3507-17.
- Zhang S, Morris ME. Effects of the flavonoids biochanin A, morin, phloretin, and silymarin on P-glycoprotein-mediated transport. *Journal of Pharmacology and Experimental Therapeutics* 2003; 304 (3):1258-67.